

**A STOCHASTIC BIOMECHANICAL MODEL FOR RISK AND RISK FACTORS OF
SUSTAINING NON-CONTACT ACL INJURIES**

Cheng-Feng Lin, MS

A dissertation submitted to the faculty of the University of North Carolina at Chapel Hill in partial fulfillment of the requirements for the degree of Doctor of Philosophy in the Program of Human Movement Science.

Chapel Hill
2006

Approved by

Chair: Bing Yu
Member: William Garrett
Member: Michael Gross
Member: Chuanshu Ji
Member: Darin Padua
Member: Paul Weinholt

ABSTRACT

Cheng-Feng Lin: A Stochastic Biomechanical Model for Risk and Risk Factors of Sustaining Non-contact ACL Injuries (Under the direction of Dr. Bing Yu)

Non-contact anterior cruciate ligament injury is one of the most commonly seen injuries in sports with an estimated total cost for treatment over \$2 billion per year. To prevent non-contact ACL injuries, several possible risk factors have been proposed. No studies to date, however, have shown conclusive evidence that any of the proposed risk factors are indeed risk factors for sustaining non-contact ACL injuries.

In this study, a sagittal plane knee model was developed to enhance the understanding of the effects of sagittal plane biomechanics on the ACL loading. Knee geometry data were obtained from x-ray films of 10 male and 10 female collegiate aged recreational athletes. The patellar tendon-tibial shaft angle, patella-patellar tendon angle, quadriceps tendon-patella angle, and hamstring tendon-tibial shaft angle were expressed as functions of knee flexion angle, and incorporated into the sagittal plane knee model to estimate the ACL loading. *In vivo* lower extremity kinematic and kinetic data of a stop-jump task collected from 80 college aged recreational athletes were used for computer simulation with the sagittal plane knee model. A stochastic biomechanical model was developed and used to determine the risk and risk factors of sustaining non-contact ACL injuries during landing of the stop-jump task.

The results of the computer simulation with sagittal plane inverse dynamic knee model showed that the lower extremity sagittal plane biomechanics simulated did affect the ACL loading. The results of the stochastic biomechanical model presented that females had higher

risk of non-contact ACL injuries than males did. The gender difference in the risk of non-contact ACL injuries was affected by the differences in the lower extremity motion patterns, ACL ultimate load, and knee anatomy between genders. Biomechanical characteristics during the stop-jump task were significantly different between injured and uninjured jumps or between females and males. During the stop-jump task, the isolated sagittal plane loading alone can injure the ACL while the isolated non-sagittal plane loading alone may not. Knee flexion angle and peak posterior ground reaction force are two important risk factors for the gender difference in the risk of non-contact ACL injuries during the stop-jump task.

DEDICATION

To my parents Shui-Lung Lin and Yu-Chiao Huang and my fiancé Jen-Chieh Liao

ACKNOWLEDGEMENTS

I would like to thank my committee for their critical and constructive suggestions in the conduct and completion of this dissertation. Special thanks to Dr. Bing Yu for his tremendous support and guidance throughout my doctoral study. Thanks for being my academic advisor and chairing my dissertation committee. I also want to express my special thanks to Dr. William Garrett and Dr. Michael Gross for being positive role models as good combination of clinician and researcher. Thanks to Dr. Paul Weinholt for delivery of clear concepts in biomechanics during my doctoral study. Special thanks also to Dr. Chuanshu Ji for ensuring my probability concepts and to Dr. Darin Padua for critical suggestions and careful review of my dissertation.

I also would like to thank Prof. Fong-Chin Su, my academic and thesis advisor while I was in the master program of Biomedical Engineering at the National Cheng Kung University in Taiwan, for opening the door to biomechanics for me and setting the basis for my studies at the doctoral level.

Also, I would like to extend my appreciation to my family and my fiancé Jen-Chieh for their caring and unlimited support and love. Finally, I would like to thank my friends in Taiwan and United States for their support in my life.

Cheng-Feng Connie Lin

Chapel Hill, NC.

September, 2006

TABLE OF CONTENTS

	Page
ABSTRACT	ii
DEDICATION.....	iv
ACKNOWLEDGEMENTS	v
TABLE OF CONTENTS	vi
LIST OF FIGURES	xi
LIST OF TABLES	xvii
LIST OF ABBREVIATIONS AND SYMBOLS	xix
 CHAPTER	
I. INTRODUCTION	1
Statement of Purposes	5
 II. REVIEW OF LITERATURE	6
ACL Injuries	6
ACL Injury Mechanism	8
ACL Loading Mechanism	8
Effects of the Quadriceps Muscle Force on the ACL loading	11
Effects of the Knee Flexion Angle on the ACL Loading.....	13
Effects of the Ground Reaction Forces on the ACL Loading	15

Effects of the Hamstring Co-contraction on the ACL Loading.....	17
Effects of the Gastrocnemius Muscle Force on the ACL loading.....	21
Effects of the Knee Valgus-varus and Internal-external Rotation Moment on the ACL Loading	22
Potential Risk Factors	27
Non-modifiable Intrinsic Risk Factors	28
Motor Control Related Biomechanical Risk Factors	28
Effect of the Training Programs on the Prevention of Non-contact ACL Injuries ...	33
Research Methods to Determine Risk Factors for Sustaining Non-contact ACL Injuries	38
Traditional Epidemiological Research Methods.....	38
Stochastic Biomechanical Modeling	40
Summary.....	42
III. METHODS	44
The Sagittal Plane Knee Model	44
Determination of the ACL Loading	45
Determination of the Quadriceps Muscle Force	51
Determination of the Patella tendon-tibia shaft angle, Patella-patella tendon angle, Quadriceps tendon-patella angle, and Hamstring tendon-tibial shaft angle.....	53
Determination of the Moment Arms	56
Determination of the ACL Elevation Angle	57
Collection and Reduction of Lower Extremity Kinetics, Kinematics, and EMG in a Stop-Jump Task	59
Data Collection	59

Data Reduction	62
Computer Simulation of the Effects of Sagittal Biomechanics on the ACL Loading.....	63
The Stochastic Biomechanical Model of the Probability of Sustaining Non-contact ACL Injuries	66
Determination of Density Distributions of the Primary Independent Variables.....	66
Determination of Cumulative Distribution Functions of the Primary Independent Variables	69
Determination of the Secondary Independent Variables.....	71
Monte Carlo Simulation for Estimate of the Probability of Sustaining Non-contact ACL Injuries	72
Normalization of Moment Arms of Muscles	73
Determination of Mean and Standard Deviation of Muscle Forces.....	73
Determination of the ACL Loading.....	74
Sensitivity Analysis of the ACL Ultimate Load.....	76
Monte Carlo Simulation for Determining Risk Factors of Sustaining Non-Contact ACL Injuries	81
Assumptions of Models.....	81
Assumptions for the Sagittal Plane Inverse Dynamic Knee Model	82
Assumptions for the Stochastic Biomechanical Model	83
IV. RESULTS	84
Computer Simulation of Effects of Sagittal Plane Lower Extremity Biomechanics on Peak ACL Loading during the landing of the Stop-jump Task.....	84
Monte Carlo Simulation of Simulated Non-contact ACL Injuries during the Stop-jump Task	106

Goodness-of-fit Test for Independent Variables	106
Sensitivity Analysis of ACL Ultimate Load during the Stop-jump Task.....	115
Probability and Characteristics of Simulated Injured and Uninjured Jumps...	117
Risk Factors of Simulated Non-contact ACL Injuries.....	123
V. DISCUSSION.....	126
Effects of Assumptions on the Validity of the Sagittal Plane Inverse Dynamic Model of the Knee.....	126
Effects of Assumptions on the Validity of the Stochastic Biomechanical Model of the Probability of Sustaining Non-contact ACL injuries.....	130
Effects of Sagittal Plane Biomechanics on the Peak ACL loading.....	131
Effect of the Knee Flexion Angle on the ACL Loading.....	131
Effect of the Peak Posterior Ground Reaction Force on the ACL Loading	136
Effect of Landing Styles on the ACL Loading.....	140
Effect of Hamstrings Force on the ACL Loading.....	145
Effect of Gastrocnemius Force on the ACL Loading.....	148
Monte Carlo Simulation of the Probability of Sustaining Non-contact ACL Injuries during the Stop-jump Task.....	150
Sensitivity of Simulated Relative Risk of Non-contact ACL injury.....	150
Biomechanical Characteristics of Simulated Non-contact ACL Injuries.....	153
Comparison of Injured and Uninjured Jumps.....	153
Comparison of Injured Jumps between Genders	159
Comparison of Uninjured Jumps between Genders	159
Risk Factors of Simulated Non-contact ACL Injuries.....	161
Limitations of the Stochastic Biomechanical Model.....	165

Significance and Recommended Future Studies.....	166
Conclusion.....	172
 APPENDICES	
Appendix A: Effect of Sagittal Plane Biomechanics on the Peak ACL Loading.....	174
Appendix B: Density Distribution of Independent Variables of Stochastic Biomechanical Models	182
Appendix C: Probability Distribution of Independent Variables of Stochastic Biomechanical Models.....	188
 REFERENCES	194

LIST OF FIGURES

Figure	Page	
3.1	The horizontal ($F_{GRF,x}$) and vertical ($F_{GRF,z}$) ground reaction forces in the laboratory reference frame and representation of the tibial tilting angle (σ) ...	46
3.2	The knee geometry to show the definition of knee flexion angle (θ), patellar tendon-tibial shaft angle (α), hamstring tendon-tibial shaft angle (γ), and ACL elevation angle (ϕ)	50
3.3	Definition of the quadriceps tendon-patella angle (ϕ) and patella-patellar tendon angle (β)	52
3.4	Relationship between probability density function and cumulative distribution function. (a) Probability Density Function: $f(x)$. (b) Cumulative Distribution Function: $0 \leq F(x) \leq 1$. The integral of $f(x)$ with respect to a (the gray area under curve) was the cumulative distribution function $F(a)$ ($0 \leq F(a) \leq 1$), which was a randomly generated number. GRN: generated random number.....	70
3.5	A flow chart of one iteration of the Monte Carlo Simulation.....	80
4.1	Effect of the knee flexion angle at peak posterior ground reaction force on the simulated ACL loading for males at different posterior ground reaction forces during the landing of the stop-jump task. The inputs of other independent variables during computer simulation were fixed with the corresponding values at peak posterior ground reaction force.	90
4.2	Effect of the knee flexion angle at peak posterior ground reaction force on the simulated ACL loading for females at different posterior ground reaction forces during the landing of the stop-jump task. The inputs of other independent variables during computer simulation were fixed with the corresponding values at peak posterior ground reaction force. The inputs of other independent variables during computer simulation were fixed with the corresponding values at peak posterior ground reaction force	91
4.3	Effect of the posterior ground reaction force on the simulated ACL loading for males at different knee flexion angles during the landing of the stop-jump task. The inputs of other independent variables during computer simulation were fixed with the corresponding values at peak posterior ground reaction force.....	92
4.4	Effect of the posterior ground reaction force on the simulated ACL loading	

	for females at different knee flexion angles during the landing of the stop-jump task. The inputs of other independent variables during computer simulation were fixed with the corresponding values at peak posterior ground reaction force.....	93
4.5	Effect of landing-on-heels and landing-on-toes on the simulated ACL loading for males during the landing of the stop-jump task. The inputs of other independent variables during computer simulation were fixed with the corresponding values at peak posterior ground reaction force	94
4.6	Effect of landing-on-heels and landing-on-toes on the simulated ACL loading for females during the landing of the stop-jump task. The inputs of other independent variables during computer simulation were fixed with the corresponding values at peak posterior ground reaction force	95
4.7	Effect of the anterior(+)-posterior(-) tibial tilting angle on the simulated ACL loading for males at different posterior ground reaction forces during the landing of the stop-jump task. The inputs of other independent variables during computer simulation were fixed with the corresponding values at peak posterior ground reaction force	96
4.8	Effect of the anterior(+)-posterior(-) tibial tilting angle on the simulated ACL loading for females at different posterior ground reaction forces during the landing of the stop-jump task. The inputs of other independent variables during computer simulation were fixed with the corresponding values at peak posterior ground reaction force	97
4.9	Effect of the hamstring force on the simulated ACL loading for males at 500 N of posterior ground reaction force and at different knee flexion angles during landing of the stop-jump task. The inputs of other independent variables during computer simulation were fixed with the corresponding values at peak posterior ground reaction force	98
4.10	Effect of the hamstring force on the simulated ACL loading for males at 1000 N posterior ground reaction force and at different knee flexion angles during the landing of the stop-jump task. The inputs of other independent variables during computer simulation were fixed with the corresponding values at peak posterior ground reaction force.....	99
4.11	Effect of the hamstring force on the simulated ACL loading for females at 500 N of posterior ground reaction force and at different knee flexion angles during the landing of the stop-jump task. The inputs of other independent variables during computer simulation were fixed with the corresponding values at peak posterior ground reaction force	100
4.12	Effect of the hamstring force on the simulated ACL loading for females at	

	1000 N of posterior ground reaction force and at different knee flexion angles during the landing of the stop-jump task. The inputs of other independent variables during computer simulation were fixed with the corresponding values at peak posterior ground reaction force	101
4.13	Effect of the gastrocnemius force on the simulated ACL loading for males 500 N of posterior ground reaction force and at different knee flexion angles during the landing of the stop-jump task. The inputs of other independent variables during computer simulation were fixed with the corresponding values at peak posterior ground reaction force.....	102
4.14	Effect of the gastrocnemius force on the simulated ACL loading for males at 1000 N of posterior ground reaction force and at different knee flexion angles during the landing of the stop-jump task. The inputs of other independent variables during computer simulation were fixed with the corresponding values at peak posterior ground reaction force	103
4.15	Effect of the gastrocnemius force on the simulated ACL loading for females at 500 N of posterior ground reaction force and at different knee flexion angles during the landing of the stop-jump task. The inputs of other independent variables during computer simulation were fixed with the corresponding values at peak posterior ground reaction force.....	104
4.16	Effect of the gastrocnemius force on the simulated ACL loading for females at 1000 N of posterior ground reaction force and at different knee flexion angles during the landing of the stop-jump task. The inputs of other independent variables during computer simulation were fixed with the corresponding values at peak posterior ground reaction force.....	105
4.17	Q-Q plot of independent variables against the test of normal distribution for males. The abscissa represents the observed value while the ordinate represents the expected normal value. (a) knee varus-valgus moment (BH.BW); (b) knee int.-ext. rotation moment (BH.BW); (c) COP to ankle distance (m); (d) tibial tilting angle (deg); (e) knee flexion angle (deg).....	109
4.18	Q-Q plot of independent variables against the test of gamma distribution for males. The abscissa represents the observed value while the ordinate represents the expected gamma value. (a) posterior GRF (N); (b) standing height (m); (c) normalized linear envelope hamstring EMG ; (d) normalized linear envelope gastrocnemius EMG.....	110
4.19	Q-Q plot of independent variables against the test of normal distribution for females. The abscissa represents the observed value while the ordinate represents the expected normal value. (a) knee varus-valgus moment (BH.BW); (b) knee int.-ext. rotation moment (BH.BW); (c) COP to ankle distance (m); (d) tibial tilting angle (deg)	111

4.20	Q-Q plot of independent variables against the test of gamma distribution for females. The abscissa represents the observed value while the ordinate represents the expected gamma value. (a) posterior GRF (N); (b) knee flexion angle (deg); (c) standing height (m) (d) normalized linear envelope hamstring EMG ; (e) normalized linear envelope gastrocnemius EMG.....	112
5.1	A flow chart of how the knee flexion angle affects the ACL Loading.....	133
5.2	A flow chart of how the posterior ground reaction force affects the ACL Loading	138
5.3	A flow chart of how the landing style affects the ACL Loading.....	142
5.4	A flow chart of how the tibial tilting angle affects the ACL Loading.....	144
5.5	A flow chart of how the hamstring force affects the ACL Loading.....	146
5.6	A flow chart of how the gastrocnemius force affects the ACL Loading.....	149
A.1	Effect of the knee flexion angle at peak posterior ground reaction force on the simulated ACL loading for males at different posterior ground reaction forces during the landing of the stop-jump task.....	174
A.2	Effect of the knee flexion angle at peak posterior ground reaction force on the simulated ACL loading for females at different posterior ground reaction forces during the landing of the stop-jump task.....	175
A.3	Effect of the posterior ground reaction force on the simulated ACL loading for males at different knee flexion angles during the landing of the stop-jump task.....	176
A.4	Effect of the posterior ground reaction force on the simulated ACL loading for females at different knee flexion angles during the landing of the stop-jump task.....	177
A.5	Effect of the hamstring force on the simulated ACL loading for males at 500 N of posterior ground reaction force and at different knee flexion angles during the landing of the stop-jump task.....	178
A.6	Effect of the hamstring force on the simulated ACL loading for females at 500 N of posterior ground reaction force and at different knee flexion angles during the landing of the stop-jump task.....	179
A.7	Effect of the gastrocnemius force on the simulated ACL loading for males at 500 N of posterior ground reaction force and at different knee flexion angles	

	during the landing of the stop-jump task.....	180
A.8	Effect of the gastrocnemius force on the simulated ACL loading for females at 500 N of posterior ground reaction force and at different knee flexion angles during the landing of the stop-jump task	181
B.1	Density distribution of knee flexion angle of males and females. Empirical indicates the distribution based on the experimental data.	182
B.2	Density distribution of normalized peak posterior ground reaction force of males and females. Empirical indicates the distribution based on the experimental data.	183
B.3	Density distribution of normalized internal varus(+)-valgus(-) moment of males and females. Empirical indicates the distribution based on the experimental data.	184
B.4	Density distribution of normalized internal internal(+)-external(-) rotation moment of males and females. Empirical indicates the distribution based on the experimental data.	185
B.5	Density distribution of anterior(+)-posterior(-) tibial tilting angle of males and females. Empirical indicates the distribution based on the experimental data.	186
B.6	Density distribution of COP to ankle joint distance of males and females. (+): prone to land on heel; (-): prone to land on toe. Empirical indicates the distribution based on the experimental data	187
C.1	Probability distribution of knee flexion angle of males and females. Empirical indicates the distribution based on the experimental data.....	188
C.2	Probability distribution of normalized posterior ground reaction force of males and females. Empirical indicates the distribution based on the experimental data.	189
C.3	Probability distribution of normalized internal varus(+)-valgus(-) moment of males and females. Empirical indicates the distribution based on the experimental data.	190
C.4	Probability distribution of normalized internal internal(+)-external(-) rotation moment of males and females. Empirical indicates the distribution based on the experimental data.	191
C.5	Probability distribution of anterior(+)-posterior(-) tibial tilting angle of males and females. Empirical indicates the distribution based on the experimental	

	data.....	192
C.6	Probability distribution of COP to ankle joint distance of males and females (+): prone to land on heel; (-): prone to land on toe. Empirical indicates the distribution based on the experimental data	193

LIST OF TABLES

Table	Page
3.1	Pearson correlation coefficients (p-values) of peak posterior ground reaction force with peak vertical ground reaction force and peak knee joint resultants during the landing of the stop-jump task (Yu et al., 2006b) 65
3.2	ACL ultimate load (N) in pairs for sensitivity analysis 77
4.1	Anthropometric data of subjects 85
4.2	Simulated range and increment of each independent variable of the sagittal plane inverse dynamic knee model..... 86
4.3	Skewness and kurtosis of each independent variable for Monte Carlo simulation..... 107
4.4	Types of distribution and p-value of each independent variable for males and females 108
4.5	Mean and standard deviation (SD) of variables simulated as normal distribution in the stochastic biomechanical knee model 113
4.6	Shape and scale parameters and mean and standard deviation (SD) of independent variables with gamma distribution for males 114
4.7	Shape and scale parameters and mean and standard deviation (SD) of independent variables as gamma distribution for females..... 114
4.8	Average (SD) of number of simulated ACL injuries per 100,000 jumps and female to male non-contact ACL injury rate ratio with different ACL injury loadings 116
4.9	Mean (SD) of biomechanical characteristics of simulated injured and uninjured jumps with 2250 N as ACL ultimate load for males 119
4.10	Mean (SD) of biomechanical characteristics of simulated injured and uninjured jumps with 1800 N as ACL ultimate load for females 120
4.11	Mean (SD) of injured biomechanical characteristics of simulated jumps with 2250 N for males and 1800 N for females as ACL ultimate load..... 121
4.12	Mean (SD) of uninjured biomechanical characteristics of simulated jumps

	with 2250 N for males and 1800 N for females as ACL ultimate load	122
4.13	Mean of contribution from non-sagittal loadings to total ACL loading in injured jumps subjected to the change of varus-valgus moment from literature in female stochastic biomechanical model and 1800 N as ACL injury criterion.....	123
4.14	Mean of numbers of non-contact ACL injury per 100,000 jumps and female to male non-contact ACL injury rate ratio subjected to the change of each independent variable in female Monte Carlo simulations and 1800 N as ACL injury criterion.....	125

LIST OF ABBREVIATIONS AND SYMBOLS

ACL	= Anterior cruciate ligament
BW	= Body weight
BH	= Body height (standing height)
COP	= Center of pressure
EMG	= Electromyography
GRF	= Ground reaction force
Int.	= Internal
Ext.	= External
MCL	= Medial collateral ligament
N	= Newton
Nm	= Newton-meter
PTTS	= Patellar tendon-tibial shaft angle
Var	= Varus
Val	= Valgus
α (alpha)	= Patellar tendon-tibial shaft angle
β (beta)	= Patella-patellar tendon angle
ϕ (phi)	= Quadriceps tendon-patella angle
γ (gamma)	= Hamstring tendon-tibial shaft angle
θ (theta)	= Knee flexion angle
φ (phi)	= ACL elevation angle
σ (sigma)	= Tibial tilting angle

ϵ (epsilon) = Residual of ground reaction force

τ (tau) = ACL anterior load share coefficient

CHAPTER I

INTRODUCTION

Anterior cruciate ligament (ACL) injury is one of the most commonly seen injuries in sports. The incidence of ACL injuries is more than three per 1000 athletes over a single season (McCarroll et al., 1995). Arendt and Dick (1995) found that the average ACL injury rate per 1000 athlete-exposures was 0.31 and 0.29 in women soccer and basketball players, respectively, from National Collegiate Athletic Association (NCAA) database. Gottlob et al. (1999) estimated that approximately 175,000 primary ACL reconstruction surgeries were performed annually in the United States with an estimated cost of over \$2 billion.

ACL injuries have devastating influences on patients' activity levels and quality of life. Complete ACL rupture could induce other knee pathological conditions including knee instability, damage to menisci and chondral surface, and osteoarthritis. Studies have repeatedly shown that patients with complete ACL rupture had chronic knee instability and secondary damage to menisci and chondral surfaces (Finsterbush et al., 1990; Irvine and Glasgow, 1992; Kannus and Jarvinen, 1987). These debilitating consequences would influence their quality of life and severely impair patients' functional activities (Smith et al., 1993).

ACL injuries that occur without physical contact between athletes are referred to as non-contact ACL injuries (Boden et al., 2000; Feagin and Lambert, 1985; Ferretti et al., 1992). The majority of ACL injuries occur with a non-contact mechanism of injury in sports in which

sudden deceleration, landing, and pivoting maneuvers are repeatedly performed (Boden et al., 2000). Female athletes had higher incidence on the ACL injuries compared with their male counterparts (Arendt and Dick, 1995; Ferretti et al., 1992; Huston and Wojtys, 1996). Studies have shown that the incidence of female athletes is two to eight times higher than males in soccer, basketball, and volleyball (Arendt and Dick, 1995; Bjordal et al., 1997; Ferretti et al., 1992; Harmon and Ireland, 2000; Huston and Wojtys, 1996; Huston et al., 2000; Linderfeld et al., 1994).

Risk factors have to be identified to develop intervention strategies to reduce the risk of sustaining non-contact ACL injuries. A variety of risk factors of sustaining non-contact ACL injuries has been proposed in the literature. These proposed risk factors can be categorized into intrinsic and extrinsic risk factors. Intrinsic risk factors are those related to anatomic structure, physiological properties, and motor control related biomechanical factors such as Q-angle, the width of femoral condyle notch (Shambaugh et al., 1991), knee joint laxity (Wojtys et al., 1998), hormonal effects (Arendt et al, 2002), imbalanced lower extremity strength (Boden et al., 2000) and the altered lower extremity motion patterns (Boden et al., 2000; Decker et al., 2003; Malinzak et al., 2001). Extrinsic risk factors include shoe-surface interaction (Garrick and Requa, 1996) and playing surface (Powell and Schootman, 1992). Among these proposed risk factors, risk factors related to neuromuscular control and muscle strength are modifiable through intervention programs.

Extensive research efforts have been made in the last several years to identify neuromuscular control related risk factors of sustaining non-contact ACL injuries in attempts to develop training programs for reducing the risks. Several studies indicated that small knee flexion angle (Arms et al., 1984; Chappell et al., 2002; Malinzak et al., 2001), excessive knee

valgus-varus and internal-external rotation moment (Ford et al., 2003; Hewett et al., 2005; McLean et al., 2004), large ground reaction forces (DeVita and Kelly, 1992), and strong quadriceps and weak hamstring muscles activations tend to increase the load on the ACL (Arms et al., 1984; Fleming et al., 2001; Malinzak et al., 2001). Studies also proposed that excessive quadriceps activation along with a small knee flexion angle predisposed the ACL to a great strain which may injure the ACL (Arms et al., 1984; DeMorate et al., 2004; Li et al., 1999, 2004).

Although the studies mentioned previously provide some indirect evidence that the altered movement patterns during athletic task may be risk factors of sustaining non-contact ACL injuries, a recent extensive literature review failed to show conclusive evidence that any proposed risk factors related to neuromuscular control are indeed risk factors of sustaining non-contact ACL injuries. This lack of confirmation of neuromuscular control related risk factors of sustaining non-contact ACL injuries is mainly due to the difficulty in identifying neuromuscular control related risk factors. Longitudinal cohort design and a cross-sectional case-control design are two commonly used traditional epidemiological methods for identifying risk factors of sustaining an injury or disease. These two traditional epidemiological methods, however, have significant limitations when used to identify neuromuscular control related risk factors of sustaining non-contact ACL injuries. The pitfalls of the longitudinal cohort design include high cost, difficult control of independent variables during the study, and the descriptive nature of the results with lack of evidence for any cause-and-effect relationship between identified risk factors and injuries. The difficulty in determining pre-injury motion patterns is an additional critical limitation to the case-control design as a possible method to identify neuromuscular control related risk factors of sustaining

non-contact ACL injuries.

Another research design that can be used to determine risk effectively and risk factors of sustaining non-contact ACL injuries but has not been fully recognized is the stochastic biomechanical modeling. Stochastic biomechanical modeling is a research method in biomechanics to address the random outcomes of human movements using the Monte Carlo simulation technique. The Monte Carlo stochastic simulation is a method to express a dependent variable as a function of a group of random independent variables to simulate the variability of the dependent variable, and estimate the probability that the dependent variable is less or greater than a given limit. Stochastic biomechanical modeling method has been successfully applied in several recent biomechanical studies on injury prevention. Mirka and Marras (1993) applied a trunk stochastic biomechanical model for determining the variation of muscle forces during trunk bending, and to explain how repetitive lifting could injure the lower back. Hughes and An (1997) developed a shoulder stochastic biomechanical model and estimated the variation of deltoid and rotator cuff muscle forces during arm elevation and the probability of shoulder impingement. Chang et al. (2000) also developed a shoulder stochastic biomechanical model and determined the variation of shoulder muscle forces in shoulder internal rotation and the probability of rotator cuff injury, shoulder joint subluxation and dislocation. In an effort to determine the risk and risk factors of sustaining non-contact ACL injuries, McLean et al. (2003) formulated a stochastic biomechanical model of the ACL loading, and estimated the variation of ACL loading in a side cutting task. Garrett and Yu (2004) also used this method to estimate the ACL loading and ACL injury rate. The predicted gender differences in the probability of sustaining non-contact ACL injuries was similar to the gender differences in the risk of sustaining non-contact ACL injuries reported in the literature.

These studies demonstrated the feasibility of using the stochastic biomechanical modeling method to identify risk factors of sustaining non-contact ACL injuries.

Statement of Purposes

The purposes of this study were:

1. to develop a sagittal plane inverse dynamic knee model for studying the effects of lower extremity sagittal plane biomechanics on the ACL loading during landing of the stop-jump task;
2. to determine the effects of the knee flexion angle, posterior ground reaction force, hamstrings and gastrocnemius muscles contractions, tibial tilting angle, and location of center of pressure relative to the ankle joint center on the ACL loading during landing of the stop-jump task; and
3. to determine the probability of sustaining non-contact ACL injuries and the contribution of lower extremity motion patterns to the risk of sustaining non-contact ACL injuries during the stop-jump task using a stochastic biomechanical model.

CHAPTER II

REVIEW OF LITERATURE

The incidence of ACL injuries, ACL loading mechanism, possible risk factors for non-contact ACL injuries in athletes, training effects on the prevention of non-contact ACL injuries, and current research designs to identify risk factors of sustaining non-contact ACL injuries were reviewed as background information in this chapter to justify the significance of the current study. Studies using stochastic biomechanical modeling were also reviewed in this chapter to further justify the significance and establish the feasibility of the current study.

2.1. ACL Injuries

ACL injuries have raised serious concerns among athletes, coaches, and physicians in the last two decades as the population participating sports and exercises are growing. ACL injuries are common in sports and exercises with devastating consequences that significantly influence athletes' performance and quality of life, and result in secondary injuries and disorders, such as knee joint instability, knee pain, damage to menisci and chondral surfaces, and knee osteoarthritis (Finsterbush et al., 1990; Irvine and Glasgow, 1992). Griffin et al. (2000), Huston et al. (2000), and Arendt (2002) reported that nearly 80,000 ACL tears occur every year in United States. Gottlab et al. (1999), however, estimated that approximately 175,000 primary ACL reconstruction surgeries were performed annually in the United States at an estimated cost of over \$2 billions. Individuals between 15 to 25 years of age who

participated in sports in which they frequently performed pivoting maneuvers had the highest incidence of ACL injury (Griffin et al., 2000).

Female athletes have significantly greater incidence rate of ACL injuries than male athletes do. Henry and Kaeding (2001) reported that female athletes had 4 to 6 times incidence rate of contact ACL injuries when compared with their male counterparts. Huston et al. (2000) reviewed literature and reported that the incidence rate of ACL injuries of female athletes who participated in the sports in which landing and pivoting tasks were frequently performed was 2 to 8 times higher than that of the male counterparts.

The majority of ACL injuries occur with a non-contact mechanism in sports in which sudden deceleration, landing, and pivoting maneuvers are repeatedly performed (Boden et al., 2000; Feagin and Lambert, 1985; Ferretti et al, 1992; Griffin et al., 2000; McNair et al., 1990). ACL injuries that occur without physical contact between athletes at the time of injury are referred to as non-contact ACL injuries (Boden et al., 2000; Ferretti et al., 1992; McNair et al., 1990). McNair et al. (1990) and Boden et al., (2000) reported that 70% to 72% of ACL injuries occurred with non-contact mechanisms. Ferretti et al. (1992) showed that landing from a jump in the attack zone without direct contact was the most frequent injury mechanism in volleyball players.

The non-contact nature of the majority of ACL injuries indicates that the majority of ACL injuries may be preventable (Griffin et al., 2000). Like preventing other injuries or diseases, a good understanding of risk factors based on a good understanding of injury mechanisms is crucial for preventing non-contact ACL injuries.

2.2. ACL Injury Mechanisms

2.2.1. ACL Loading Mechanisms

An ACL injury occurs when an excessive tensile force is applied on the ACL. A non-contact ACL injury occurs when a person generates great forces or moments at the knee that applied excessive loading on the ACL. Research has demonstrated three ACL loading mechanisms: (1) knee anterior shear force loading, (2) knee varus-valgus loading, and (3) knee internal-external rotation loading. An understanding of these ACL loading mechanisms would set the basis for understanding non-contact ACL injury mechanisms and further research to identify the risk factors of sustaining non-contact ACL injuries.

Berns et al. (1992) studied the *in vitro* strain of the anteromedial bundle of the ACL on 13 cadaver knees subject to pure load of anterior-posterior force, varus-valgus moment, and internal-external rotation torque and combined loads. The pure load was applied when the knee flexion angle were fixed at 0°, 15°, and 30° knee flexion while the combined load were loaded in pairs at 0° and 30° knee flexion. The corresponding range of the pure anterior-posterior force, varus-valgus moment, and internal-external rotation torque were 150-200 N, 25-30 Nm, and 6-10 Nm. They found that the anterior shear force on the proximal tibia was the primary determinant of the ACL strain. Neither pure axial torque nor pure varus-valgus moment was observed to strain the anteromedial bundle of the ACL at any of the knee flexion angles. The results of this study further showed the ACL strain subject to combination of the anterior shear force and valgus torque was significantly larger than that of pure anterior shear force.

Markolf et al. (1995) investigated effects of anterior shear force at the proximal end of the tibia and knee valgus, varus, internal rotation, and external rotation moments on the ACL

loading of the cadaver knees. A 100 N anterior shear force and 10 Nm knee valgus, varus, internal rotation, and external rotation moments were applied to cadaver knees. The ACL loading was recorded as the knee was extended from 90 degrees of flexion to 5 degrees hyperextension. The results of this study showed that an anterior shear force on the proximal tibia generated significant ACL loading, while the knee valgus, varus, and internal rotation moments also generated significant ACL loading only when the ACL was loaded by the anterior shear force at the proximal end of the tibia. The results of this study further showed that the ACL loading due to the anterior shear force combined with either valgus or varus moment to the knee was greater than that due to the anterior shear force alone, while that ACL loading due to the anterior shear force combined with knee external rotation moment was lower than that due to anterior shear force alone. Furthermore, the results of this study showed that the ACL loading due to the combined knee varus and internal rotation moment loading was greater than that due to either knee varus moment loading or internal rotation moment loading alone, and that the ACL loading due to the combined knee valgus and external rotation moment loading was lower than that due to either knee valgus or external rotation moment loading alone. Finally, the results of this study showed that the ACL loading due to the anterior shear force and knee valgus, varus, and internal rotation moments increased as the knee flexion angle decreased. The results of this study combined suggest that proximal tibial anterior shear loading is a major ACL loading mechanism, and that non-sagittal plane knee moment loading have significant effects on the ACL loading only when the sagittal plane knee loadings are presented. These results are consistent with those reported by Berns et al. (1992).

Fleming et al. (2001) studied the effects of weight bearing and external tibial loading on *in vivo* ACL strain, and obtained results similar to those of Markolf et al. (1995). They

implanted a differential variable reluctance transducer to the anterior medial bundle of the ACL of 11 subjects. *In vivo* ACL strains were measured when a subject's leg was attached to a knee loading fixture that allowed independent application of anterior-posterior shear force, valgus-varus moment, and internal-external rotation moment to the tibia and to simulate the weight bearing condition. The anterior shear force was applied on the proximal end of the tibia from 0 N to 130 N in 10 N increments. The valgus-varus moment was applied to the knee from -10 Nm to 10 Nm in 1 Nm increment. The internal-external rotation moments was applied to the knee from -9 Nm to 9 Nm in 1 Nm increment. The knee was fixed at 20 degrees flexion angle during the test. The results of this study showed the ACL strain significantly increased as the anterior shear force at the proximal end of the tibia and the knee internal rotation moment increased while knee valgus-varus and external rotation moments had little effect on the ACL strain under the weight bearing condition.

The studies by Berns et al. (1992), Markolf et al. (1995), and Fleming et al. (2001) combined demonstrate that the anterior shear force on the proximal tibia is the primary ACL loading mechanism. These studies also demonstrate that the varus-valgus moments and internal rotation moment also contribute to ACL loading when combined with the proximal tibial anterior shear force loading. The study by Markolf et al. (1995) suggests that an external rotation moment on the tibia may unload the ACL when combined with the anterior shear force loading at the proximal tibia. Based on the ACL loading mechanisms revealed in these studies, strong quadriceps muscle contraction, small knee flexion angle, and large posterior ground reaction force are likely the major ACL injury mechanisms.

2.2.2. Effects of the Quadriceps Muscle Force on the ACL loading

Increasing the quadriceps muscle contraction increases the ACL loading by increasing the proximal tibial anterior shear force. Studies have shown that an isolated quadriceps contraction acting through patellar tendon results in a large anterior tibial translation and ACL strain, especially at a small knee flexion angle (Arms et al., 1984; Beynnon et al., 1995; DeMorat et al., 2004; Draganich and Vahey, 1990; Dürselen et al., 1995). Arms et al. (1984) investigated the ACL strain in normal and reconstructed ACL during active and passive knee flexion and simulated isometric and eccentric quadriceps force. The knee flexion angle was moved from 0° to 120° at 15° interval. They implanted the Hall effect transducer to the anteromedial fiber of the ACL. They found that the quadriceps activity did not significantly strain the ACL when the knee flexion angle was above 60°, but significantly strained the ACL from 0° to 45°. Effects of quadriceps on the ACL strain by Arm et al. (1984) were in conformity with the data from Beynnon et al. (1995), in which the quadriceps activity significantly strained the ACL from 0° to 45° of knee flexion, but did not strain the ACL when the knee was flexed over 60°.

Draganich and Vahey (1990) studied the *in vitro* strain of anteromedial bundle of the ACL during the application of isolated isometric quadriceps force and isometric co-contraction of quadriceps and hamstring forces from 0° to 90° knee flexion at 10° increments. Their results showed that quadriceps force induced significant ACL strain when the knee flexion angle was between 0° and 40°, but no significant ACL strain was seen when the knee flexion angle was between 50° to 90°.

Dürselen et al. (1995) investigated the effects of quadriceps, hamstring, and gastrocnemius forces and external loads on the cruciate ligament strains from 0° to 110° of

knee flexion. A Ω -transducer was attached to the anteromedial bundle of the ACL to record the change of the ACL strain subjected to isolated or combined loadings. The applied loadings included 140 N of quadriceps force, 25 N of hamstring force, and 40 N to 55 N of gastrocnemius force, 1 Nm of tibial rotation moment, and 5 Nm of varus-valgus moment. Their results demonstrated that an isolated quadriceps loading resulted in a large ACL strain when knee flexion angle was between 0° to 30° and a decreasing trend of ACL strain when the knee flexion angle was between 30° and 70° .

DeMorat et al. (2004) studied the effects of the aggressive quadriceps muscle force on the anterior laxity of the knee and evaluated how the knee kinematics associated with aggressive quadriceps muscle force simulating a non-contact ACL injury. Thirteen cadaver knees were fixed at 20° knee flexion angle with the quadriceps loading simulated with a ramp loading at a peak load of 4500 N at a rate of 4500 N/s. Anterior tibial displacement was measured with a KT-1000 arthrometer before and after 4,500 N quadriceps muscle force loading. Six out of the 11 specimens had confirmed ACL injuries. All specimens showed increased tibial anterior translation in KT-1000 tests. The result of this study also showed that quadriceps muscle contraction could cause tibial anterior translation and tibial internal rotation.

During the stop-jump and cutting movements, the quadriceps muscle contracts eccentrically at the instant of foot contact. The developed eccentric force through the patellar tendon acting on the tibia could be large enough to injure the ACL at a small knee flexion angle.

Quadriceps muscles apply an anterior shear force on the proximal end of the tibia through patellar tendon. Several investigations have proposed that the patellar tendon force

may not be equal to the quadriceps muscle force. Huberti et al. (1984) and Buff et al. (1988) have shown that the patellar tendon force to quadriceps force ratio changed with knee flexion angles. Both studies found that the patellar tendon force to quadriceps force ratio was greater than unity at knee flexion angle below 30°. These two studies provided information that patellofemoral joint was not a simple pulley system, but instead, a balance beam. Based on their results, the ACL loading can be underestimated if the patellar tendon force is considered equal to the quadriceps muscle force at a small knee flexion angle.

Overall, large quadriceps muscle force could contribute to ACL loading by increasing the patellar tendon force and proximal tibial anterior shear force at small knee flexion angle. A large quadriceps force at a small knee flexion angle, therefore, can be an important contributor to ACL loading.

2.2.3. Effects of the Knee Flexion Angle on the ACL Loading

Decreasing the knee flexion angle increases the ACL loading by increasing the patellar tendon-tibial shaft angle and the proximal tibial anterior shear force. Nunley et al. (2003) collected sagittal plane x-ray films for 10 male and 10 female college students at 0, 15, 30, 45, 60, 75, and 90 degree knee flexions with even weight bearing on each foot. Regression analyses were performed to determine the relationship between the patellar tendon-tibial shaft angle and the knee flexion angle, and compare the relationship between genders. They found that the patellar tendon-tibial shaft angle was inversely related to the knee flexion angle. The more extended knee, therefore, increased the patellar tendon-tibial shaft angle, which would increase the proximal tibial anterior shear force. The increased proximal tibial anterior shear force would increase the ACL loading and ACL strain based on the ACL loading mechanism.

The results of Nunley et al. (2003) also demonstrated that their female subjects had a mean patellar tendon-tibial shaft angle 3.7° greater than that of their male subjects, which suggest that females on average had an anterior shear force 13.2% greater than that of males with the same patellar tendon force at the same knee flexion angle. Pflum et al. (2004) also suggested that a large patellar tendon-tibial shaft angle immediately after initial contact could result in a large horizontal component of patellar tendon force and the ACL loading. These results provide a biomechanical explanation for the increased ACL loading with decreased knee flexion angle reported by Markolf et al. (1995).

Decreasing the knee flexion angle increases the ACL loading as well by increasing the ACL elevation angle. Herzog and Read (1993) and Li et al. (2005) expressed the ACL kinematics as a function of the knee flexion angle. Herzog and Read (1993) determined the line of action of the ACL as a function of the knee flexion angle. The line of action of the ACL was determined using the most anterior attachment point on the tibia and femur. Results of Herzog and Read (1993) showed that the line of action of the ACL changed with the knee flexion angle. An increase of knee flexion angle results in a more horizontal line of action of the ACL and decreases the ACL elevation angle. Li et al. (2005) determined the *in vivo* ACL elevation angle as a function of the knee flexion angle with weight bearing of five young and healthy volunteers. The ACL elevation angle at 30° , 60° , and 90° knee flexion with weight bearing were obtained using individualized dual-orthogonal fluoroscopic images and MR image-based three-dimensional models. The ACL elevation angle was defined as the angle between longitudinal axis of the ACL and the tibial plateau. Results of this study showed that ACL elevation angle increased as the knee flexion angle decreased. Both studies (Herzog and Read, 1993; Li et al., 2005) showed the important relationship between the ACL kinematics

and knee flexion angle and again provided the biomechanical explanation for Markolf et al. (1995).

2.2.4. Effects of the Ground Reaction Forces on the ACL Loading

Large ground reaction forces during the landing phase of athletic tasks can affect ACL loading by increasing the quadriceps muscle contraction. Increased posterior ground reaction force applied to the foot during the landing task can result in a large external knee flexion moment and cause the knee to flex. The increased external knee flexion moment needs to be balanced by the internal knee extension moment to avoid knee buckling. The quadriceps muscle force is the major contributor to the internal knee extension moment. As mentioned previously, a large quadriceps force results in a large patellar tendon force and therefore increases the anterior shear force on the proximal tibia to increase the ACL loading at a small knee flexion angle. A vertical ground reaction force also affects the knee extension moment. The effect of vertical ground reaction force on the knee extension moment, however, depends on the landing style. Landing on the heels and landing with less posterior-tilted tibial angle exaggerate the external knee flexion moment and require large quadriceps muscle force to balance this exaggerated external knee flexion moment. The increased quadriceps force due to ground reaction forces can possibly threaten the ACL.

Cerulli et al. (2003) and Lamontagne et al. (2005) recently demonstrated the importance of ground reaction forces in association with maximal strain of the ACL during the hop landing. Cerulli et al. (2003) recorded the anteromedial bundle of the ACL strain by a differential variable reluctance transducer of one subject during a single leg forward hop while Lamontagne et al. (2005) documented ACL strain of three subjects with the same protocols as

Cerulli et al. (2003). Force plate, EMG, and *in vivo* ACL strain were recorded simultaneously. Both studies showed the maximal ACL strain occurred almost at the same time as occurrence of peak vertical ground reaction force. Large ACL strain was maintained throughout the landing phase with small knee flexion angle. Simonsen et al. (2000) demonstrated the first peak of knee extension moment after initial contact was in conjunction with the onset of peak posterior ground reaction force during a side-cutting. A computer simulation with a 3-D model to calculate the ACL loading of ACL-deficient knee and ACL-intact knee during walking showed peak ACL loading, peak anterior shear force, peak patellar tendon force, and peak quadriceps force were concurrent (Shelburne et al., 2004a, b). A recent study by Yu et al. (2006b) demonstrated that peak posterior ground reaction force and peak knee extension moment occurred essentially at the same time as peak vertical ground reaction force occurred during the stop-jump task.

The tibial anterior shear force, another possible contributor to non-contact ACL injuries, may be associated with ground reaction forces. The tibial anterior shear force was determined from the inverse dynamics and the free body diagram by consideration of the horizontal and vertical ground reaction forces in a 2D sagittal plane lower extremity model. McNair and Marshall (1994) found a significant positive correlation between vertical ground reaction force and the tibial anterior acceleration during a hop-landing task for all subjects, including normal and ACL-deficient subjects. This result indicated that a significant correlation between vertical ground reaction force and proximal tibial anterior shear force might exist because the force on a segment is the product of segment mass and segment acceleration. They concluded that results of this study also demonstrated that the ground reaction forces may be important parameters affecting the tibial anterior shear force. This

result is consistent with a study by Yu et al. (2006b), in which the peak proximal tibial anterior shear force was significantly correlated with peak vertical and posterior ground reaction force during landing of the stop-jump task.

In summary of the studies on the ACL loading and lower extremity kinetics, the peak ACL strain occurs at the peak vertical ground reaction force while peak posterior ground reaction force and peak knee extension moment occur essentially at the same time as the vertical ground reaction force occurs. The peak ground reaction forces, peak anterior shear force, and peak knee extension moment are significantly correlated to each other. These results demonstrated an association of the ACL loading with peak posterior ground reaction force, peak quadriceps force, peak proximal tibial anterior shear force, and peak knee extension moment.

2.2.5. Effects of the Hamstring Co-contraction on the ACL Loading

The effect of the hamstring muscle co-contraction on the ACL has been investigated *in vivo* (Beynnon et al., 1995; Kingma et al., 2004), *in vitro* (Draganich and Vahey, 1990; Dürselen et al., 1995; Li et al., 1999; MacWilliams et al., 1999), or by computer modeling (O'Connor, 1993; Shelburne and Pandey, 1997; Yu and Garrett, 2005). Beynnon et al. (1995) investigated the *in vivo* ACL strain during selected rehabilitation exercise by implantation of the Hall effect transducer into normal ACL. The ACL strain was recorded from 15° to 90° at 15° interval in a relax and an approximately 80% of maximum effort conditions. They found that the isolated isometric hamstring contraction did not significantly reduce the ACL strain among the knee flexion angles tested. The simultaneous contraction of the quadriceps and hamstring muscles, however, produced significant ACL strain value relative to the relax

condition at 15° knee flexion, but no significant increases were observed in rest of knee flexion angles. The co-contraction of quadriceps and hamstring muscles produced significantly greater ACL strains at 15° and 30° of knee flexion than those at 60° and 90° of knee flexion. This study showed that the effect of the hamstring on the ACL strain is knee flexion angle dependent.

Kingma et al. (2004) studied the knee flexor and extensor electromyography during a quasi-isometric task for a range of 5° to 50° in a 5° interval with the external flexion moments of 20, 50, and 80 Nm. Their results showed that the hamstring activation increased only from 1.3 to 2.0 times the activation at the lowest extension moment level while knee extension moment increased from 2.7 to 3.4 times the lowest level of extension moment. They concluded that the hamstring muscle activation did not increase proportionally with the anterior shear force induced by the quadriceps muscle and the hamstring activation may not be protective for the ACL during isometric extension efforts. The increase in co-contraction of hamstrings between the ranges of 20 to 50 degrees irrespective of the effect of moment levels, however, could support that the hamstring muscle is protective for the ACL.

O'Connor (1993) used a computer-based sagittal knee model to study the cruciate ligament forces induced by the co-contraction of knee flexor and extensor muscles. They modeled the tibial plateau as a flat line and the lines of action of the muscle, the moment arms, ligament forces, and contact forces were expressed as functions of knee flexion angle. The result of O'Connor (1993) showed that the hamstring muscle force could produce effective posterior-directed force as long as the knee flexion angle was greater than 22°. O'Connor (1993) pointed out that anterior component of the patellar tendon force was greater than the posterior pull force of hamstring muscle when the knee flexion angle was smaller than 22° and

that was the reason the hamstring force was not protective at small knee flexion angle. Simulated results further showed that the co-contraction of the quadriceps, hamstring, and gastrocnemius muscles could unload the ACL when the knee flexion angle was greater than 22°. Shelburne and Pandy (1997) used a sagittal plane knee model to simulate the ligament force in three tasks: quadriceps leg raise, maximum isometric knee extension, and maximum isometric knee flexion. They found that the ACL forces were much lower for maximum isometric flexion than for extension. They also reported that isolated hamstring force could not unload the ACL when the knee flexion angle was below 10°. Yu and Garrett (2005) also investigated the effects of hamstring contraction by computer simulation with a sagittal plane knee model. They considered relevant knee geometries as functions of knee flexion angle in their sagittal plane knee model and had empirical data of 60 subjects as inputs. They found that the ACL loading increased as the hamstring co-contraction increased at knee flexion angle smaller than 15° for males and 20° for females. All these three studies (O'Connor, 1993; Shelburne and Pandy, 1997; Yu and Garrett, 2005) investigated the ACL loading by using computer model and computer simulation and all showed that the hamstring muscle could not reduce the ACL loading at small knee flexion angle.

Draganich and Vahey (1990) found that ACL strain induced by the simultaneous application of isometric quadriceps and hamstring forces did not significantly differ from zero at any of the knee flexion angles tested. The simultaneous application of isometric quadriceps and hamstring forces, however, significantly reduced the ACL strain at 10°, 20°, and 90° when compared to the ACL strain induced by the isolated quadriceps force. Dürselen et al. (1995) found isolated hamstring force caused lower ACL strain than that of passive motion between 70° to 110° knee flexion, but the difference was not statistically significant. Result of the effect

of hamstring muscle on the ACL strain by Dürselen et al. (1995) was unable to be compared with other studies because the hamstring muscle was assumed not active at knee flexion angle below 70 degree.

A study by Li et al. (1999) also investigated the effects of the quadriceps and hamstring muscle loadings on the tibial kinematics and ACL loading in 10 cadaver knees. Their results showed that the *in situ* ACL loading at 15° was significantly higher than that at other knee flexion angles when subjected to either isolated quadriceps force or combined quadriceps and hamstring forces. They also reported that addition of hamstring force significantly reduced the *in situ* ACL loading at 15°, 30°, and 60° and the tibial anterior and lateral translation and tibial internal rotation when the knee flexion angle is greater than 30° when compared to isolated quadriceps contraction. The *in situ* ACL loading increased as knee flexion angle decreased when the quadriceps muscle was loaded regardless of the hamstring muscle loading conditions. Some other studies also demonstrated that significant reduction in tibial internal rotation, anterior displacement, and anterior shear force when the hamstring load was added to the isolated quadriceps activation during knee flexion (MacWilliams et al., 1999; More et al., 1993; Yanagawa et al., 2002).

McNair and Marshall (1994) showed that higher activation of lateral hamstring muscle had lower vertical ground reaction force during the landing task and lower vertical ground reaction force had lower anterior tibial acceleration. Their results indicate that the activation of hamstring muscle reduces anterior tibial translation.

Simonsen et al. (2000), however, found that low activation of hamstring EMG and rapid contraction of hamstring muscle may not produce sufficient force to protect the ACL during the side-cutting maneuver. The ACL force estimated by their 2D sagittal knee model

was an average of 520 ± 68 N. They claimed that such a force was unlikely to injure the ACL compared to the 2000 N ultimate strength of the ACL (Woo et al., 1991). This underestimated ACL loading maybe due to the assumption in their 2D model, in which the ACL loading was assumed to equal proximal tibial shear force. Lack of consideration of the ACL elevation angle in their 2-D model may underestimate the ACL force.

2.2.6. Effects of the Gastrocnemius Muscle Force on the ACL loading

The contribution of gastrocnemius muscle to the ACL loading is inconsistent in current literature. Some studies hypothesized that its contraction could pull tibia anteriorly, load the ACL, and increase the ACL strain because of its geometrical orientation (Fleming et al., 2001; O'Connor, 1993; Pflum et al., 2004). Fleming et al. (2001) studied *in vivo* ACL strain of 6 subjects with implantation of differential variable reluctant transducer in the anteromedial bundle of the ACL. A four-channel transcutaneous electrical muscle stimulation (TEMS) was used to generate isometric contraction of quadriceps, hamstring, and gastrocnemius muscles. They found the ACL strain produced by TEMS was dependent of the knee flexion angle and ankle torque. An increase of ankle torque corresponds to the increase of ACL strain. They found that the isolated gastrocnemius stimulation that produced 15 Nm ankle torque could result in significantly greater ACL strain at 5° and 15° knee flexion than the same torque level at 30° and 45° of knee flexion angle. They also observed that the co-contraction of the quadriceps and gastrocnemius muscles significantly increased the ACL strain compared to the contraction of the quadriceps muscle alone. The hamstring and gastrocnemius muscles co-contractions resulted in a significantly greater ACL strain than the contraction of the hamstring muscle alone. These results demonstrated that gastrocnemius muscle activation

could increase the ACL strain, especially when the knee was near extension. O'Connor (1993) showed the identical results that co-contraction of quadriceps and gastrocnemius muscles loaded the ACL throughout the knee flexion angles. Pflum et al. (2004) used a 3-D model of body to simulate a drop-landing task. The input of muscle excitations were adjusted until the performance of the model matched the *in vivo* data. They reported that the gastrocnemius muscle applied an anteriorly directed force on the tibia, but may have limited effects on the ACL loading because the gastrocnemius muscle applied a relatively small anterior shear force to the lower leg.

Several other studies, however, showed opposite effects of the gastrocnemius muscle on the ACL loading (Dürselen et al., 1995; Shelburne and Pandy, 1997). A computer modeling showed that isolated gastrocnemius muscle force could reduce the ACL loading at the knee flexions angle from 0° to 90° (Shelburne and Pandy, 1997). Although Dürselen et al. (1995) found that the gastrocnemius muscle force had no significant effect on the ACL strain when compared to the strain at 60° knee flexion without muscle force, the activation of the gastrocnemius muscle could significantly strain the posterior cruciate ligament. Based on their results, this posterior pull of the tibia due to the contraction of gastrocnemius muscle may reduce the ACL loading. The controversial findings of the effects of the gastrocnemius muscle contraction on the ACL loading highlight the need of more research on this topic.

2.2.7. Effects of the Knee Valgus-varus and Internal-external Rotation Moment on the ACL Loading

Several studies suggest that knee valgus-varus and internal-external rotation moments are major ACL loading mechanisms. McLean et al. (2003, 2004) studied the variation of ACL loading during a side-cutting task by using a stochastic model with forward dynamics. Their

simulation results showed that on average the sagittal plane biomechanics contributed about 1,000 N. The authors, however, claimed that the sagittal plane biomechanics cannot injure the ACL based on their simulation results, and concluded that the knee valgus moment loading was the major ACL loading mechanism. This conclusion was apparently subjective without careful considerations of the limitations and validity of their model and methods. Their results showed that sagittal plane biomechanics on average could generate 1,000 N ACL loading. Compared to the 2,160 N ACL ultimate strength (Woo et al., 1991), the reported ACL loading from sagittal plane biomechanics was about 46% of ACL injury loading and should have been considered as a significant contribution to ACL loading. The authors ignored this result and subjectively claimed that sagittal plane biomechanics could not injure the ACL. Further, the ACL loading in this study was significantly underestimated. The ACL loading in this study was approximated as the knee shear force balanced by the ACL without consideration of the ACL elevation angle. With a 55 degree ACL elevation angle and 1,000 N knee shear force balanced by the ACL, the axial force on the ACL would be over 1,700 N or 79% of the ACL ultimate strength. In addition, the validity of the forward dynamic model in this study was questionable. The results of simulation showed a posterior knee resultant shear force greater than 1,000 N while the horizontal ground reaction force was also in the posterior direction, which was inconsistent to *in vivo* results of other studies. The mass of the lower leg plus the foot segment is less than 5 kg. This means that the posterior knee resultant shear force observed in this study alone could generate a lower leg posterior linear acceleration greater than 22 g, which appeared to be far away from reality.

Chaudhari and Andriachii (2006) also used modeling approach to study the effects of knee valgus-varus moment loading on the ACL loading. Their results showed that the

importance of lower limb alignment on the ACL injury threshold which was defined as the maximal sustainable axial force that the limb could tolerate before the knee joint opened medially or laterally more than 8°. A three-link frontal plane model was used to investigate the consequences of dynamic alignment and muscle contraction on the ACL injury threshold. The results indicated that valgus or varus alignment reduced the injury threshold, but contraction of hip abductors and adductors increased the injury threshold. Chaudhari and Andriachii (2006) claimed that a publication by Woo et al. (1999) showed that the ACL became tensed before the MCL was tensed when the knee is subject to a knee valgus moment loading. A careful review of the publication by Woo et al. (1999) and the original study by Inoue et al. (1987) failed to show any direct and indirect evidence to support Chaudhari and Andriachii's claim.

The results of the two above described studies of McLean et al. (2004) and Chaudhari and Andriachii (2006) were not supported by other studies. As mentioned previously, Markolf et al. (1995) investigated effects of anterior shear force at the proximal end of the tibia and knee valgus, varus, internal rotation, and external rotation moments on the ACL loading of the cadaver knees. The results of this study not only demonstrated that the proximal tibial anterior shear loading as a major ACL loading mechanism, but also showed that each of the knee valgus, varus, and internal rotation moments alone could not generate significant ACL loading unless combined with proximal tibia anterior shear loading. Fleming et al. (2001) studied the effects of weight bearing and tibial external loading on *in vivo* ACL strain and obtained results similar to those of Markolf et al. (1995).

Arms et al. (1984), as mentioned previously, investigated the ACL strain in normal and reconstructed ACL during active and passive knee flexion, with and without knee varus-valgus torque (15 Nm) and internal-external rotation torque (13.6 Nm). They found that the normal

pattern of ACL strain showed a minimum strain between 30 and 35° of knee flexion. The passive varus moment increased ACL strain throughout the range of knee flexion angle tested. The passive internal rotation torque markedly increased the strain when compared to the passive normal strain curve. The passive external rotation torque resulted in less strain during the first few degrees of flexion. They also found that the ACL strain measured at combined eccentric quadriceps force and varus moment or combined eccentric quadriceps force and valgus moment had greater strain than the eccentric quadriceps force alone when the knee flexion angle was at around 30°. They concluded that the varus and internal rotation moments increased the ACL strain and the ACL strain was significantly different depending on active or passive flexion of the knee. The results of Arms et al. (1984), to certain extent, agree with the results of Markolf et al. (1995) in which the varus moment and internal rotation torque can increase the ACL loading.

Bendjaballah et al. (1997) studied knee ligaments loading responses to knee valgus-varus moment of up to 15 Nm using a finite element model of the knee joint. The loading was applied to the femur while the tibia was remained fixed. Their results demonstrated that the collateral ligaments were the primary knee valgus-varus load bearing structures, and cruciate ligaments were the primary knee valgus-varus load bearing structures only when collateral ligaments were injured. The simulated ACL loading due to a 15 Nm knee valgus moment loading in this study was similar to that obtained in the study by Markolf et al. (1995).

The result of Bendjaballah et al. (1997) is supported by a study by Mazzocca et al. (2003) as well. Mazzocca et al. (2003) examined the effects of the applied valgus loading on the ACL damage and rupture of the MCL. Six unpaired cadaver knees were separated into

experimental and control group. The cadaver knees in the experimental group were held at 30 degrees of flexion while under a 200 N valgus force applied a displacement rate of 2 mm/second. Control specimens were not subjected to valgus loading. These six unpaired femur-ACL-tibia specimens were then aligned vertically with a tensile preload of 10 N applied. The ACL was loaded to failure at a displacement rate of 2 mm/second. A differential variable reluctance transducer was implanted into ACL to measure the ACL strain. The study by Mazzocca et al. (2003) showed that minimal ACL strain occurred during valgus loading before MCL rupture, but the ACL strain increased substantially after MCL rupture in the cadaver study. Their results showed that ACL still have about 60% of its original strength after complete MCL ruptures due to knee valgus loading. The results of this study also demonstrated that the ACL is the major constraint to valgus loading only when the MCL is ruptured. The findings of Bendjaballah et al. (1997) and Mazzocca et al. (2003) together demonstrate that it is unlikely that the cruciate ligaments were tensed before the collateral ligaments were tensed.

Dürselen et al. (1995) also studied the effects external loads on cruciate ligament strain from 0° to 110° of knee flexion. The applied external loadings were 1 Nm of tibial rotation moment, and 5 Nm of varus-valgus moment. They found that the strain of the anteromedial bundle of the ACL induced by the combined external valgus and external rotation moment was smaller than the combined external varus and internal rotation moment throughout the knee flexion angle tested. The results of Dürselen et al. (1995) were consistent with Markolf et al. (1995) in which they also found that the ACL strain was greater in the combined varus moment and internal rotation moment than that of combined valgus moment and external rotation moment.

Based on this extensive review of literature of the effects of non-sagittal plane loading on the ACL loading and ACL strain, we need to be careful when interpreting the non-sagittal plane loading alone as the major ACL loading mechanism. Although the role of knee valgus-varus and internal-external rotation moments in non-contact ACL injuries may be still open to debate and need further research, current literature does not support these non-sagittal plane knee moments as major ACL loading mechanisms.

2.3. Potential Risk Factors

As an attempt to prevent non-contact ACL injuries, many investigations have been conducted to identify risk factors of sustaining non-contact ACL injuries. A variety of potential risk factors of sustaining non-contact ACL injuries have been proposed in literature. These potential risk factors have been categorized into two groups: intrinsic and extrinsic (Arendt and Dick, 1995; Boden et al., 2000). Intrinsic risk factors include anatomic, physiologic, and motor control related risk factors, such as static musculoskeletal alignment (e.g. quadriceps angle), the knee joint laxity, the hormonal effect, size of the ACL, and the altered lower extremity motion patterns. Motor control related risk factors such as altered lower extremity motion patterns and muscle co-activation, particularly co-contractions of the quadriceps, hamstring, and gastrocnemius muscles are considered as modifiable while anatomic and physiological factors are considered as non-modifiable intrinsic risk factors. Extrinsic risk factors include shoe-surface interaction (Garrick and Requa, 1996) and playing surface (Powell and Schootman, 1992). Intrinsic motor control related biomechanical risk factors were the focus of this chapter and discussed in great detail because they are modifiable through training programs and would be the focus of future prevention programs.

2.3.1. Non-modifiable Intrinsic Risk Factors

A number of investigations have demonstrated the association between intrinsic risk factors and non-contact ACL injuries. Anderson et al. (2001) and Chandrashekar et al. (2005) showed that females had smaller ACL size in comparison to that of males. Several other investigators have reported that females had wider pelvis, greater Q-angle and knee joint laxity than did males, which might contribute to the gender differences in the non-contact ACL injury rate (Hewett, 2000; Wojtys et al., 1998). Wojtys et al. (1998) and Hewett (2000) both observed that female athletes had increased ligament laxity and altered neuromuscular performance during menstruation. Arendt et al. (2002) studied the association of ACL injuries in female athletes with menstrual cycles, and found that most of the ACL injuries occurred mainly in follicular and luteal phases. These results suggest that hormonal effect might play a role in the ACL injuries.

A recent extensive literature review, however, failed to reveal any epidemiological studies that established the cause-and-effect relationships between the non-modifiable intrinsic risk factors and the non-contact ACL injuries. Risk factors other than the non-modifiable intrinsic risk factors, therefore, need to be considered and investigated.

2.3.2. Motor Control Related Biomechanical Risk Factors

Malinzak et al. (2001) compared the knee joint motion patterns and lower extremity electromyography between male and female recreational athletes in running, side-cutting, and cross-cutting activities. They found that female athletes tended to have less knee flexion angle, more knee valgus angle, larger quadriceps muscle activation and lower hamstring muscles

activation than did male athletes during the stance phase of each activity. Chappell et al. (2002) investigated the knee kinetics and kinematics of male and female recreational athletes during the stop-jump task. They found women exhibited larger proximal tibial anterior shear force, knee extension moment, and valgus moment, and smaller knee flexion angle at the peak proximal tibial anterior shear force during the landing phase of the stop-jump task than men did. Lephart et al. (2002) evaluated kinematics and vertical ground reaction force in single leg forward hop and drop landing tasks, and strength measures of healthy collegiate female basketball, volleyball, and soccer players and the height, age, and activity level matched male athletes. Subjects were asked to perform a single-leg forward hop and a single-leg drop landing from 20 cm platform with their dominant leg. Results of this study showed that female athletes had less knee flexion angle and lower leg internal rotation angle in both tasks compared to matched male athletes. Female athletes also exhibited less normalized peak isokinetic knee flexion and extension torque. The results, however, did not show significant gender difference in vertical ground reaction force in two tasks. Decker et al. (2003) studied lower extremity kinematics and kinetics of 12 male and 9 female athletes during the landing after a 60 cm drop. Participants were recreational athletes who played sports of volleyball and basketball. During the task of stepping off a 60 cm box, they were instructed to fold their arms across their chest and step off the box without jumping up. The results of their study showed that female athletes landed with a more erect posture than males. The investigators, however, did not find significant gender differences in the ground reaction force during the landing. James et al. (2004) examined the kinematics and ground reaction force differences between genders in a cutting maneuver. A total of 38 high school and collegiate basketball players participated in this study with doing a 60° cutting angle of side-cut. The results showed that

female athletes exhibited a smaller knee flexion angle at initial contact, smaller maximal knee flexion angle, and larger ground reaction forces at the maximal knee flexion than male athletes did during the stance phase of the cutting maneuver.

Ford et al. (2003) studied knee valgus motion of 81 high school basketball players. Subjects were asked to perform a drop vertical jump off a 31 cm height box. The drop vertical jump task consisted of dropping off a box, landing and immediately performing a maximum vertical jump. Only the first landing phase off the box was analyzed. Their results showed that female subjects had greater valgus angle through the stance phase of the drop-jump and the significantly greater maximal valgus angle than male counterparts. No significant differences in knee flexion angle at initial contact and at peak were observed in this study. Kernozek et al. (2005) investigated the gender differences in the lower extremity kinematics and kinetics for age-matched and skill-matched college recreational athletes during the drop-jump task. Their results showed female subjects had greater valgus angle through stance phase of the drop-jump and significantly larger maximal valgus angle than male counterparts, which were partly consistent with Ford et al. (2003). Both studies showed no significant differences in knee flexion angle at initial contact and at peak. Kernozek et al. (2005), however, found male subjects had significantly lower ground reaction forces than did females.

These studies combined found female athletes on average had smaller knee flexion angle, greater knee valgus angle, greater ground reaction forces, greater proximal tibial anterior shear force, and greater knee extension moment during the landing phase of selected athletic tasks when compared to their male counterparts. These altered lower extremity motion patterns in females may link to why females have higher injury rate of non-contact ACL injuries than males.

A small hip flexion angle during landing triggers a large knee extension torque to accelerate the tibia anteriorly to injure the ACL (Griffin et al., 2000), especially when it is seen simultaneously with the large transferred ground reaction forces at a small knee flexion angle. The more extended hip position maximizes the quadriceps demand and minimizes the countering effect of the hamstrings forces on the proximal tibial anterior shear force. A study revealed the knee isometric Hamstrings/Quadriceps ratio was significantly increased from 38% to 99% when the hip angle was increased from 10° to 90° for the 10° to 90° knee conditions (Ball et al., 1999). The authors concluded that the flexed hip and knee postures can be implied to facilitate the ACL-protective hamstring tension.

Landing on the heels requires large quadriceps demand as well to bring the trunk forward (Griffin et al., 2000) and to balance the exaggerated external knee flexion moment. This exerted large quadriceps force transferred to the patellar tendon can contribute to a large proximal tibial anterior shear force to likely injure the ACL, especially at a small knee flexion angle. It has been shown that the more anteriorly placed center of pressure predicted greater plantar flexion moment and less knee extensor moment. Landing on the toes, therefore, may be a protective landing style of the non-contact ACL injuries while landing on the heels may possibly increase the ACL loading.

Increased ankle eversion contributes to great foot pronation. When the foot pronation occurs, the obligatory tibial internal rotation happens subsequently (Inman, 1981). A study has shown that a nearly positive trend between foot eversion and tibial internal rotation angle during running (Bellchamber and van den Bogert, 2000). Ford et al. (2005) also showed that female athletes had greater maximum ankle eversion during the stance phase of cutting than male athletes did. Whether the increased tibial internal rotation due to the foot eversion can

contribute to ACL loading during athletic tasks is still unclear and needs further research.

The developmental physical change along with the age may associate with non-contact ACL injuries. Yu et al. (2005) and Swartz et al. (2005) both investigated the effects of the age and gender on the lower extremity motion patterns during landing. Yu et al. (2005) found that female adolescent recreational soccer athletes have decreased knee and hip flexion angle at initial foot contact and decreased knee and hip motions during landing of the stop-jump task when compared to their male counterparts. The significant gender differences in the knee and hip motion patterns of the youth recreational soccer players occur after 12 years of age and increase with age before 16 years of age. The results of Yu et al. (2005) demonstrated the selected lower extremity motion patterns may be risk factors of sustaining non-contact ACL injuries because literature has indicated that the ACL injury rate in adolescents increases linearly after 12 years of age and that adolescent at 17 and 18 years of age have the highest ACL injury rate (Shea et al., 2004).

The study by Swartz et al. (2005) showed that children (mean age: 9.41 ± 0.99 yr) had significantly greater knee valgus and less hip flexion angle at initial contact, and smaller knee flexion angle, greater valgus angle, and less hip flexion angle at maximal vertical ground reaction force and impulse, and a shorter time to maximal vertical force than adults (mean age: 23.90 ± 2.76 yr). No significant gender differences, however, were observed on the selected kinematic variables in children and adults (Swartz et al., 2005). The authors claimed that the ability to modulate the vertical ground reaction force improves with the age and this may mainly due to physical maturation, skill levels, and experience.

2.4. Effect of the Training Programs on the Prevention of Non-contact ACL Injuries

Training programs based on the proposed possible risk factors for the non-contact ACL injuries in current literature were developed and applied in the clinical practice. The effect of the developed training programs on the prevention of the non-contact ACL injuries has been investigated and demonstrated the effect in altering the lower extremity motion patterns.

Neuromuscular and proprioception trainings alter the lower extremity motion patterns in athletic tasks. Hewett et al. (1996) investigated the effects of a plyometric training program on the peak vertical ground reaction force in landing after a volleyball block jump. They reported a 22% decrease in the peak vertical ground reaction force and a 50% decrease in the knee valgus-varus moment after training. Irmischer et al. (2004) studied the effects of a nine-week and low-intensity plyometric training program on the peak vertical ground reaction force and rate of the development of the peak vertical ground reaction force during a vertical jump-landing-jump task. The authors found that the training group significantly decreased their peak vertical ground reaction force and the rate of development of the peak ground reaction force during landing. Lephart et al. (2005) compared the effects of a plyometric training program and a basic resistance training program on the lower extremity neuromuscular and biomechanical characteristics. The results demonstrated that subjects in both training programs increased quadriceps muscle strength, hip and knee flexion angles and decreased hip and knee flexion moments during landing of a jump-landing task after the training programs. No significant differences in post-training lower extremity motion patterns between training programs were observed. Myer et al. (2005) evaluated the effects of a comprehensive neuromuscular training program on the lower extremity motion patterns in a drop landing-vertical jump task. The results of this study revealed that subjects significantly

decreased the maximum valgus (28%) and varus (38%) moments for their right knee during the stance phase of the drop landing-vertical jump task. This study showed that the combination of multiple-injury prevention-exercise components into a comprehensive program improved performance and modified lower extremity motion patterns. Myer et al. (2006) further studied the effects of the plyometric exercise on the dynamic stabilization and the balance exercises on the lower extremity motion patterns in vertical and medial drop landing tasks. The results of this study further demonstrated that subjects in the plyometric training group significantly increased knee flexion angle during the vertical drop jump task but did not significantly change the knee flexion angle during the medial drop landing task. In contrast, subjects in the balance training group significantly increased knee flexion angle during the medial drop landing task but did not significantly change the knee flexion angle during the drop landing task. Pollard et al. (2006) investigated how the practice combined with the injury prevention programs affects the lower extremity motion patterns in a drop-landing task in a longitudinal pre-post intervention study. The injury prevention program included warm-up, stretching, strengthening, plyometrics, and agilities drills. They reported that the significantly decreased hip internal rotation angle and increased hip abduction angle were observed, but no differences in the knee flexion angle and valgus angle between the pre-intervention and post-intervention were observed.

Neuromuscular and proprioception trainings may decrease the ACL injury rates in athletic tasks. Caraffa et al. (1996) studied the effect of the proprioceptive training programs on the incidence of the ACL injuries in 600 soccer player in a prospective controlled training. Their results showed that incidence significantly decreased to 1.15 ACL injuries per team per year in the proprioceptively trained group. Myklebust et al. (2003) investigated the effect of

the neuromuscular training programs on the incidence of the ACL injury rate in team handball players for three seasons. The three consecutive seasons were control season, first intervention season, and second intervention season. They reported the total number of injuries reduced for the group of team handball players who completed the neuromuscular training programs, but only the elite group had significant reduction of the ACL injury rate when completed the neuromuscular training programs. They concluded that the neuromuscular training for the female team handball players was possibly to prevent the ACL injuries. Mandelbaum et al. (2005) also showed that the neuromuscular training resulted in 88% reduction of ACL injuries in the enrolled subjects compared to the control group for the year 1 and 74% reduction in anterior cruciate ligament tears for the year 2 in female soccer players.

Trainings with instruction and feedback also alter lower extremity motion patterns. McNair et al. (2000) compared the effects of different feedback techniques on the peak vertical ground reaction force during landing. They reported that using the verbal instructions and the sound of landing as feedback to modify landing techniques have the same effects in reducing the peak vertical ground reaction force during landing. Cowling et al. (2003) investigated how the different verbal instructions affect the landing biomechanics during an abrupt single limb landing. The verbal instructions included normal landing; repeat normal landing; landing after instruction to increase knee flexion; and landing after instruction to recruit hamstring muscles earlier. Their results showed that the instruction condition “landing after instruction to increase knee flexion” significantly increased the knee flexion angle and decreased the posterior ground reaction force. Onate et al. (2005) investigated the effects of using video images as feedback in landing technique training to reduce peak ground reaction force. Their results demonstrated that all training groups and the control group increased their knee flexion

motion and reduced peak vertical ground reaction force during a vertical drop landing after the training time period.

The current literature supports the evidence of altering lower extremity motion patterns through trainings; current literature on the prevention of non-contact ACL injuries, however, has no convincing evidence in the reduction of the risk of the non-contact ACL injuries. Based on the literature reviewed, only one study presented dramatic decrease after training. In addition, current literature has not scientifically demonstrated the association of the reduction in the risk of sustaining non-contact ACL injuries with the changes in the lower extremity motion patterns. The lack of scientific support in current literature is the major obstacle for developing effective training programs for the reduction of the risk of the non-contact ACL injuries. The well developed training programs based on the scientifically determined risk factors are needed for prevention the non-contact ACL injuries.

After an extensive literature review, it is clear that the proximal tibial anterior shear force is the major cause of ACL loading, while the valgus-varus and internal rotation moments are minor ACL loading mechanisms (Berns et al., 1992; Markolf et al., 1995; Fleming et al., 2001). An increased anterior shear force on the proximal end of the tibia has been shown to significantly increase ACL strain. The valgus-varus and internal rotation moments can also load the ACL; but only when anterior shear force on the proximal part of the tibia is applied simultaneously. In addition, studies by Dürselen et al. (1995) and Markolf et al. (1995) indicated that the combined external valgus moment and external rotation moment can unload the ACL. Several investigations (Ford et al., 2003; McLean et al., 2004; Hewett et al., 2005; Kernozek et al. 2005) argued that the knee valgus angle and knee valgus moment observed during the landing phase of selected athletic tasks are risk factors for non-contact ACL injuries.

They, however, did not realize dynamic valgus is the valgus angle often coupled with tibial external rotation, which can unload the ACL (Dürselen et al., 1995; Markolf et al., 1995). Care must be exercised when making inferences about the knee valgus-varus angle and moment, and knee internal rotation moment as risk factors for sustaining non-contact ACL injuries. It is true that ACL loading is composed of: the anterior shear force on the proximal part of the tibia, the knee valgus-varus moment, and the knee internal rotation moment. Factors that contribute to these three loading sources can be considered as possible risk factors for non-contact ACL injuries. The current literature, however, demonstrates that the major loading mechanism is the anterior shear force on the proximal tibia. Based on this point of view, factors that contribute to an increase in proximal tibial anterior shear force need to be strongly considered.

Based on the discussion of the ACL loading mechanisms and the findings of current research, sagittal lower extremity biomechanics seem to be the dominant risk factors for sustaining non-contact ACL injuries. A large quadriceps muscle force, a small knee flexion angle, and a large posterior ground reaction force during the landing phase of selected athletic tasks are likely to be major risk factors for sustaining non-contact ACL injuries, because all these factors can significantly contribute to an increase in proximal tibial anterior shear force and ACL loading. Non-sagittal plane risk factors may also contribute to ACL loading, but may not be major risk factors of sustaining non-contact ACL injuries.

Although the above-mentioned studies indicated that altered lower extremity motion patterns may be possible risk factors, no study provides cause-and-effect evidence to support that they are indeed risk factors. Future research focusing on the identification of actual risk factors for sustaining a non-contact injury is desperately needed for the prevention of non-contact ACL injuries.

2.5. Research Methods to Determine Risk Factors of Sustaining Non-Contact ACL Injuries

Although many modifiable motor control related risk factors of sustaining non-contact ACL injuries have been proposed, a recent extensive review of literature failed to provide strong evidence that any of those proposed motor control related biomechanical risk factors of sustaining non-contact ACL injuries are indeed risk factors. It is difficult to develop evidence based and effective intervention strategies to reduce non-contact ACL injury rate without scientifically identified risk factors. The lack of scientific evidence for motor control related biomechanical risk factors, to a large degree, is due to the limitations in research methods used in current research on risk factors of sustaining non-contact ACL injuries, and lack of recognition of new and advanced research methods.

2.5.1. Traditional Epidemiological Research Methods

Case-control and cohort designs are two traditional research designs in epidemiological research on risk factors for a disease or injury. Case-control design is categorized as an exploratory research design in epidemiology (Portney and Watkins, 2000). A case is defined as an individual who has the disease or injury of interest while a control is defined as an individual who does not have the disease or injury of interest. The objective of using this method is to compare differences in the proposed risk measures between a group of cases and a group of controls to assess the relationship between the exposure to proposed risk factors and the development of a disease or injury. Pre-disease or pre-injury data are collected through post-disease or post-injury interviews, surveys, and medical records. An odds ratio is used to

express the degree to which risk factor exposure increases the probability of disease relative to those not exposed to the risk factor.

The cohort design is categorized as an exploratory research design in epidemiology as well. When this method is applied in a research, a group of subjects who are free of the disease or injury of interest will be recruited. These subjects will be exposed to the risk of sustaining the disease or injury of interest after the pre-disease or injury data are collected. Subjects will be followed for a period of time during which adequate number of disease or injury cases will be obtained. Then, the pre-disease or -injury data of the cases will be compared with those subjects who have not been infected or injured to determine which pre-disease or -injury factors are associated with the disease or injury of interest. Careful selection of subjects for cohort studies is important to prevent invalid results. Subjects selected for cohort study should be free of the disease or injury of interest and on the basis of exposure variable. Logistic regression is often used for this kind of research design to determine how much a factor can explain the distribution of the disease or injury of interest within the selected group of subjects.

Major limitations of these two traditional epidemiologic research designs include that results are descriptive in nature and lack cause-and-effect relationships of the disease or injury of interest with the associated factors. The lack of cause-and-effect relationships of the independent variables with the outcome makes the interpretation of associate factors as risk factors difficult. A misinterpretation of the associations of the independent variables with the outcome may mislead clinical practice. In addition, these traditional epidemiological research designs lack ability to determine risk and risk factors without a large number of injury cases, which makes these two traditional epidemiological research designs very labor intensive and expensive when used in research to identify risk factors of sustaining non-contact ACL

injuries.

2.5.2. Stochastic Biomechanical Modeling

The stochastic biomechanical modeling is a biomechanical modeling paradigm that represents random variations of human motions. It can be used to evaluate the probability of random outcomes of human motions. Monte Carlo simulation method is the core of the stochastic biomechanical modeling.

Monte Carlo simulation is a method to express a dependent variable as a function of the independent random variables and to simulate the variability of a dependent variable based on the distributions of independent variables. Monte Carlo simulation is a useful tool to study the risk and risk factors of sustaining an injury if the injury can be quantitatively defined as a function of potential risk factors based on actual physical principles. Physically defined relationships of the potential risk factors with injury measures set the cause-and-effect relationships of the potential risk factors with the injury.

Monte Carlo simulation can also allow investigators to study the risk and risk factors without actual injury cases. Most of the injuries occurred when several extreme conditions are satisfied at the same time. Monte Carlo simulation is a technique to estimate the probability that multiple extreme conditions are satisfied, which allows researchers to predict the risk of sustaining an injury before actual injuries occur. The ability to predict the risk of sustaining an injury before the injury actually occurs make the stochastic biomechanical modeling very attractive as a research method as well as a clinical tool in injury prevention.

The stochastic biomechanical modeling approach has been successfully applied in injury prevention studies. Mirka and Marras (1993) developed the stochastic model based on the empirical EMG data of trunk muscles when subjects were doing the repeated bending

motions. This EMG-based stochastic model assessed the magnitude and variability of spine reaction forces during bending. It can also assess the range of spinal loads that would be expected with a particular task and to estimate various trunk muscle co-activation and to explain how repetitive lifting could injure the lower back. Hughes and An (1997) used the Monte Carlo simulation to predict the distribution of deltoid and rotator cuff muscle forces during static arm elevation. The parameters of the Monte Carlo simulation were modeled either independent or dependent to each other. Their results showed that the correlation between moment arms of different muscles affected the distribution of muscle force predictions, but would not affect the median predicted forces. The results also showed the utility of the Monte Carlo simulation in estimating variability of biomechanical measures. Chang et al. (2000) modeled the physiological cross sectional area, EMG, and muscle moment arm of muscles involved in shoulder internal rotation by Monte Carlo simulation to integrate population variability. The variability of physiological cross sectional area and EMG were modeled with log-normal distributions while muscle moment arm with normal distribution. These generated parameters were taken as input of the EMG-driven muscle model to predict the muscle forces. They indicated that this model can be applied to analyze the data of patients with rotator cuff injuries and would provide more significant information about injury mechanism and shoulder impingement prevention. Garrett and Yu (2004) also used this method to estimate the ACL loading and the non-contact ACL injury rate. The ACL loading was estimated from peak proximal tibial anterior shear force, knee valgus-varus, and internal-external rotation moment at peak proximal tibial anterior shear force. The ACL injury loading was set at 3 times body weight. The predicted injury rate of non-contact ACL injury for females to males was 7 to 1. The injury rate predicted from their model was very close to

the injury rate previously reported in the literature. McLean et al. (2003, 2004) used this method with forward dynamics to estimate the variability of 3D knee loadings and predict the ACL injuries. Ten male and 10 female athletes were used to generate subject-specific forward dynamics musculoskeletal model. Random perturbations were applied to initial contact conditions and quadriceps/hamstring activation levels to stimulate their effect on the peak 3D knee loadings. The anterior drawer force greater than 2000 N was considered as an injury event contributed from the sagittal plane mechanism. Although the model of McLean's needs to be further critically validated, all these examples demonstrated the usefulness and effectiveness of stochastic biomechanical modeling as a research method in injury prevention studies.

Summary

ACL rupture is one of the most commonly seen knee injuries in sports and exercise with devastating consequences. The majority of the ACL injuries are non-contact injuries. To prevent non-contact ACL injuries, several motor control related biomechanical risk factors of the sustaining non-contact ACL injuries have been proposed in the literature. Although tremendous research efforts have been made in the last decades, the associations of lower extremity motion patterns with the risk of the ACL injuries have not been scientifically established with convincing cause-and-effect relationships. Traditional epidemiological research designs have significant limitations when applied to studies on the risk factors of sustaining non-contact ACL injuries and evaluation of the effects of the training programs. Stochastic biomechanical modeling is a new technique in the biomechanical field that can be used to determine the risk and risk factors of sustaining non-contact ACL injuries. This

proposed study explored the application of this new technique in the prevention of the non-contact ACL injuries.

CHAPTER III

METHODS

The methods used to address the three major objectives for this project were described in detail in four sections of this chapter: (1) development of a sagittal plane knee model, (2) collection and reduction of *in vivo* lower extremity kinetics, kinematics, and electromyography during the stop-jump task, (3) determination of the effects of the sagittal plane biomechanics on the ACL loading by using computer simulation with model approach, and (4) estimate of the probability and determination of the motor control related risk factors of sustaining non-contact ACL injuries using a stochastic biomechanical model.

3.1. The Sagittal Plane Knee Model

A sagittal plane inverse dynamic knee model was developed in this study for understanding the effects of sagittal plane biomechanics on the ACL loading. This sagittal plane inverse dynamic knee model expressed the quadriceps force and the ACL loading as functions of relevant knee geometries, knee flexion angle, tibial tilting angle, location of center of pressure relative to the ankle joint center, ground reaction forces, and hamstring and gastrocnemius muscle forces. The patellar tendon-tibial shaft angle, the patella-patellar tendon angle, the quadriceps tendon- patella angle, the hamstring tendon-tibial shaft angle, the ACL elevation angle, and the knee flexion-extension moment arms of patellar tendon, hamstring muscle and gastrocnemius muscle were expressed as functions of the knee flexion angle.

3.1.1. Determination of the ACL loading

The resultant horizontal and vertical forces at the knee in the laboratory reference frame ($F_{k,x}$ and $F_{k,z}$) were determined as

$$\begin{aligned} F_{k,x} &= -F_{GRF,x} \\ F_{k,z} &= -F_{GRF,z} \end{aligned} \tag{3.1}$$

where $F_{GRF,x}$ and $F_{GRF,z}$ were horizontal and vertical ground reaction forces in the laboratory reference frame (Figure 3.1). The resultant proximal tibial anterior shear force at the knee in the tibial reference frame ($F_{k,AP}$) was expressed as

$$F_{k,AP} = F_{k,x} \cos \sigma + F_{k,z} \sin \sigma \tag{3.2}$$

where σ was tibial tilting angle defined as the angle between the longitudinal axis of the tibia and the vertical axis of the laboratory reference frame (Figure 3.1).

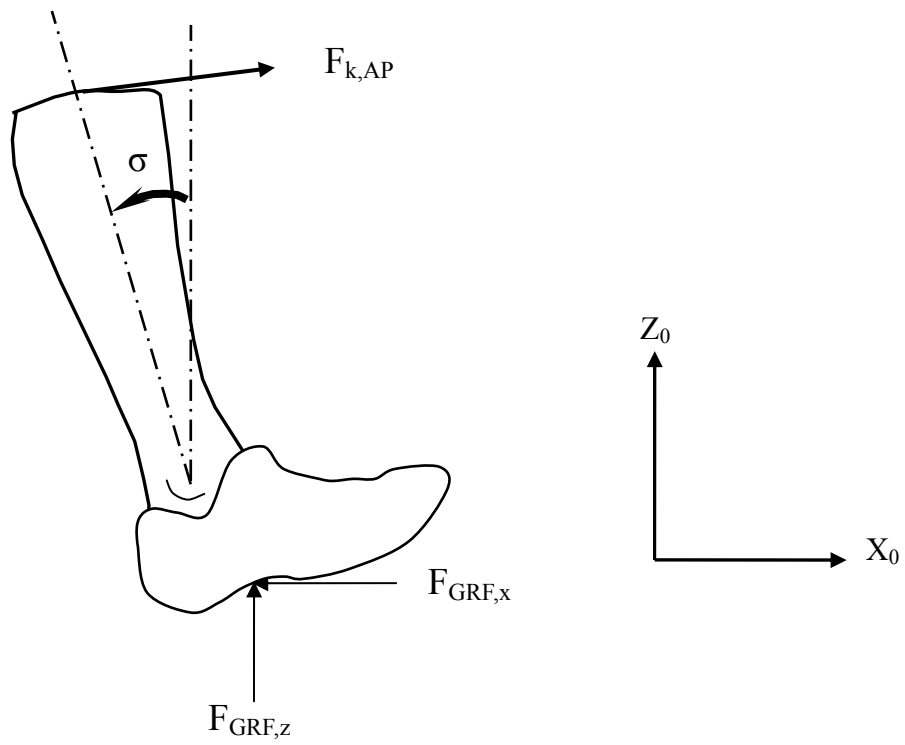


FIGURE 3.1 The horizontal ($F_{GRF,x}$) and vertical ($F_{GRF,z}$) ground reaction forces in the laboratory reference frame and representation of the tibial tilting angle (σ).

The knee flexion-extension moment on the tibia due to ground reaction forces ($M'_{k,ef}$) was determined as

$$M'_{k,ef} = (L_T \cos \sigma + z_a - z_{COP}) \times F_{GRF,x} + (L_T \sin \sigma + x_a - x_{COP}) \times F_{GRF,z} \quad (3.3)$$

where L_T was the length of the tibia; z_a and z_{COP} were the vertical coordinates of the ankle joint center and center of pressure, respectively; and x_a and x_{COP} were the horizontal coordinates of the ankle joint center and center of pressure, respectively. The knee joint resultant flexion-extension moment ($M_{k,ef}$) generated by knee flexors and extensors was

$$M_{k,ef} = -M'_{k,ef} \quad (3.4)$$

where $M_{k,ef}$ was in extension when its value was in negative while $M_{k,ef}$ was in flexion when its value was in positive. The $M_{k,ef}$ was decomposed as the sum of the patellar tendon moment, hamstring moment, and gastrocnemius moment

$$M_{k,ef} = r_{HAM} \times F_{HAM} + r_{GAS} \times F_{GAS} - r_{PT} \times F_{PT} \quad (3.5)$$

where r_{HAM} , r_{GAS} , and r_{PT} were the hamstring, gastrocnemius, and patellar tendon knee moment arms, respectively; and F_{HAM} , F_{GAS} , and F_{PT} were the hamstring, gastrocnemius, and patellar tendon forces, respectively. With a known magnitude of knee extension moment ($M_{k,ef}$), hamstring muscle force (F_{HAM}), gastrocnemius muscle force (F_{GAS}), hamstring moment arm (r_{HAM}), gastrocnemius moment arm (r_{GAS}), and patella tendon moment arm (r_{PT}), the patellar

tendon fore (F_{PT}) was determined as

$$F_{PT} = \frac{r_{HAM} \times F_{HAM} + r_{GAS} \times F_{GAS} - M_{k,ef}}{r_{PT}} \quad (3.6)$$

The resultant proximal tibial anterior shear force ($F_{k,AP}$) determined using Equation (3.2) was decomposed as the sum of the anterior shear component of the patellar tendon force on the tibia (F_{PT}), posterior component of the hamstring force on the tibia (F_{HMA}), and anterior-posterior component of the other soft tissues forces around the knee on the tibia ($F_{ST,AP}$)

$$F_{k,AP} = F_{PT} \times \sin \alpha - F_{HAM} \times \sin \gamma - F_{ST,AP} \quad (3.7)$$

where α was the patellar tendon-tibial shaft angle; and γ was the hamstring tendon-tibial shaft angle (Figure 3.2). From Equation 3.7, the anterior-posterior component of the other soft tissue force around the knee joint was determined as

$$F_{ST,AP} = F_{PT} \times \sin \alpha - F_{HAM} \times \sin \gamma - F_{k,AP} \quad (3.8)$$

with known $F_{ST,AP}$, the ACL loading due to sagittal plane biomechanics, $F_{ACL,Sagittal}$ was determined as

$$F_{\text{ACL,SAGITTAL}} = \frac{F_{\text{ST,AP}} \times \tau}{\cos \varphi} \quad (3.9)$$

where φ was the ACL elevation angle (Figure 3.2); and τ was ACL anterior-posterior loading share coefficient. The ACL anterior-posterior loading share coefficient was determined as a function of knee flexion angle using a regression analysis based the anterior shear forces and ACL loadings by Markolf et al. (1995) and ACL elevation angles by Li et al. (2005).

$$\tau = 0.6559 + 4.564 \times 10^{-3} \theta - 1.84 \times 10^{-4} \theta^2 + 1.33 \times 10^{-6} \theta^3 \quad (3.10)$$

where θ was the knee flexion angle (Figure 3.2).

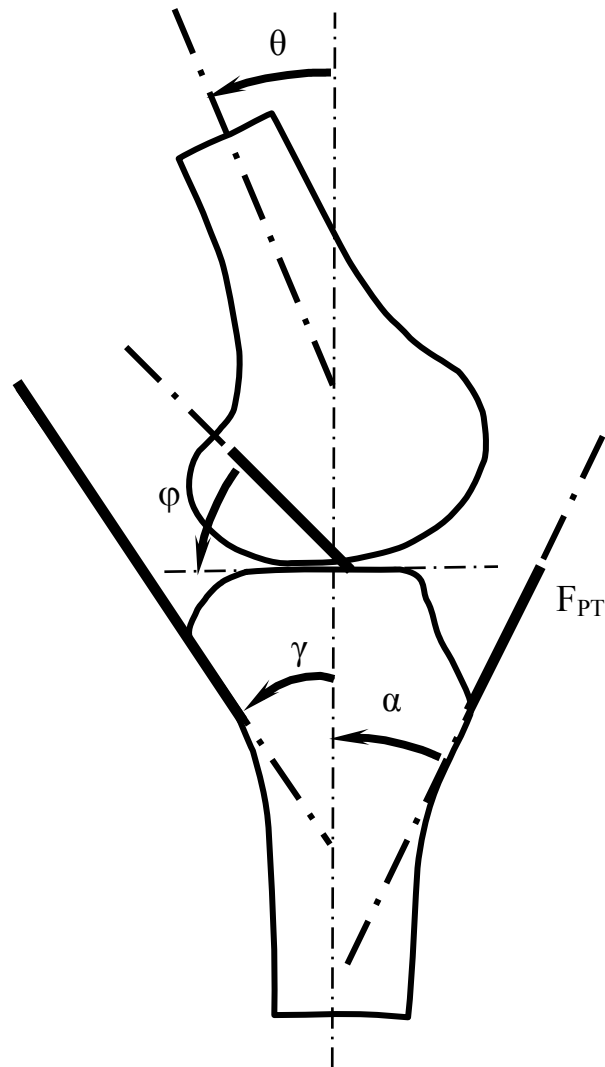


FIGURE 3.2 The knee geometry to show the definition of the knee flexion angle (θ), patellar tendon-tibial shaft angle (α), hamstring tendon-tibial shaft angle (γ), and ACL elevation angle (φ).

3.1.2. Determination of the Quadriceps Muscle Force

Assuming that the friction force between the patella and femur was negligible, the quadriceps muscle force on the patella, patellar tendon force on the patella, and the pressure force on the patella perpendicular to the longitudinal axis of the patella were in equilibrium (Figure 3.3)

$$F_{\text{QAD}} \cos \phi = F_{\text{PT}} \cos \beta \quad (3.11)$$

where F_{QAD} was the quadriceps muscle tendon force; and ϕ and β were the quadriceps tendon-patella angle and patella-patellar tendon angle, respectively. Based on this equilibrium, the quadriceps muscle force could then be determined as

$$F_{\text{QAD}} = \frac{F_{\text{PT}} \cos \beta}{\cos \phi} \quad (3.12)$$

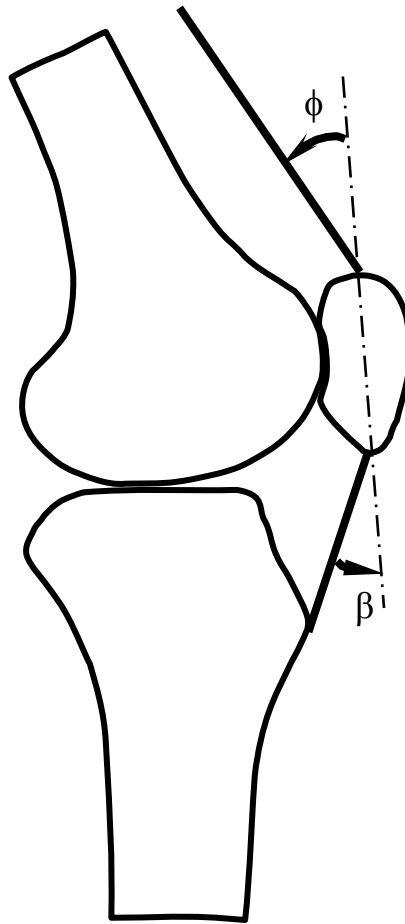


FIGURE 3.3 Definition of the quadriceps tendon-patella angle (ϕ) and patella-patellar tendon angle (β).

3.1.3. Determination of the Patellar tendon-tibial shaft Angle, Patella-patellar tendon Angle, Quadriceps tendon-patella Angle, and Hamstring tendon-tibial shaft Angle

The relationship between the patellar tendon-tibial shaft angle and the knee flexion angle was determined using the x-ray data collected by Nunley et al. (2003). The data were collected from 10 male and 10 female recreational athletes. The mean age, height, and weight were 24.5 ± 1.3 years, 1.78 ± 0.03 m, and 76.1 ± 9.9 kg, respectively, for male subjects, and 23.7 ± 1.9 years, 1.70 ± 0.05 m, and 59.8 ± 5.0 kg, respectively, for female subjects. Each subject was asked to squat and evenly bear the body weight on the two legs. A goniometer was used to measure the knee flexion angle and a scale was used to monitor their weight distribution. The trunk position was controlled as described by Ohkoshi et al. (1991). Lateral x-ray film was taken for the dominant side at each knee flexion angle, starting from 0° to 90° of knee flexions with 15° increments. The leg used for measurement was required to be in the neutral position without any tibial rotation.

Two parallel lines were drawn in the femur perpendicular to the mid-shaft of the femur; the longitudinal axis of the femur was the straight line passing two midpoints of these two parallel lines. Two parallel lines were also drawn in the tibia paralleling to the tibial plateau for determination of the longitudinal axis of the tibia. The longitudinal axis of the tibia was determined as the straight line passing the midpoints of two lines parallel to the tibial plateau. The angle formed by the longitudinal axis of the femur and the tibia was defined as actual angle of knee flexion. The longitudinal axis of the patellar tendon was the line going through the attachment points of the patellar tendon on the patella and tibia. The patella tendon-tibial shaft angle was defined as the angle between the longitudinal axis of the patellar tendon and the longitudinal axis of the tibial shaft.

The patella-patellar tendon angle, quadriceps tendon-patella angle, and hamstring tendon-tibial shaft angle were determined from the same database. The patella-patellar tendon angle was defined as the angle between the longitudinal axis of the patella and patellar tendon. The longitudinal axis of the patella was the straight line connecting the most distal and proximal point of the patella.

The quadriceps tendon-patella angle was the angle between the line of action of the quadriceps muscle group and the longitudinal axis of the patella. The line of action of the quadriceps muscle group was determined by digitizing the estimated centroid of attached points on the top of the patella and anterior inferior iliac spine. The hamstring tendon-tibial shaft angle was the angle between the line of action of the hamstrings muscle and the longitudinal axis of the tibial shaft. The line of action of the hamstring muscle group was a line connecting attached centroid points on the ischial tuberosity and tibial condyle.

The multiple regression analyses were performed to determine the relationship of the patellar tendon-tibial shaft angle, the patella-patellar tendon angle, the quadriceps tendon-patella angle, and the hamstring tendon-tibial shaft angle as functions of the knee flexion angle. The regression model used for these analyses was in a form of a polynomial

$$y = \sum_{n=0}^N (a_n \theta^n + \eta b_n \theta^n) \quad (3.13)$$

where y was the dependent variable (patellar tendon-tibial shaft angle, patella-patellar tendon angle, quadriceps tendon-patella angle, or hamstring tendon-tibial shaft angle); θ was the knee flexion angle. N was the order of the best regression equation; a_n and b_n were regression coefficients at order n , η was a dummy variable representing gender ($\eta=0$ for males and $\eta=1$

for females). The order of the best polynomial equation of y as a function of θ , N was determined as the order of the regression equation when a_{N+1} , b_{N+1} , a_{N+2} , b_{N+2} had no significant contribution to the regression greater than 2% of the total variation of observed y values.

The best regression equations of the patellar tendon-tibial shaft angle (α) as a function of knee flexion angle (θ) obtained through this analysis was in a form of

$$\alpha = 22.03 - 0.30\theta \quad (3.14)$$

for males, and

$$\alpha = 25.70 - 0.30\theta \quad (3.15)$$

for females. The best regression equation of the patella-patellar tendon angle (β) as a function of knee flexion angle (θ) obtained through this analysis was in a form of

$$\beta = 26.617 + 0.228\theta + 0.002\theta^2 \quad (3.16)$$

for both genders. The best regression equation of the quadriceps tendon-patella angle (ϕ) as a function of knee flexion angle (θ) was in a form of

$$\phi = 0.48 + 0.67\theta \quad (3.17)$$

for both genders. The best regression equation of the hamstring tendon-tibial shaft angle (γ) as a function of knee flexion angle (θ) was in a form of

$$\gamma = 0.001 + 0.89\theta \quad (3.18)$$

for both genders.

3.1.4. Determination of the Moment Arms

The knee flexion-extension moment arms of the patellar tendon, and hamstring and gastrocnemius muscles were expressed as functions of knee flexion angle. The moment arms of the patellar tendon, and hamstring and gastrocnemius muscles at variety of knee flexion angles were retrieved from the study by Imran et al. (2000) because this paper provided complete information about moment arm of patellar tendon, hamstring, and gastrocnemius muscles at different knee flexion angles and muscle forces. A four-bar linkage of the knee model in the sagittal plane was used to determine the corresponding moment arms. The determined moment arm was the perpendicular distance from the lines of action of the muscle force to the point of intersection of the lines of action of the tibiofemoral contact force and the cruciate ligament force. Each moment arm was calculated at 0°, 30°, 60°, 90°, and 120° of knee flexion angle with the isometric quadriceps force of 2500 N and hamstring and gastrocnemius muscle forces of 1000 N.

A nonlinear regression was used to determine the relationship of the moment arm as a function of the knee flexion angle. The equation of the moment arm of each muscle was expressed as polynomial function of knee flexion angle

$$r = \sum_{n=0}^3 (c_n \theta^n) \quad (3.19)$$

where r was estimated moment arm in meter of the muscle of interest; c_n was regression coefficient of order n of the power of the best regression equation; and θ was the knee flexion angle. The order of the power of the best regression equation was determined as the order of the power where c_{n+1} and c_{n+2} had no significant contribution to the regression greater than 2% of the total variation of observed r values.

The regression equation of each moment arm as a function of the knee flexion angle were in forms of

$$r_{PT} = 0.0508 + 0.000217\theta - 4.45 \times 10^{-6} \theta^2 + 1.676 \times 10^{-8} \theta^3 \quad (3.20)$$

$$r_{HAM} = 0.0270 + 5.35 \times 10^{-4} \theta - 4.614 \times 10^{-6} \theta^2 \quad (3.21)$$

$$r_{GAS} = 0.0288 - 5.742 \times 10^{-5} \theta + 4.07 \times 10^{-7} \theta^2 \quad (3.22)$$

for both genders, where r_{PT} , r_{HAM} , r_{GAS} were moment arms of the patellar tendon, hamstring muscle and gastrocnemius muscle, respectively.

3.1.5. Determination of the ACL Elevation Angle

The ACL elevation angle expressed as a function of knee flexion angle was determined

based on the literature of Li et al. (2005). Five young and healthy subjects were asked to do a single leg lunge from a full knee extension to 90° knee flexion with 30° interval. The 3-D knee model with relative position of the ACL insertion areas on the femur and tibia was constructed by a MR imaging, fluoroscope, solid modeling software, and virtual C-arm. The ACL elevation angle was defined as the angle between the ACL and tibial plateau. They found that the ACL elevation angle significantly decreased as the knee flexion angle increased, which was shown as $64.9^\circ \pm 10.7^\circ$ at 0° knee flexion angle and $43.2^\circ \pm 4.0^\circ$ at 90° knee flexion angle. For more details on the setup of the experiment to determine the ACL elevation angle the reader is referred to the original reference (Li et al., 2005).

An exponential regression model was used to determine the relationship between the ACL elevation angle and the knee flexion angle

$$\varphi = \exp\left(\sum_{n=0}^N a_n \theta^n\right) \quad (3.23)$$

where φ was the ACL elevation angle; θ was the knee flexion angle; N was the order of the power of the best regression equation; and a_n was the regression coefficient at order n of the power of the best regression equation. The order of the power of the best regression equation was determined as the order of the power where a_{n+1} and a_{n+2} had no significant contribution to the regression greater than 2% of the total variation of observed φ values.

The best regression equation of the ACL elevation angle as a function of the knee flexion angle obtained was in a form of

$$\varphi = \exp(4.1862 - 7.9 \times 10^{-3} \theta + 3.6 \times 10^{-5} \theta^2) \quad (3.24)$$

for both genders.

3.2. Collection and Reduction of Lower Extremity Kinetics, Kinematics, and EMG in a Stop-Jump Task

In vivo lower extremity kinematics and kinetics were collected and reduced. The *in vivo* data were used as inputs of the sagittal plane inverse dynamic knee model that was later used to determine the effects of lower extremity kinematics and kinetics on the ACL loading at the peak posterior ground reaction force during landing of a stop-jump task. The *in vivo* data were also used in the stochastic biomechanical model to determine the risk and risk factors of sustaining non-contact ACL injuries.

3.2.1. Data Collection

A total of 40 male and 40 female recreational athletes without known history of lower extremity disorders were recruited as the subjects for this study. The mean age, height, and weight were 22.4 ± 3.1 years, 1.78 ± 0.06 m, 78.8 ± 9.4 kg, respectively, for male subjects, and 23.2 ± 2.7 years, 1.63 ± 0.07 m, 60.1 ± 11.5 kg, respectively, for female subjects. Each subject was asked to perform a stop-jump task. The stop-jump task consisted of a running approach of up to five steps, a two-footed landing, and vertical take off for maximum jumping height. The approaching speed was self-selected by the subject after they were instructed to run as fast as they could but felt comfortable for the maximum effort in the vertical jump. The stop-jump task was described to the subject before warm up and practice. The specific technique was not demonstrated in detail to avoid coaching effect.

Seventeen 20 mm passive reflective markers were attached to the recommended landmarks for kinematic analyses. Markers were placed on the bilateral anterior superior iliac spines, lateral thighs, anterior superior shanks, anterior inferior shanks, lateral malleoli, heels, 1st and 5th metatarsophalangeal joints. Another marker was placed between the lumbar vertebrae 4 and 5. The subject performed the stop-jump task with the above-described markers. Each subject performed five successful trials of the stop-jump task at the self-selected maximum approach run speed and vertical jump effort. A successful trial was defined as a trial in which the subject performed the stop-jump task as instructed and landed each foot on the force plates as required.

Three-dimensional (3-D) videographic and two force plates (Bertec Corp., Worthington, OH, USA) data were collected for each subject in a vertical stop-jump task. A videographic system with six infrared video cameras was used to collect the trajectories of markers on the subject at a frame rate of 120 frames/s. Cameras were adjusted so that each marker could be viewed by at least two cameras throughout a movement cycle. The calibration volume for the six infrared cameras used in the performance of the stop-jump task was 3.0 m long×2.5 m wide×2.5 m high. Two Type 4060A Bertec force plates (Bertec Corporation, Worthington, OH, USA) were used to collect the ground reaction force signals at a sample rate of 1200 samples/channel/second. The videographic and ground reaction force signals were recorded by the Peak Performance Motus videographic and analog data acquisition system (Peak Performance Technology, Inc., Englewood, CO, USA). The videographic and force plate data collection were time-synchronized to 1200 frames/second and 1200 samples/channel/second using a linear interpolation method.

A static standing trial with six additional markers was captured after collections of all

stop-jump trials. Additional six markers were placed on bilateral medial and lateral femoral condyles and lateral malleoli. These six additional markers were used to estimate critical body landmarks needed for calculation of joint centers. The subject was required to stand in the center of the calibration volume which the 3-D videographic data of all 23 markers was captured.

A 16-channels telemetry electromyography (EMG) system (Konigsburg Instruments, Pasadena, CA) was used to collect EMG of seven muscles of the lower extremity on the dominant side. Seven muscles were vastus medialis, rectus femoris, vastus lateralis, semimembranosus, biceps femoris, medial, and lateral head of gastrocnemius muscles. The skin was prepared for surface electrodes placement by cleaning the skin with alcohol and shaving hair if necessary. Two disposable pre-jelled surface electrodes (Type 720-00S, Ambu Inc., Glen Burnie, Maryland) were placed in series parallel to the muscle fibers for each muscle according to the guidelines of Delagi and Perotto (1979). Pre-taping underwrap was used to secure electrodes and wires to avoid any move artifact. Three movements were performed prior to data collection to ensure the electrodes were well attached and were transmitting clean signals. Squatting was used to examine three components of quadriceps muscles and two components of hamstring muscles. Resisted knee flexion was also performed to examine the electrode placements for hamstring muscles. Electrodes on gastrocnemius muscles were examined by toe-raising. One ground electrode was placed over the area between tibial tuberosity and lower tip of the patella.

The electrodes were then connected to a telemetry transmitter at a gain setting of 2000 Hz (Konigsburg Instruments, Pasadena, CA). The transmitter was secured to the subject to reduce any movement artifact. Each of the 7 EMG channels had a differential input amplifier.

The input to each amplifier was capacitively coupled, with a high-pass corner frequency at 10 Hz. The common mode rejection ratio (CMRR) was above 70 dB for the amplifier used in current study. The signal to noise ratio of the encoder sections of the transmitter was 60 dB.

3.2.2. Data Reduction

The raw 3-D coordinates of the markers during each stop-jump trial were filtered through a Butterworth low-pass digital filter at estimated optimum cutoff frequencies (Yu et al., 1999). The 3-D local coordinates of bilateral medial and lateral femoral condyles and medial malleolus were estimated from the 3-D coordinates of markers on the tibia in the standing trial. The 3-D coordinates of the hip joint centers in stop-jump trials were estimated from the 3-D coordinates of the reflective markers on the right and left ASISs and L4-L5 joint and anatomical data (Bell et al., 1990). The 3-D coordinates of the medial and lateral femoral condyles and medial malleolus in stop-jump trials were estimated from the local coordinates of the corresponding markers in the standing trials through the direction cosine matrices of the tibia defined by the 3-D coordinates of the markers on the tibia in stop-jump trials. The knee joint center was defined as the middle point between the medial and lateral femoral condyles. The ankle joint center was defined as the middle point between the medial and lateral malleoli. The 3-D coordinates of the knee and ankle joint centers and medial and lateral malleolus were used to define the tibia reference frame. The 3-D coordinates of the knee and hip joint centers and medial and lateral femoral condyles were used to define the femoral reference frame. The knee joint angles were determined as Euler angles of the tibial reference frame relative to the femur reference frame rotated in an order of (1) flexion-extension (z-axis), (2) valgus-varus (y-axis), and (3) internal-external rotation (x-axis) (Chao, 1980). The electric signals from the

force plates were converted to forces. Knee joint resultants were calculated using an inverse dynamic procedure (Greenwood, 1987).

A stance phase was analyzed in the stop-jump task and was defined as the duration from the time of initial foot contact to takeoff. A stance phase was divided into two phases: landing phase and jumping phase. Landing phase duration was defined from the instant the vertical ground reaction force greater than zero to the instant of maximal knee flexion angle. Jumping phase duration was defined from the instant the maximal knee angle began to decrease to the instant of takeoff.

Raw EMG signals of four muscles were rectified and band-pass filtered at 20 Hz (high-pass) and 400 Hz (low-pass). The linear envelope EMG of each muscle was obtained by 10 Hz low-pass filter. The linear envelope EMG was then normalized to the maximal linear envelope EMG occurred during each trial. The normalized linear envelope EMG of semimembranosus and biceps femoris muscles were averaged to represent the activation of the hamstring muscle. The normalized linear envelope EMG of medial gastrocnemius and lateral gastrocnemius muscles were averaged to represent the activation of the gastrocnemius muscle. All signal processing and data reduction were performed using MotionSoft 3-D motion data reduction program package version 6.5 (MotionSoft, Inc., Chapel Hill, NC, USA).

3.3. Computer Simulation of the Effects of the Sagittal Biomechanics on the ACL Loading

To understand the sagittal plane ACL loading mechanisms during the stop-jump task, a computer simulation was performed to study the relationships of sagittal plane ACL loading with lower extremity sagittal plane kinematics and kinetics. The sagittal plane inverse

dynamic knee model described previously was instrumented in the computer simulation, with the sagittal plane ACL loading at the peak posterior ground reaction force during landing as the dependent variable. The empirical biomechanical data of 40 male and 40 female recreational athletes during the stop-jump task were inputs of the sagittal plane inverse dynamic knee model. The input independent variables used for the computer simulation were the peak posterior ground reaction forces, the knee flexion angle, the tibial tilting angle, the location of the center of pressure relative to the ankle joint center, and the hamstring and gastrocnemius muscle forces.

A preliminary study (Yu et al., 2006b) showed that the lower extremity kinetics at the peak posterior ground reaction forces were correlated to each other (Table 3.1). Based on these results, the posterior ground reaction force, the location of the COP relative to the ankle joint, the tibial tilting angle, and the knee flexion angle were considered as the primary independent variables of the sagittal plane inverse dynamic knee model while the vertical ground reaction force was considered as the secondary independent variable. The magnitude of the secondary variable was estimated from the primary independent variable based on the regression equation determined through regression analysis and the regression equation was expressed as

$$F_{\text{VGRF}} = 567.884 + 1.406 \times F_{\text{PGRF}} \quad (P < 0.001; R=0.637) \quad (3.25)$$

for males, and

$$F_{\text{VGRF}} = 335.081 + 1.45 \times F_{\text{PGRF}} \quad (P < 0.001; R=0.663) \quad (3.26)$$

for females where F_{VGRF} was vertical ground reaction force in Newton and F_{PGRF} was posterior ground reaction force in Newton.

Table 3.1 Pearson correlation coefficients (p-values) of peak posterior ground reaction force with peak vertical ground reaction force and peak knee joint resultants during the landing of the stop-jump task (Yu et al., 2006b)

	Peak vertical ground reaction force	Peak proximal tibia anterior shear force	Peak knee extension moment
Peak posterior ground reaction force	0.67 (<0.001)	0.85 (<0.001)	0.86 (<0.001)

The patellar tendon-tibial shaft angle, the patella-patellar tendon angle, the quadriceps tendon-patella angle, the hamstrings tendon-tibial shaft angle, the ACL elevation angle, the corresponding knee moment arms of the patellar tendon, the hamstring muscle, and the gastrocnemius muscle used in the sagittal plane inverse dynamic knee model were changed along with a given knee flexion angle based on the best regression equations described previously since these variables were expressed as functions of knee flexion angle.

During computer simulations, the independent variables were systematically changed within their observed ranges to determine their effects on the ACL loading. The range of an independent variable was defined as the interval between corresponding observed minimum and maximum. The posterior ground reaction force was changed from 100 N to 1700 N with 100 N increments. The knee flexion angle was changed from 0 degree to 90 degree with 5 degrees increments and tibial tilting angle was changed from 5 degree to -20 degree with 1 degree increment. The location of center of pressure relative to the ankle joint center was

simulated for landing on toes and landing on heels of each gender. The hamstring muscle force was simulated from 0 N to 500 N with 100 N increments and the gastrocnemius muscle forces was changed from 0 N to 200 N with 100 N increments. The simulated ranges of the muscle forces were based on the muscle forces estimated from computer modeling during a drop-jump task (Pflum et al., 2004).

3.4. The Stochastic Biomechanical Model of the Probability of Sustaining Non-contact ACL Injuries

A stochastic biomechanical model was developed to estimate the probability of sustaining non-contact ACL injuries and to determine the motor control related biomechanical risk factors. The stochastic biomechanical model consisted of five major components: (1) determination of density distributions of primary independent variables of the biomechanical model for estimate of the ACL loading, (2) determination of cumulative distribution functions of the primary independent variables, (3) determination of the secondary independent variables of the biomechanical model for estimate of the ACL loading, (4) Monte Carlo simulation for determining the probability of sustaining a non-contact ACL injury, and (5) Monte Carlo simulation for determining the motor control related biomechanical risk factors of sustaining non-contact ACL injuries.

3.4.1. Determination of Density Distributions of the Primary Independent Variables

The mean, standard deviation, and the density distribution of each primary input variable for the Monte Carlo simulation needed to be determined to imitate the stochastic nature of the variability of human motions. The biomechanical input variables for the Monte

Carlo simulation in this study included the knee flexion angle at peak posterior ground reaction force, peak posterior ground reaction forces during landing, location of center of pressure relative to the ankle joint center at peak posterior ground reaction force, hamstring and gastrocnemius muscle forces at peak posterior ground reaction force, knee valgus-varus moment at peak posterior ground reaction force, and knee internal-external rotation moment at peak posterior ground reaction force. The density distribution, mean, and standard deviation of the input variables were determined based on the empirical data of 40 male and 40 female subjects during the stop-jump task and grouped by gender.

The quantile-by-quantile (Q-Q) plot was used to examine the quantile of a distribution of a variable against the quantile of any of test distributions. The points would cluster along a straight line if the selected variable distribution matches the test distribution. Skewness and kurtosis of each independent variable were examined where skewness expressed the symmetry of the curve while the kurtosis represented how heavy the tail was. Normality test were used to further determine whether the data were normally distributed with significant level at 0.05.

Two major types of probability density distributions were constructed for different kinematic and kinetic variables in this study. One was the normal density distribution and the other one was the gamma density distribution. The general form for the probability density function of a random variable x having normal density distribution was expressed as

$$y = f(x|\mu, \sigma) = \frac{1}{\sigma\sqrt{2\pi}} \exp\left[-\frac{(x-\mu)^2}{2\sigma^2}\right] \quad (3.27)$$

where μ and σ were the observed sample mean and standard deviation, respectively.

The general form for the probability density function of a random variable x having

gamma distribution was expressed as

$$y = f(x|a,b) = \frac{1}{b^a \Gamma(a)} x^{a-1} \exp\left[-\frac{x}{b}\right] \quad (3.28)$$

where a and b were the parameters that determined the shape and scale of the gamma probability density function; $\Gamma(a)$ was the gamma function. The effect of the scale parameter was to stretch out the density distribution and to determine the practical range of the given density distribution while the shape parameter allowed the distribution to take on a variety of shapes and was to determine the profile of the given density distribution.

The shape parameter a and scale parameter b were determined from the mean and variance of the independent variable by solving the following system of equations

$$\text{Mean} = a \times b \quad (3.29)$$

$$\text{Variance} = a \times b^2 \quad (3.30)$$

gamma function, $\Gamma(a)$, was expressed as

$$\Gamma(a) = \int_0^{\infty} e^{-x} x^{a-1} dx \quad (3.31)$$

3.4.2. Determination of the Cumulative Distribution Functions of the Primary Independent Variables

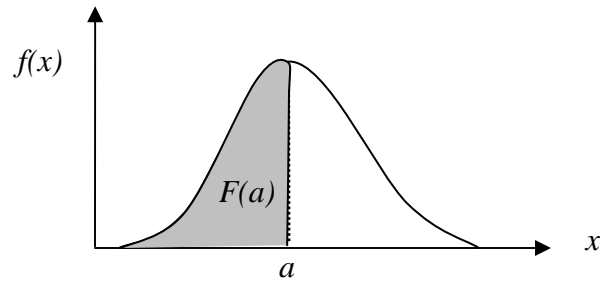
The cumulative distribution function of one primary independent variable was determined based on the relationship with the probability density function and was expressed as

$$F(a) = p\{X \leq a\} = \int_{-\infty}^a f(x)dx \quad (3.32)$$

where $F(a)$ was the cumulative function that represented the probability of random number x ($0 \leq F(a) \leq 1$) when $x \leq a$; $f(x)$ was the probability density function of an independent variable X .

The cumulative distribution value ($0 \leq F(a) \leq 1$) was the integral of the probability density function and equal to a randomly generated number. With the known magnitude of cumulative distribution function $F(a)$, the corresponding magnitude of a could be numerically determined from the graphic relationship between $F(x)$ and x (Figure 3.4).

(a) Probability Density Function: $f(x)$



(b) Cumulative Distribution Function: $0 \leq F(x) \leq 1$

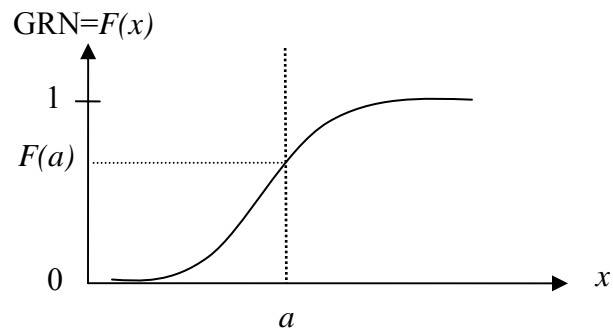


FIGURE 3.4 Relationship between probability density function and cumulative distribution function. (a) Probability Density Function: $f(x)$. (b) Cumulative Distribution Function: $0 \leq F(x) \leq 1$. The integral of $f(x)$ with respect to a (the gray area under curve) was the cumulative distribution function $F(a)$ ($0 \leq F(a) \leq 1$), which was a randomly generated number. GRN: generated random number.

3.4.3. Determination of the Secondary Independent Variables

The magnitude of a secondary independent variable was determined as

$$y = f(x) + e \quad (3.33)$$

where y was the secondary independent variable; x was the primary independent variable correlated to the y ; $y = f(x)$ was the regression equation obtained previously from the empirical data; and e was the regression residual. The regression residual was considered to have a normal density distribution with zero mean. The density distribution of the regression residual was determined for each secondary variable based on the data obtained previously.

Body mass and vertical ground reaction forces (normalized to body weight) were two secondary variables used for stochastic biomechanical model. Body mass used in the Monte Carlo simulation was predicted by the regression equation with the randomly generated standing height as the independent variable and was expressed as

$$BM = -99.33 + 98.916 \times BH \quad (P < 0.001; R = 0.694) \quad (3.34)$$

for both genders where BM was body mass in kg; BH was standing height in meter. The vertical ground reaction in the Monte Carlo simulations was expressed as functions of posterior ground reaction force and the random residual. The vertical ground reaction force normalized to body weight was expressed as

$$F_{VGRF} = 0.717 + 1.414 \times F_{PGRF} + \varepsilon_1 \quad (3.35)$$

for males, and

$$F_{\text{VGRF}} = 0.592 + 1.443 \times F_{\text{PGRF}} + \varepsilon_2 \quad (3.36)$$

for females where the F_{VGRF} and F_{PGRF} was vertical ground reaction force normalized to body weight and posterior ground reaction force normalized to body weight, respectively. The ε_1 and ε_2 were residual determined from regression analysis based on male and female ground reaction forces, respectively.

3.4.4. Monte Carlo Simulation for Estimate of the Probability of Sustaining Non-contact ACL Injuries

The Monte Carlo simulation in this study had three major components: (1) random samples of the primary independent variables, (2) determination of the magnitudes of the secondary independent variables, and (3) determination of the ACL loading from the random sampled independent variables.

With the known probability density function and cumulative distribution function of the primary independent variable determined based on the methods discussed previously, a random number generation was used to randomly generate a cumulative distribution value $F(x)$. The corresponding magnitude of x was determined from the relationship between x and $F(x)$ as described in Equation 3.32 and Figure 4. With the known value of a randomly sampled primary independent variable, x , the magnitude of the secondary independent variable of the ACL loading model was determined using Equation 3.33-3.36.

Normalization of Moment Arms of Muscles

Since the differences of physique between genders and the body height would affect the moment arm, the body height was considered in the predicted moment arms obtained from computer simulation data of Imran et al. (2000). The moment arm normalization was processed with a known predicted moment arm at a given knee flexion angle divided by the mean body height 1.76 m, reported by Smidt (1973), times the randomly selected body height. The equation was expressed as

$$r_{\text{norm}} = \frac{r_{\text{predicted}}}{1.76} \times \text{BH}_{\text{random}} \quad (3.37)$$

where r_{norm} was normalized moment arm of patellar tendon, hamstring and gastrocnemius muscles; $r_{\text{predicted}}$ was predicted moment arm at a given knee flexion angle from the corresponding regression equation for patellar tendon, hamstring muscle, and gastrocnemius muscle; and $\text{BH}_{\text{random}}$ was randomly generated body height in meter. The major reason to compromise the use of the reported body height from Smidt (1973) was due to lack of anthropometric information from Imran et al. (2000) and the magnitudes and the curve of the patellar tendon moment arm obtained from computer simulation data (Imran et al., 2000) used for this study was similar to the results of Smidt (1973).

Determination of Mean and Standard Deviation of Muscle Forces

The mean and standard deviation of the distribution pattern of the hamstring and gastrocnemius forces were obtained and determined from Pflum et al. (2004) and the collected empirical normalized linear envelope EMG. Pflum et al. (2004) used a computer model to

predict the muscle forces and ACL loading during the drop-jump landing. The calculated hamstring and gastrocnemius muscle forces at peak ground reaction force were about 500 N and 200 N, respectively. The two values were considered as mean of the corresponding muscle forces in the present stochastic biomechanical model. Since they did not report the standard deviation of each muscle force, the standard deviation for the corresponding density distribution was determined as

$$SD_{\text{HAM_FORCE}} = \frac{F_{\text{HAM}}}{\text{Norm}_{\text{HAM_EMG}}} \times SD_{\text{HAM_EMG}} \quad (3.38)$$

$$SD_{\text{GAS_FORCE}} = \frac{F_{\text{GAS}}}{\text{Norm}_{\text{GAS_EMG}}} \times SD_{\text{GAS_EMG}} \quad (3.39)$$

where $SD_{\text{HAM_FORCE}}$ and $SD_{\text{GAS_FORCE}}$ was the corresponding standard deviation of hamstring and gastrocnemius forces; F_{HAM} and F_{GAS} was the mean of the hamstring and gastrocnemius forces, respectively; $\text{Norm}_{\text{HAM_EMG}}$ and $\text{Norm}_{\text{GAS_EMG}}$ was normalized linear envelope EMG of hamstring and gastrocnemius muscles, respectively; $SD_{\text{HAM_EMG}}$ and $SD_{\text{GAS_EMG}}$ was the corresponding standard deviation of normalized linear envelope EMG of hamstring and gastrocnemius muscles. With the known mean and the determined standard deviation, the density distribution of muscle force can be determined and the muscle force could be simulated as desired distribution and randomly sampled.

Determination of the ACL Loading

The ACL loading model was used to determine the ACL loading with the random

sampled independent variables. The total ACL loading (F_{ACL}) was an additive function of ACL force due to sagittal plane biomechanics and the ACL force contributed by knee valgus-varus loading and internal-external rotation loading

$$F_{ACL} = F_{ACL,SAGITTAL} + F_{ACL,VV} + F_{ACL,IE} \quad (3.40)$$

where $F_{ACL,SAGITTAL}$ was the ACL loading due to sagittal plane biomechanics determined using Equation 3.9; $F_{ACL,VV}$ was the ACL loading due to knee varus-valgus moment; and $F_{ACL,IE}$ was the force due to the knee internal-external rotation moment.

The relationships of the ACL loadings with the knee valgus-varus and internal-external rotation moments were expressed as functions of knee flexion angle using regression analysis based on the *in vitro* ACL loading data by Markolf et al. (1995). When ACL loading due to sagittal plane biomechanics was greater than zero, the ACL loadings due to knee valgus-varus moment (M_{VV}) and internal-external rotation moment (M_{IE}) were expressed as

$$F_{ACL,VV} = (4.179 - 0.1108\theta + 9.43 \times 10^{-4} \theta^2) \times M_{VV} \quad (3.41)$$

For M_{VV} in varus,

$$F_{ACL,VV} = (0.357 + 0.5628\theta - 1.09 \times 10^{-2} \theta^2 + 5.858 \times 10^{-5} \theta^3) \times M_{VV} \quad (3.42)$$

for M_{VV} in valgus,

$$F_{ACL,IE} = (11.815 - 0.7035\theta + 9.47 \times 10^{-3} \theta^2 - 3.92 \times 10^{-5} \theta^3) \times M_{IE} \quad (3.43)$$

for M_{IE} in internal rotation direction, and

$$F_{ACL,IE} = (-3.3527 - 8.19 \times 10^{-2} \theta + 5.08 \times 10^{-4} \theta^2) \times M_{IE} \quad (3.44)$$

for M_{IE} in external rotation direction. The knee valgus-varus and internal-external rotation moments in Equations 3.41 to 3.44 were in Nm.

Sensitivity Analysis of the ACL Ultimate Load

Sensitivity analysis was performed to examine the effects of ACL ultimate load on the results of Monte Carlo simulations for the relative probability of sustaining non-contact ACL injuries. The outcome of the sensitivity analysis was the female to male injury rate ratio. The ACL ultimate load was changed in pairs to the magnitudes of 1250 N for females and 1800 N for males (Chandrashekar et al., 2006), 2000 N for both genders (McLean et al., 2003, 2004), and 2160 N for both genders (Mazzocca et al. 2003; Woo et al., 1991).

Besides the gender effect on the ACL strength, the specimen size was taken into consideration based on the study of Stapleton et al. (1998). They provided the data of ACL strength in terms of the gender and specimen size. The male specimen sizes tested were extra-large and large, and the female specimen sizes tested were medium and small. The force interval between sizes was assumed equivalent in either genders. The ACL strength in male medium size was then determined as the ACL strength of male large minus the interval

between the male large and extra-large. The ACL strength of male medium was therefore equal to 2250 N. The ACL strength of female large was the ACL strength of female medium plus the interval between the female medium and female small size. The ACL strength of female large was 2025 N. The ACL ultimate load therefore for large specimen was 2550 N and 2025 N for males and females, respectively, and 2250 N for males and 1800 N for females in medium specimen (Table 3.2.).

Table 3.2 ACL ultimate load (N) in pairs for sensitivity analysis

Source	Male	Female
Stapleton et al. (1998)	2550	2025
Stapleton et al. (1998)	2250	1800
Woo et al. (1991)& Mazzocca et al. (2003)	2160	2160
McLean et al. (2003, 2004)	2000	2000
Chandrashekar et al. (2006)	1800	1250

The female to male non-contact ACL injury rate ratio obtained from each pair of ACL ultimate load was then compared to the 5:1 non-contact ACL injury rate ratio of female basketball players to their male counterparts (Arendt and Dick, 1995). The ACL ultimate load that resulted in a simulated non-contact ACL injury rate ratio of females to males closest to 5:1 was taken as the non-contact ACL injury criteria in the corresponding male and female stochastic biomechanical models. A non-contact ACL injury occurred when the calculated ACL loading exceeded the injury criteria in the Monte Carlo simulation. Ten Monte Carlo simulations were performed for each ACL ultimate load with 100,000 iterations in each Monte

Carlo simulation. The mean and standard deviation of the number of simulated ACL injuries and the magnitudes of the independent variables of all simulated ACL injuries were documented (Figure 3.5). The probability of sustaining non contact ACL injuries was defined as relative frequency which is the number of simulated non-contact ACL injuries divided by 100,000.

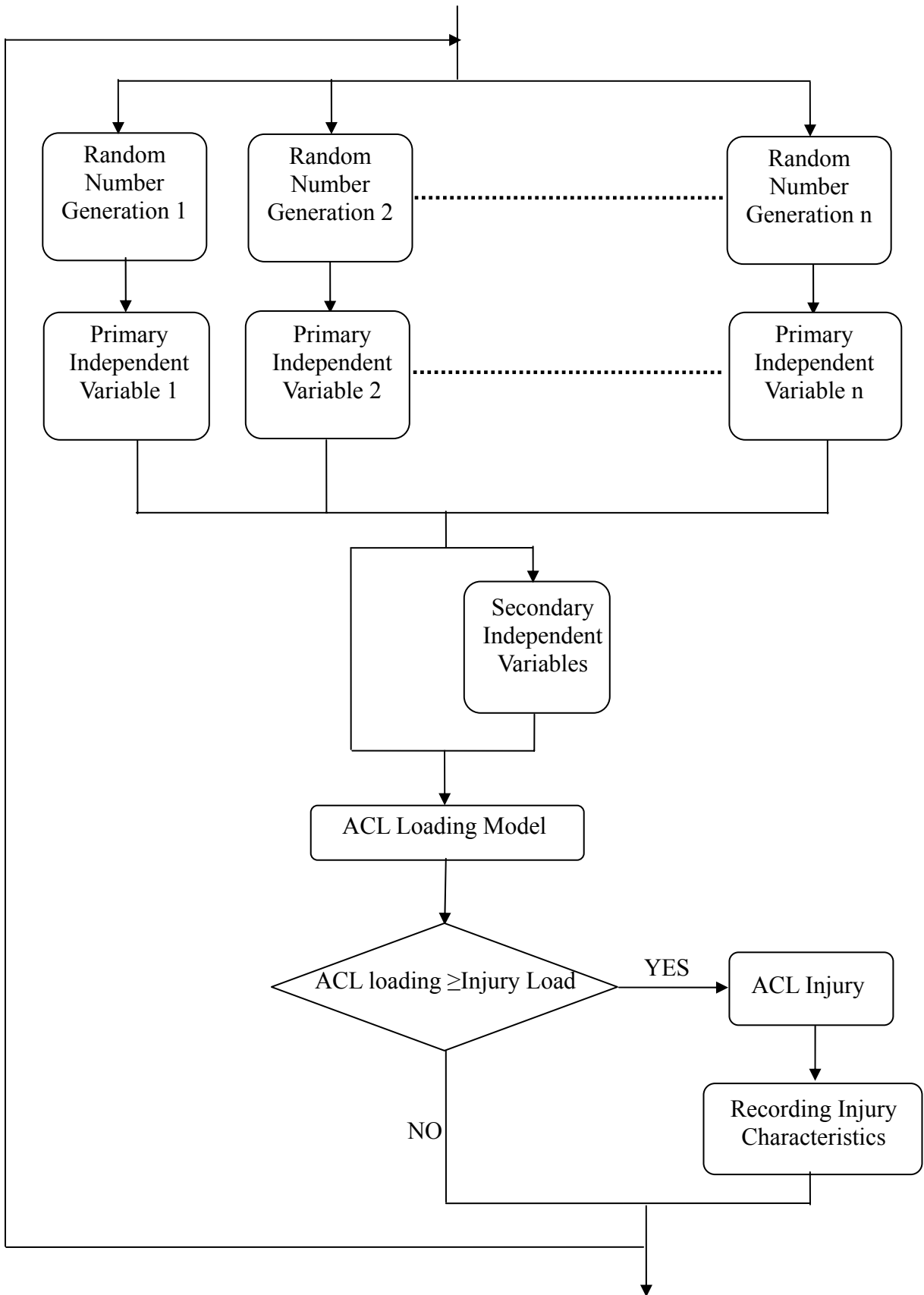


FIGURE 3.5 A flow chart of one iteration of the Monte Carlo simulation.

3.4.5. Monte Carlo Simulation for Determining Risk Factors of Sustaining Non-contact ACL Injuries

The Monte Carlo simulation was repeated with the systematically altered probability density distribution of each primary independent variable to determine the effects of each primary independent variable on the risk of sustaining non-contact ACL injuries. The probability density distribution of each primary independent variable of female subjects was replaced with the probability density distribution of the corresponding variable of male subjects. The Monte Carlo simulation was repeated 10 times with 100,000 iterations in each simulation to estimate the probability of sustaining non-contact ACL injuries for the altered probability density distribution of each altered primary independent variable. The injury probability ratio of females to males was recalculated. The results of simulations demonstrated the sensitivity of the probability of sustaining non-contact ACL injuries to each independent variable. A t-test was performed to determine if the probability of non-contact ACL injuries in females and the female-to-male injury probability ratio was significantly decreased by replacing the probability density distribution of each primary independent variable of females' with males'. A type I error rate of 0.05 was chosen to indicate statistical significance. All these procedures of the random number generation, random sampling, and Monte Carlo simulations were programmed using MATLAB computer programming language version 7.0.1. (The Mathworks Inc., Natick, MA, USA).

3.5. Assumptions of Models

Biomechanical computer modeling has been used widely to determine the effects of selected variables on the ligamentous loading. These published models included complicated

3-D knee model (McLean et al., 2003; Shelburne et al., 2004a, b) and 2-D knee model (Shelburne and Pandey, 1997; Zatsiorsky and O'Connor, 1992a, b). The simplified sagittal plane inverse dynamic knee model was developed in this study to facilitate the understanding of the effect of sagittal plane biomechanics on the ACL loading with consideration of important relevant knee geometries. The sagittal plane inverse dynamic knee model is simplistic but useful and the validity of inverse dynamic model has been well established (Nisell, 1985; Zatsiorsky, 2002). Assumptions for the sagittal plane inverse dynamic model and stochastic biomechanical model follow.

3.5.1. Assumptions for the Sagittal Plane Inverse Dynamic Knee Model

Several assumptions were made for the sagittal plane inverse dynamic knee model. These assumptions include: (1) the masses of the tibia and foot were small, and their effects on calculated joint resultants and results of Monte Carlo simulations were negligible, (2) the moments generated by passive connective tissues such as collateral ligament and joint capsule were small, and their effects on the calculated patellar tendon and quadriceps forces were negligible, (3) the effects friction force between the femur and tibia and the friction force between the femur and patella on estimated ACL loading and quadriceps muscle force were small and negligible, (4) the effect of muscle activation on the length and orientation of the muscle moment arm was small and negligible, and (5) the effects of tibial plateau tilt angle on the estimated joint resultant forces and ACL loading were small and negligible, and (6) the knee joint compressive force was ignored.

3.5.2. Assumptions for the Stochastic Biomechanical Model

The stochastic biomechanical model in this study was constructed by instrumenting the ACL loading model into the Monte Carlo simulation. The assumptions of the ACL loading model were similar to the assumptions for the sagittal plane inverse dynamic knee model. The additional assumptions of the stochastic biomechanical model include: (1) the relationship between EMG and muscle force was linear; and (2) the ACL loadings due to knee valgus-varus and internal-external rotation moments were independent to each other and additive.

CHAPTER IV

RESULTS

The empirical data used for computer simulations with a sagittal plane inverse dynamics knee model and Monte Carlo simulation were collected from 40 male and 40 female recreational athletes during the stop-jump task. The results of this study were described in four major sections in this Chapter. The first was the effects of the sagittal plane lower extremity motion patterns on the simulated ACL loading. The second part was the sensitivity analysis to determine the ACL ultimate load in male and female stochastic biomechanical models. The third section was the Monte Carlo simulations to determine the probability and the biomechanical characteristics of simulated non-contact ACL injuries. The fourth part was the Monte Carlo simulations to determine the risk factors of simulated non-contact ACL injuries.

4.1. Computer Simulation of Effects of Sagittal Plane Lower Extremity Biomechanics on Peak ACL Loading during landing of the Stop-jump Task

The relative tibial length, relative foot length, relative ankle height, and relative rear foot length were estimated from the 3-D landmark coordinates (Table 4.1) and used as critical anthropometric parameters of the sagittal plane inverse dynamic knee model. The ranges of the peak posterior ground reaction force during the landing of the stop-jump task, and the knee flexion angle, tibial tilting angle, and the location of the COP relative to the ankle joint center at the peak posterior ground reaction force were determined from the *in vivo* kinematic and

kinetic data of the 40 male and 40 female subjects (Table 4.2). The ranges of hamstring and gastrocnemius muscle forces at the peak posterior ground reaction force during the landing of the stop-jump task were obtained from the literature (Table 4.2). These data were used as independent variables to simulate peak ACL loading due to sagittal plane biomechanics during landing of the stop-jump task using the sagittal plane inverse dynamic knee model.

Table 4.1. Anthropometric data of subjects.

		Male	Female
Standing Height (m)	Mean	1.78	1.63
	SD	0.06	0.07
Body Mass (kg)	Mean	78.70	60.00
	SD	9.38	11.10
Relative Tibial Length (to Standing Height)	Mean	0.2266	0.2296
	SD	0.0073	0.0092
Relative Foot Length (to Standing Height)	Mean	0.1327	0.1319
	SD	0.0069	0.0072
Relative Ankle Height (to Standing Height)	Mean	0.0680	0.0715
	SD	0.0102	0.0094
Relative Rearfoot Length (to Foot Length)	Mean	0.4221	0.4239
	SD	0.0479	0.0430

Table 4.2. Simulated range and increment of each independent variable of the sagittal plane inverse dynamic knee model.

		Male	Female
Knee Flexion Angle (Deg)	Max.	90	90
	Min.	0	0
	Increment	5	5
Posterior Ground Reaction Force (N)	Max.	1700	1700
	Min.	100	100
	Increment	100	100
COP horizontal location relative to heel (m) (Landing on Toes/ Heels)	Max.	0.135	0.131
	Min.	0.059	0.054
	Increment		
Tibial Tilting Angle (Deg)	Max.	20	20
	Min.	-5	-5
	Increment	1	1
Hamstring Force (N)	Max.	500	500*
	Min.	0	0
	Increment	100	100
Gastrocnemius Force (N)	Max.	200	200*
	Min.	0	0
	Increment	100	100

Max=maximum; Min=minimum; N= Newton; COP= center of pressure.

*: Mean muscle force determined from Pflum et al. (2004)

The ACL loading increased as the knee flexion angle at the peak posterior ground reaction force decreased (Figure 4.1, 4.2). The rate of increase of the ACL loading increased as the peak posterior ground reaction force increased. ACL was not loaded when the knee flexion angle at the peak posterior ground reaction force was greater than 55 degrees for males and 65 degrees for females within the observed posterior ground reaction force. ACL loading was not greater than 2000 N even when the knee flexion angle at the peak posterior ground reaction force was zero degree if the peak posterior ground reaction force was less than 670 N for males and 545 N for females. The ACL loading due to the sagittal plane biomechanics could be over 2000 N if the knee flexion angle at peak posterior ground reaction force was less than 30 degrees in males and 35 degrees in females at 1700 N of posterior ground reaction force. Females' peak ACL loading was always greater than males' with the same knee flexion angle and same peak posterior ground reaction force.

The simulated ACL loading increased as the peak posterior ground reaction force increased during the landing of the stop-jump task for both genders (Figures 4.3 and 4.4). The rate of change of simulated peak ACL loading increased as the knee flexion angle at peak posterior ground reaction force decreased. The simulated peak ACL loading was not over 2000 N even when large posterior ground reaction force was applied if males landed with knee flexion angle at peak posterior ground reaction force greater than 25 degrees and females landed with knee flexion angle greater at peak posterior ground reaction force than 35 degrees.

Peak ACL loading was increased when landing on the heel in comparison to landing on the toe for both genders (Figures 4.5 and 4.6). Landing on toes with knee flexion angle at peak posterior ground reaction force greater than 26 degrees for males and 35 degrees for females,

respectively, could avoid peak ACL loading over 2000 N within the observed posterior ground reaction force (Figures 4.5 and 4.6).

The increase of posterior-tilted tibial angle decreased the simulated peak ACL loading (Figures 4.7 and 4.8). The simulated peak ACL loading at 35 degrees of knee flexion in males was below 2000 N through the entire simulated range of tibial tilting angles even when the posterior ground reaction force was increased to 2000 N. The peak ACL loading in females did not exceed 2000 N if landing at 35 degrees knee flexion angle with posterior ground reaction force smaller than 1400 N at any simulated tibial tilting angles. Females had greater peak ACL loading than males did at the same tibial tilting angle.

The effect of the hamstring force on the peak ACL loading depended on the knee flexion angle. The increase of hamstring muscle force decreased the peak ACL loading when the knee flexion angle was greater than 13 degrees in males and 16 degrees in females (Figures 4.9 and 4.11). The peak ACL loading was below 2000 N even in a landing with zero degree of knee flexion angle at 500 N of posterior ground reaction force regardless the magnitude of hamstring force. Landing at knee flexion angle at peak posterior ground reaction force smaller than 13 degrees for males and 21 degrees for females at 1000 N of posterior ground reaction force could result in a peak ACL loading greater than 2000 N if the hamstring force was increased to 500 N (Figures 4.10 and 4.12).

The peak ACL loading increased as the gastrocnemius muscle force increased for both genders. The peak ACL loading was below 2000 N in a landing with 500 N of peak posterior ground reaction force and a 200 N gastrocnemius force, a zero degree knee flexion angle at the peak posterior ground reaction force (Figures 4.13 and 4.15). The peak ACL loading increased to 2000 N if males landed at knee flexion angle smaller than 13 degrees and females landed at

knee flexion angle smaller than 21 degrees at 1000 N of posterior ground reaction force and 200 N of gastrocnemius force (Figures 4.14 and 4.16).

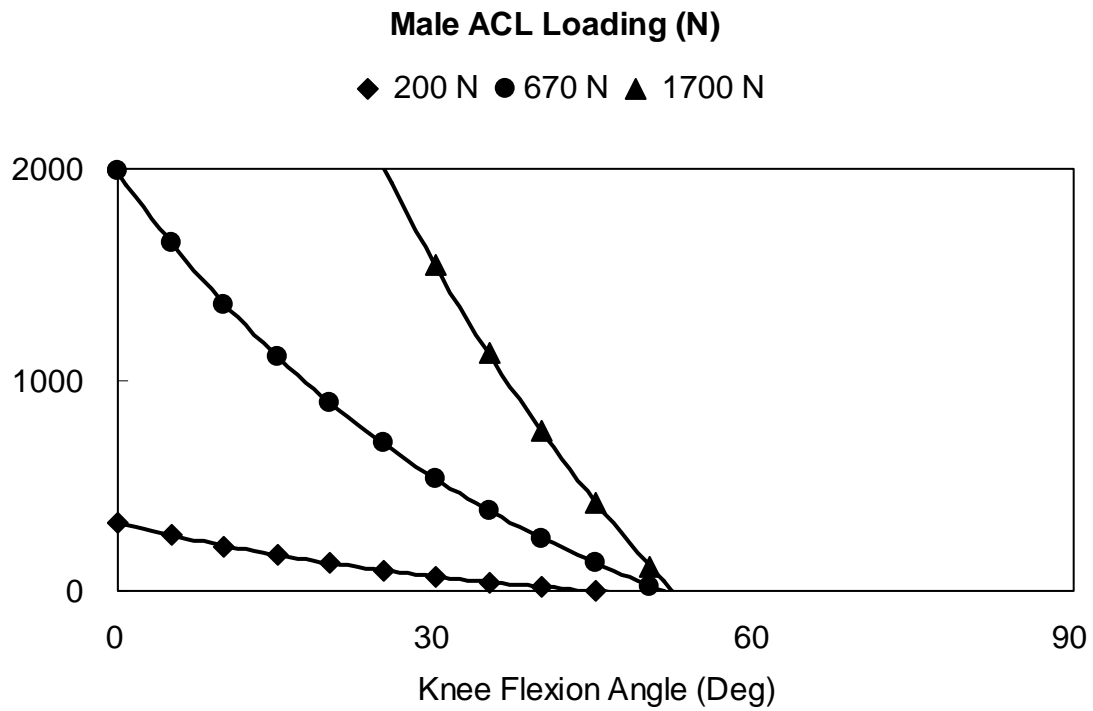


Figure 4.1. Effect of the knee flexion angle at peak posterior ground reaction force on the simulated ACL loading for males at different posterior ground reaction forces during the landing of the stop-jump task. The inputs of other independent variables during computer simulation were fixed with the corresponding values at peak posterior ground reaction force.

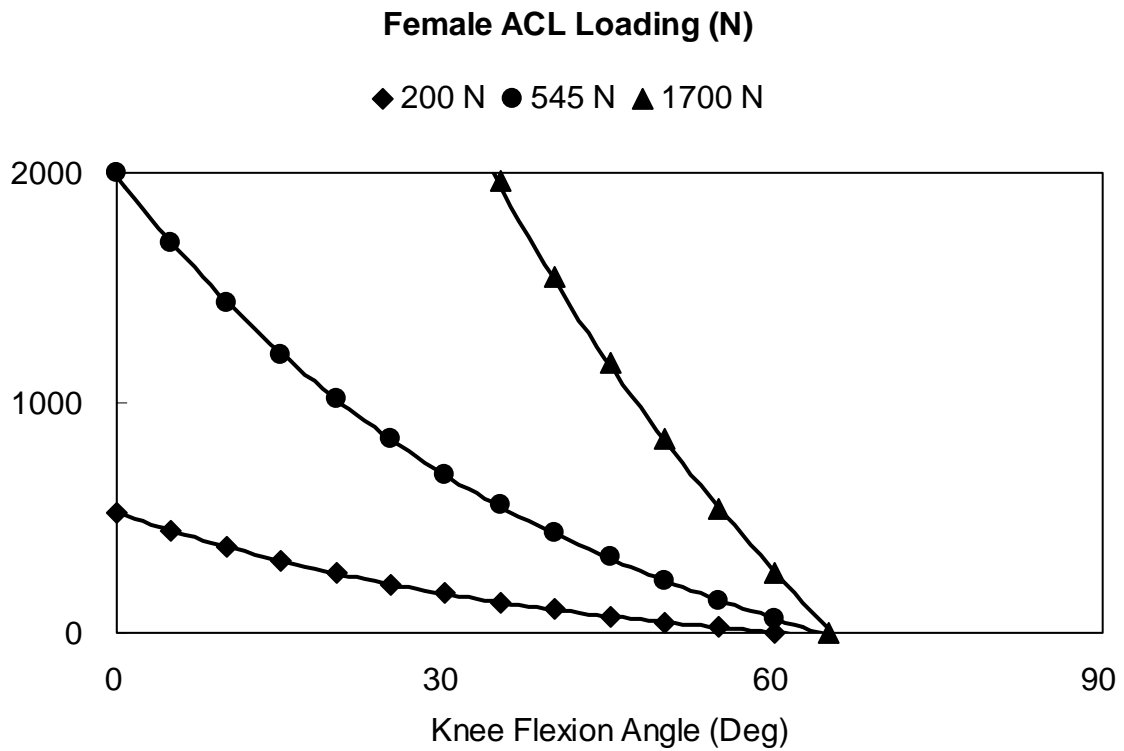


Figure 4.2. Effect of the knee flexion angle at peak posterior ground reaction force on the simulated ACL loading for females at different posterior ground reaction forces during the landing of the stop-jump task. The inputs of other independent variables during computer simulation were fixed with the corresponding values at peak posterior ground reaction force.

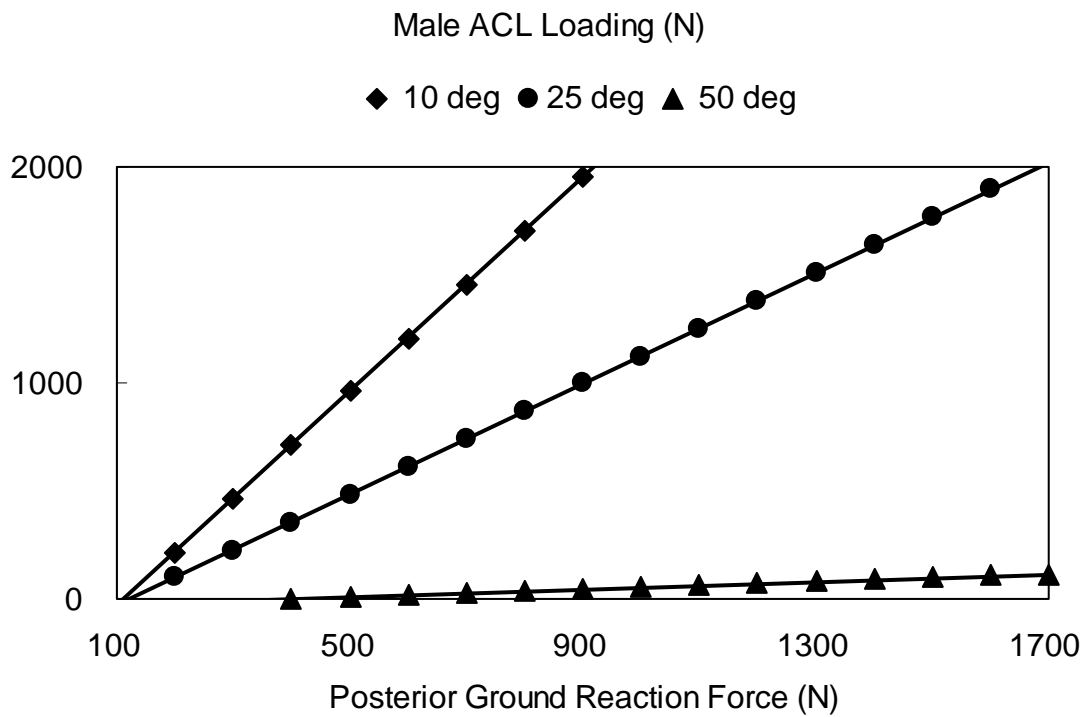


Figure 4.3. Effect of the posterior ground reaction force on the simulated ACL loading for males at different knee flexion angles during the landing of the stop-jump task. The inputs of other independent variables during computer simulation were fixed with the corresponding values at peak posterior ground reaction force.

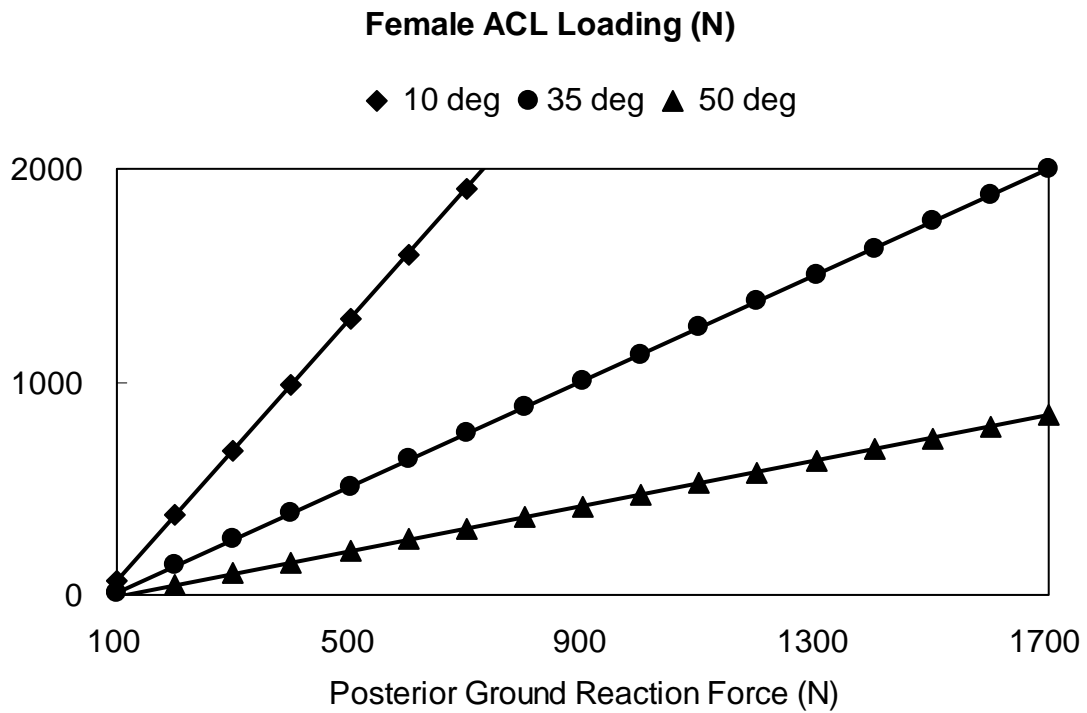


Figure 4.4. Effect of the posterior ground reaction force on the simulated ACL loading for females at different knee flexion angles during the landing of the stop-jump task. The inputs of other independent variables during computer simulation were fixed with the corresponding values at peak posterior ground reaction force.

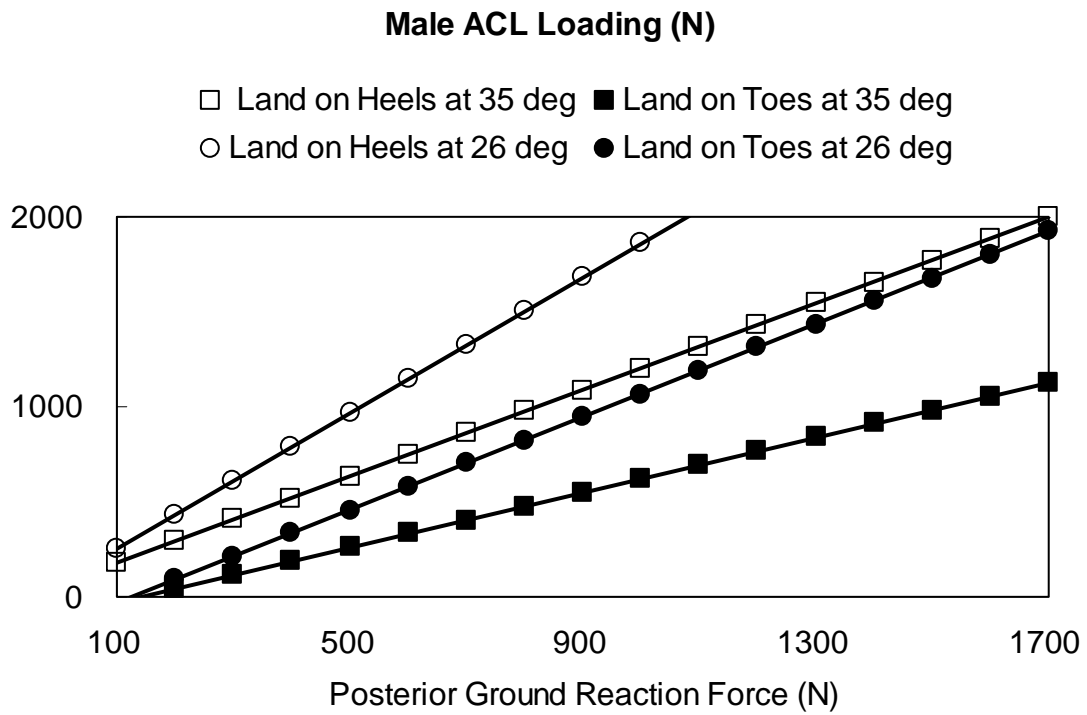


Figure 4.5. Effect of landing-on-heels and landing-on-toes on the simulated ACL loading for males during the landing of the stop-jump task. The inputs of other independent variables during computer simulation were fixed with the corresponding values at peak posterior ground reaction force.

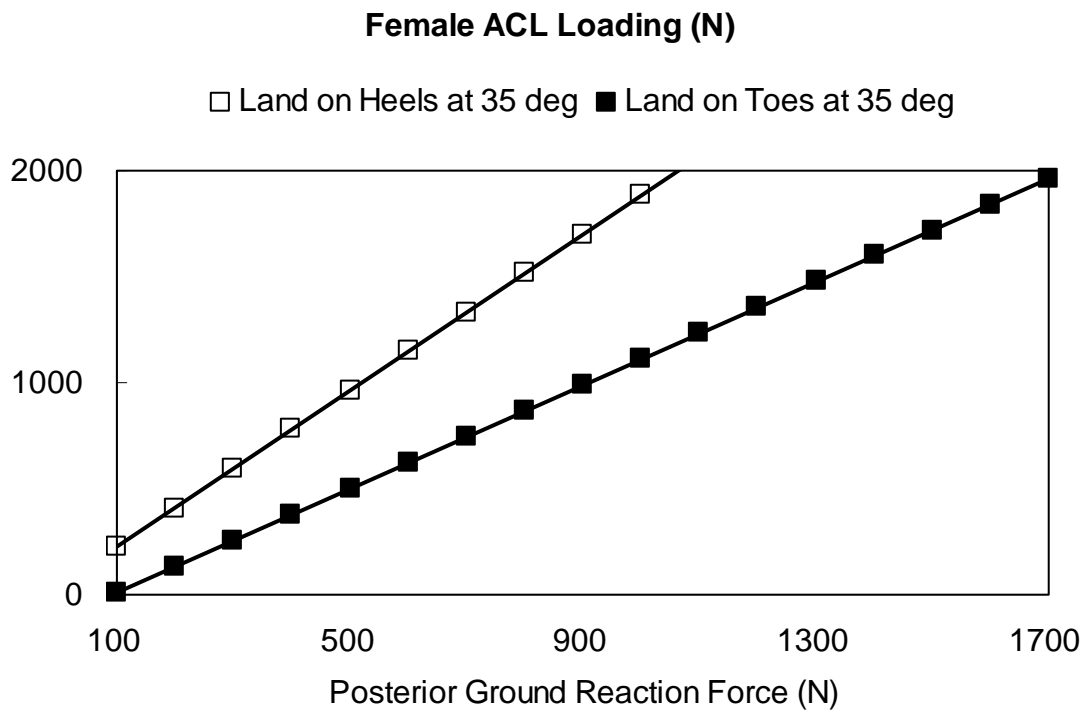


Figure 4.6. Effect of landing-on-heels and landing-on-toes on the simulated ACL loading for females during the landing of the stop-jump task. The inputs of other independent variables during computer simulation were fixed with the corresponding values at peak posterior ground reaction force.

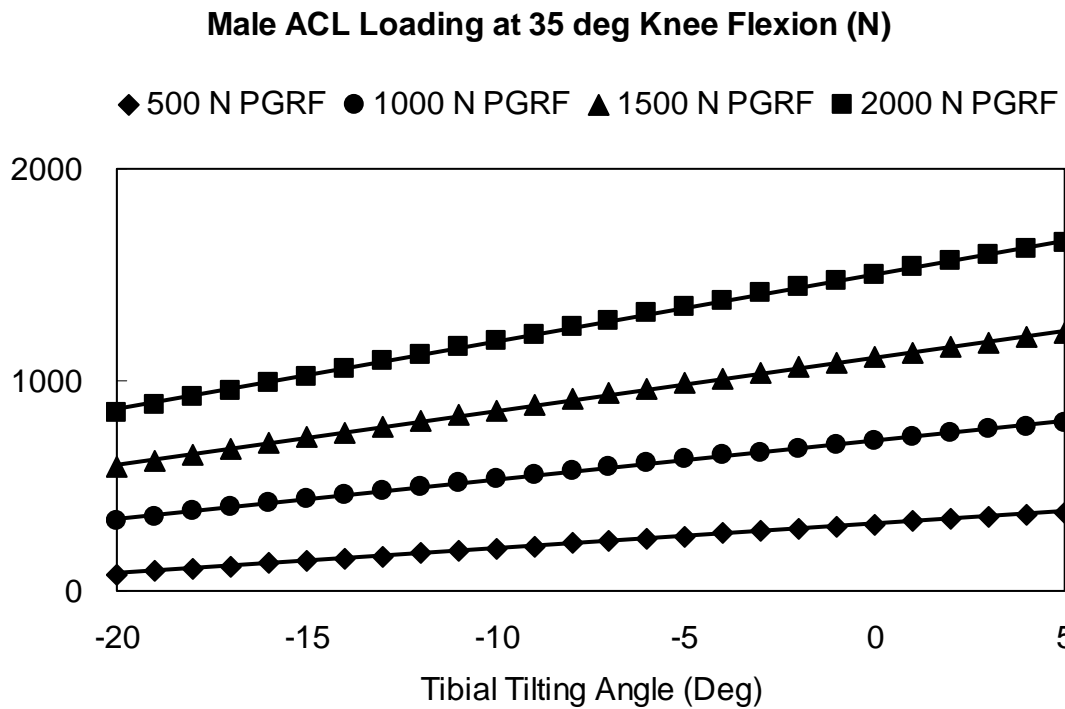


Figure 4.7. Effect of the anterior(+)-posterior(-) tibial tilting angle on the simulated ACL loading for males at different posterior ground reaction forces during the landing of the stop-jump task. The inputs of other independent variables during computer simulation were fixed with the corresponding values at peak posterior ground reaction force.

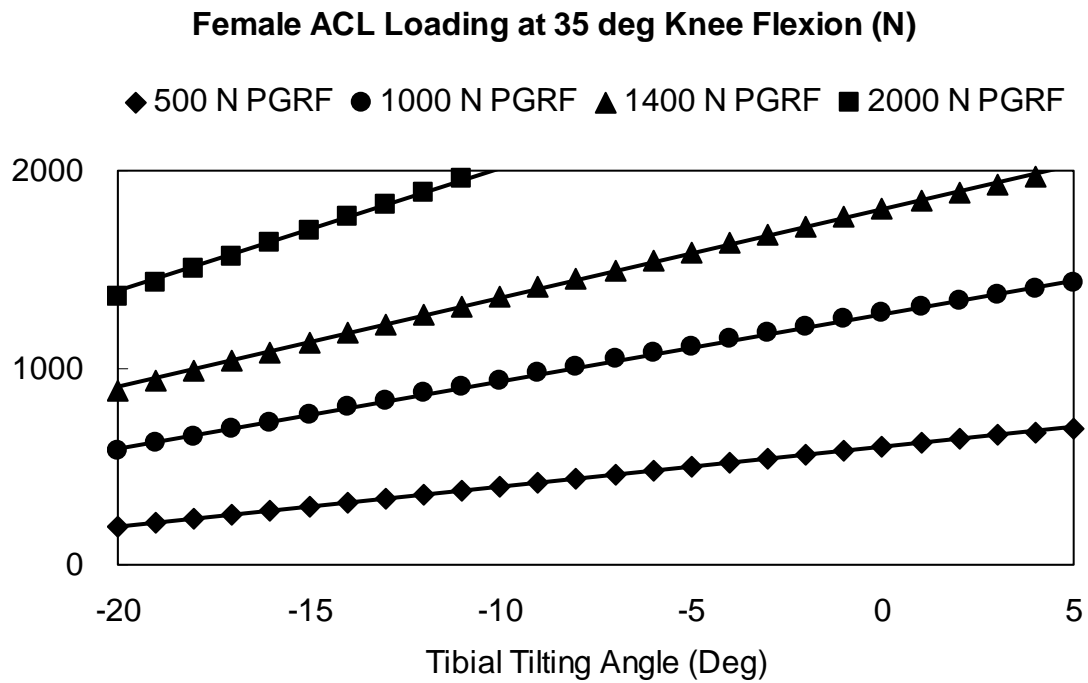


Figure 4.8. Effect of the anterior(+)-posterior(-) tibial tilting angle on the simulated ACL loading for females at different posterior ground reaction forces during the landing of the stop-jump task. The inputs of other independent variables during computer simulation were fixed with the corresponding values at peak posterior ground reaction force.

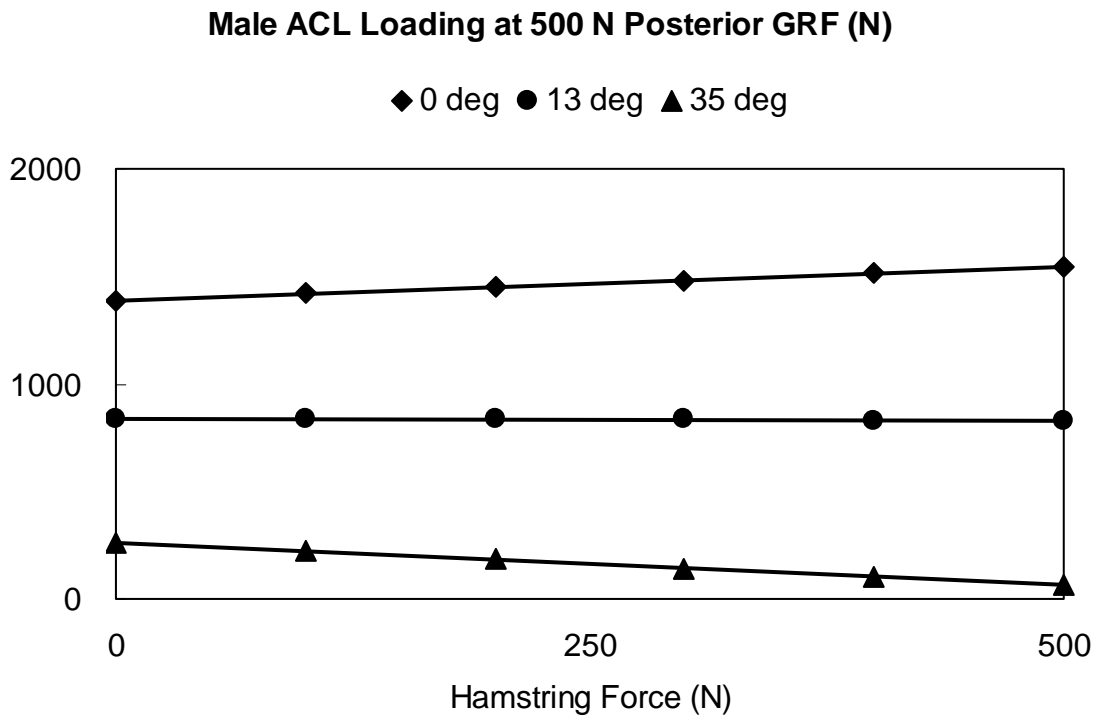


Figure 4.9. Effect of the hamstring force on the simulated ACL loading for males at 500 N of posterior ground reaction force and at different knee flexion angles during the landing of the stop-jump task. The inputs of other independent variables during computer simulation were fixed with the corresponding values at peak posterior ground reaction force.

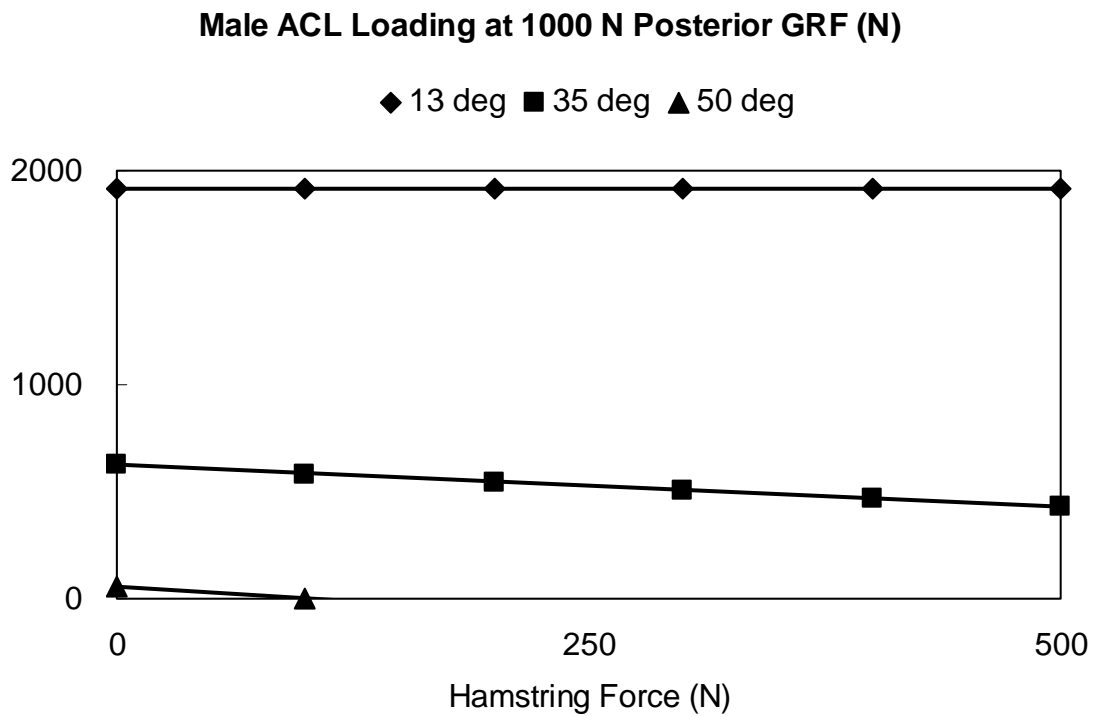


Figure 4.10. Effect of the hamstring force on the simulated ACL loading for males at 1000 N posterior ground reaction force and at different knee flexion angles during the landing of the stop-jump task. The inputs of other independent variables during computer simulation were fixed with the corresponding values at peak posterior ground reaction force.

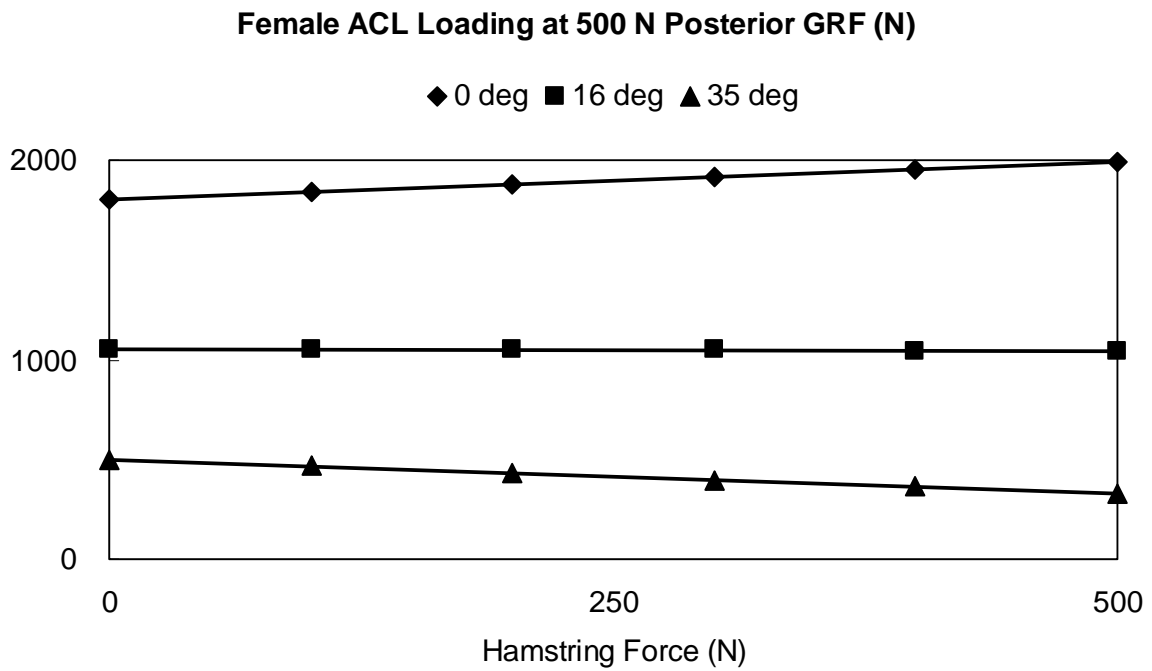


Figure 4.11. Effect of the hamstring force on the simulated ACL loading for females at 500 N of posterior ground reaction force and at different knee flexion angles during landing of the stop-jump task. The inputs of other independent variables during computer simulation were fixed with the corresponding values at peak posterior ground reaction force.

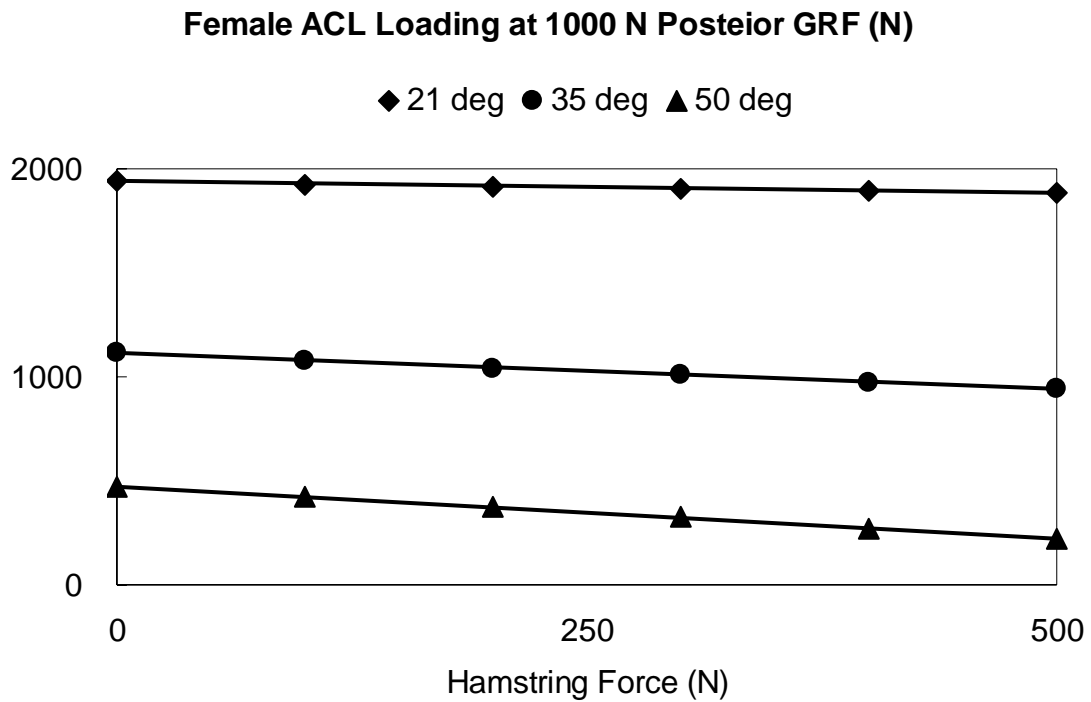


Figure 4.12. Effect of the hamstring force on the simulated ACL loading for females at 1000 N of posterior ground reaction force and at different knee flexion angles during the landing of the stop-jump task. The inputs of other independent variables during computer simulation were fixed with the corresponding values at peak posterior ground reaction force.

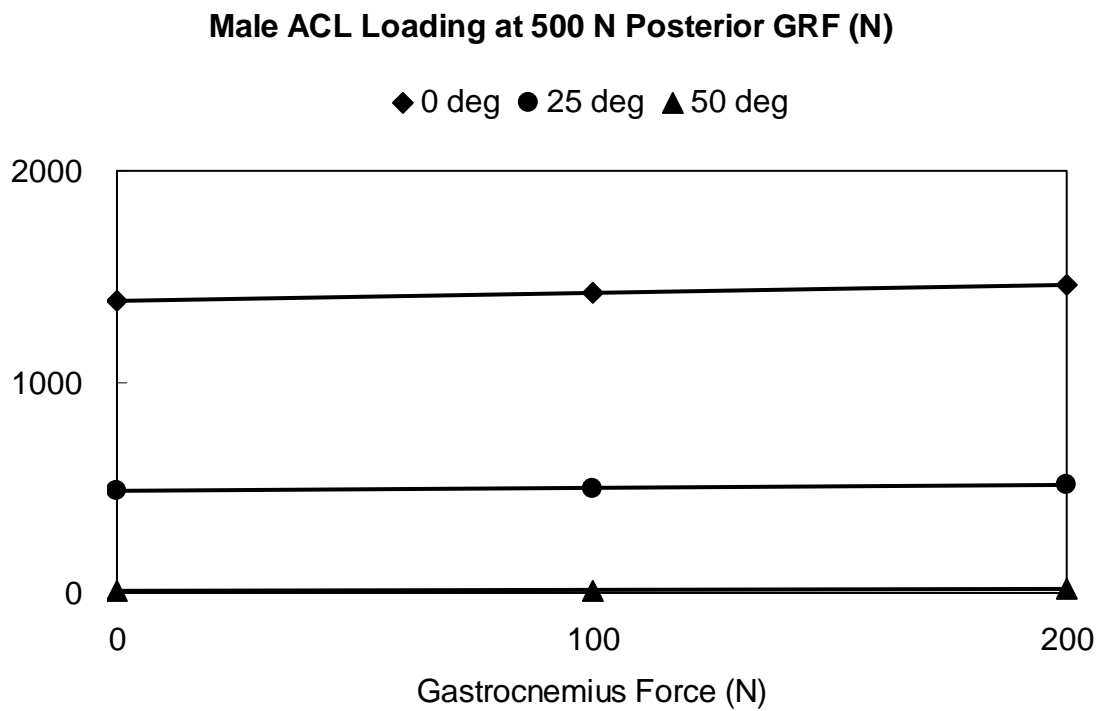


Figure 4.13. Effect of the gastrocnemius force on the simulated ACL loading for males 500 N of posterior ground reaction force and at different knee flexion angles during the landing of the stop-jump task. The inputs of other independent variables during computer simulation were fixed with the corresponding values at peak posterior ground reaction force.

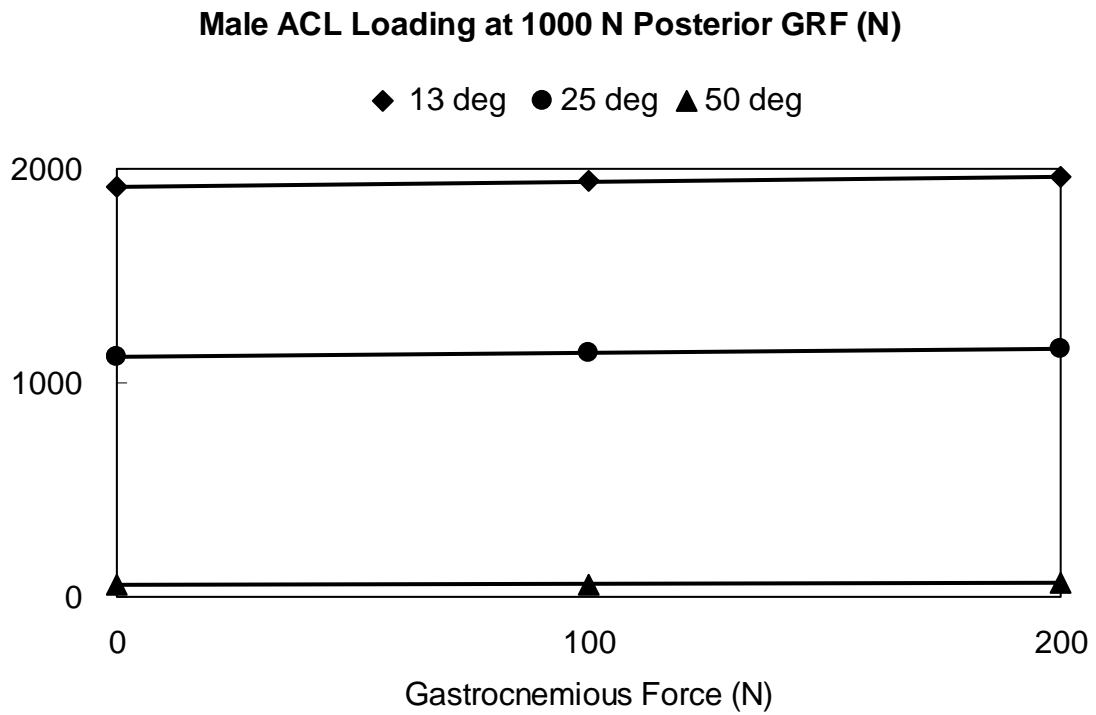


Figure 4.14. Effect of the gastrocnemius force on the simulated ACL loading for males at 1000 N of posterior ground reaction force and at different knee flexion angles during the landing of the stop-jump task. The inputs of other independent variables during computer simulation were fixed with the corresponding values at peak posterior ground reaction force.

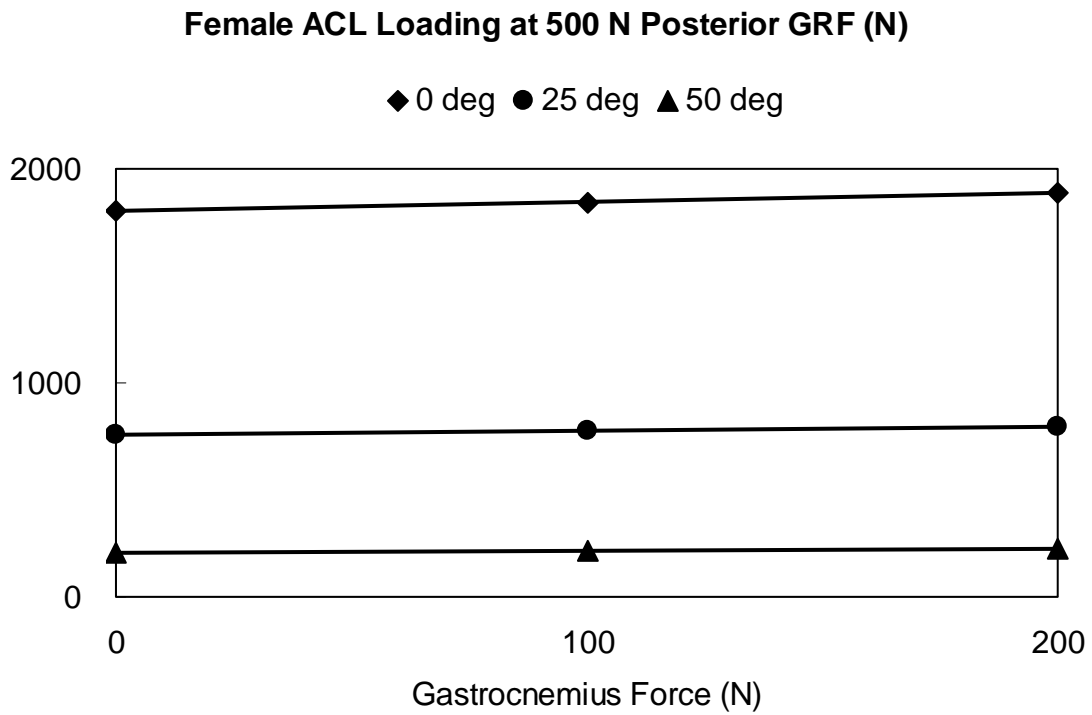


Figure 4.15. Effect of the gastrocnemius force on the simulated ACL loading for females at 500 N of posterior ground reaction force and at different knee flexion angles during the landing of the stop-jump task. The inputs of other independent variables during computer simulation were fixed with the corresponding values at peak posterior ground reaction force.

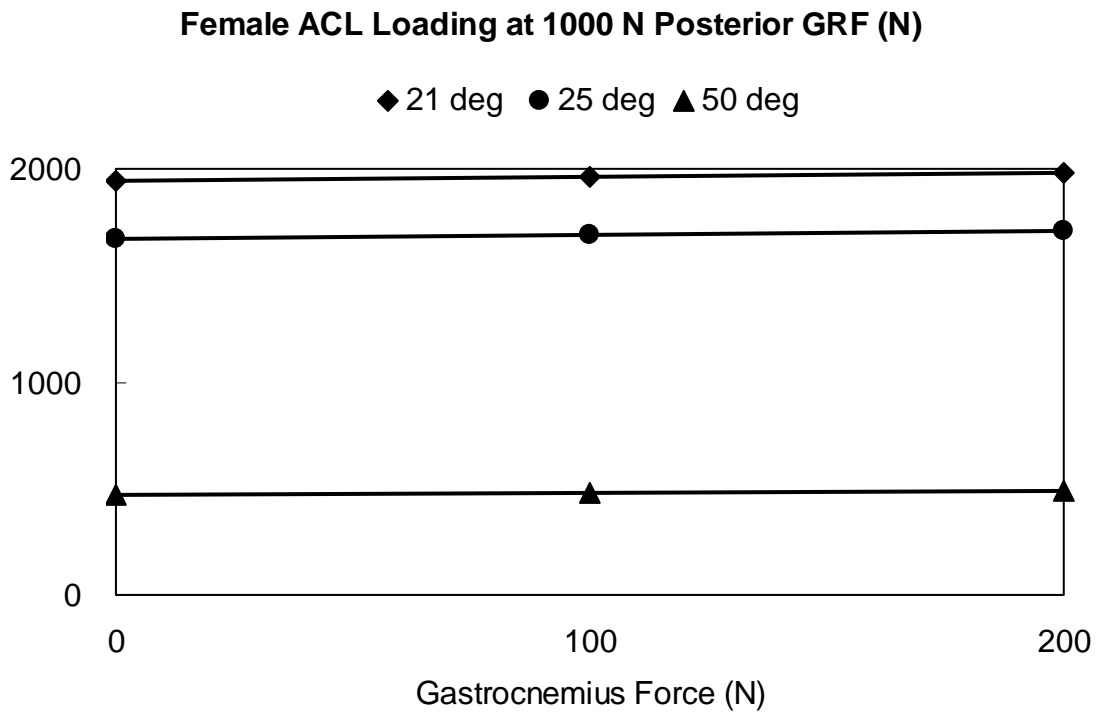


Figure 4.16. Effect of the gastrocnemius force on the simulated ACL loading for females at 1000 N of posterior ground reaction force and at different knee flexion angles during the landing of the stop-jump task. The inputs of other independent variables during computer simulation were fixed with the corresponding values at peak posterior ground reaction force.

4.2. Monte Carlo Simulation of Simulated Non-contact ACL Injuries during the Stop-jump Task

4.2.1. Goodness-of-fit Test for Independent Variables

COP to ankle joint distance, posterior ground reaction force, and gastrocnemius EMG had obvious skewness (Table 3.4). Male posterior ground reaction force and female knee flexion angle had heavy tails of the density distributions (Table 3.4).

Q-Q plot of each independent variable showed that the empirical distribution fitted well with the corresponding distribution tested (Figures 4.17 to Figure 4.20). The Q-Q plot suggested that density distribution of knee varus-valgus moment, internal-external rotation moment, tibial tilting angle, COP to ankle joint distance, and male knee flexion angle were normal distributions. The Q-Q plot suggested that density distribution of posterior ground reaction force, standing height, hamstring EMG, gastrocnemius EMG, and female knee flexion angle were gamma distributions.

Normality test accepted the normality of the density distribution of knee varus-valgus moment, internal-external rotation moment, tibial tilting angle, and male knee flexion angle. The posterior ground reaction force, standing height, hamstring EMG, and gastrocnemius EMG, and female knee flexion angle were rejected by normality test and were simulated as gamma distribution (Table 4.4). The COP to ankle joint distance was simulated as normal distribution for its value across zero and well-fitted Q-Q plot against normal distribution even though the normality test was rejected (Table 4.4).

Table 4.3. Skewness and kurtosis of each independent variable for Monte Carlo simulation.

	Male		Female	
	Skewness	Kurtosis	Skewness	Kurtosis
Knee Var-Val Moment	0.04	3.02	-0.15	2.62
Knee Int.-Ext. Rot. Moment	0.20	2.99	-0.07	2.62
COP to Ankle Distance	-0.65	3.68	-0.68	3.42
Tibial Tilting Angle	-0.02	3.63	0.09	2.64
Knee Flexion Angle	0.25	3.38	0.05	4.81
Posterior GRF	1.09	4.01	0.66	2.94
Standing Height	-0.11	1.79	-0.11	1.79
Hamstring EMG	0.24	2.28	0.11	2.20
Gastrocnemius EMG	0.58	2.55	0.40	2.23

Table 4.4. Types of distribution and p-value of each independent variable for males and females.

	Male		Female	
	Distribution	P-Value	Distribution	P-Value
Knee Var-Val Moment	Normal	0.059	Normal	0.200
Knee Int.-Ext. Rot. Moment	Normal	0.200	Normal	0.200
COP to Ankle Distance	Normal	0.000	Normal	0.000
Tibial Tilting Angle	Normal	0.200	Normal	0.200
Knee Flexion Angle	Normal	0.130	Gamma	0.000
Posterior GRF	Gamma	0.000	Gamma	0.000
Standing Height	Gamma	0.000	Gamma	0.000
Hamstring EMG	Gamma	0.008	Gamma	0.000
Gastrocnemius EMG	Gamma	0.000	Gamma	0.000

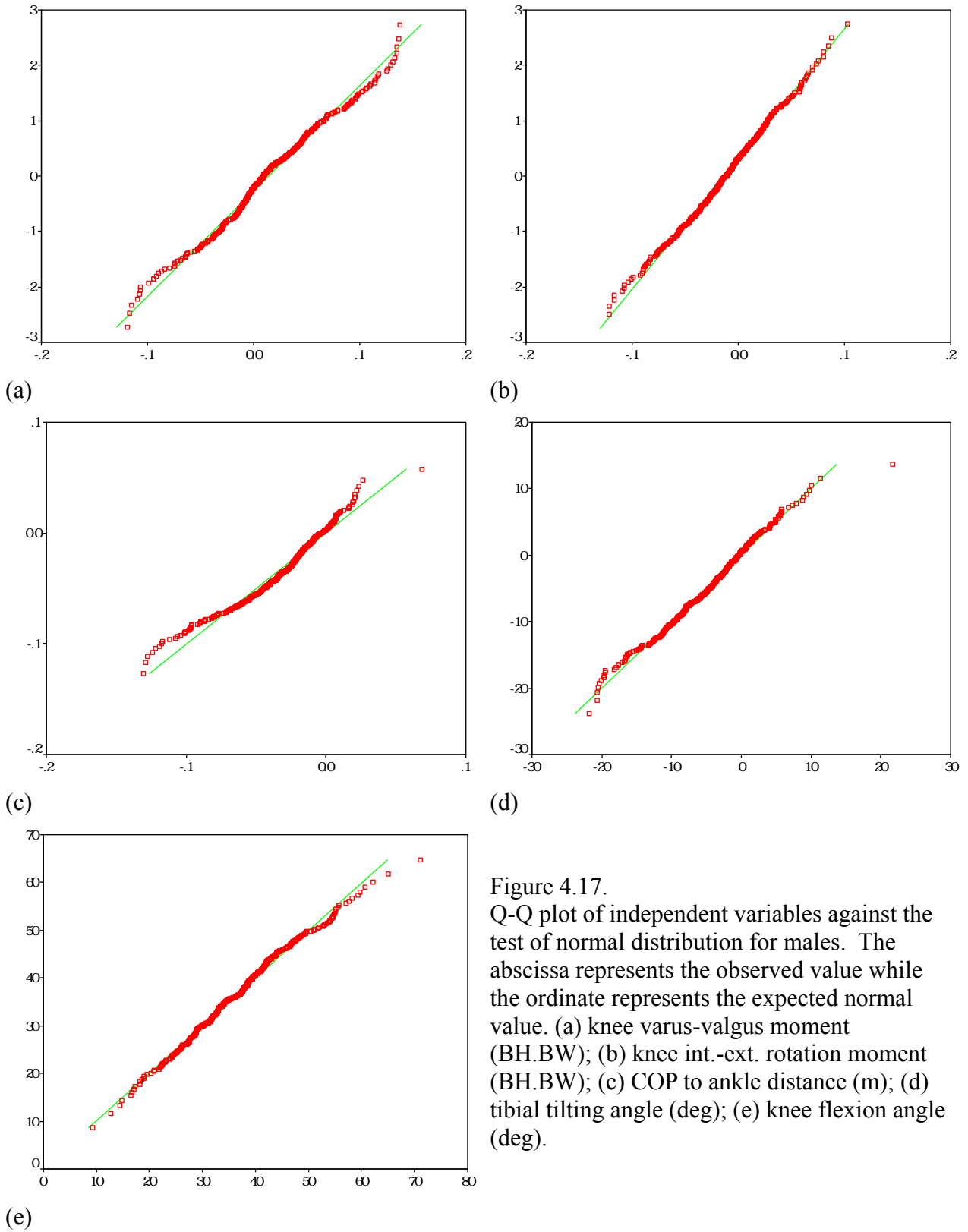


Figure 4.17.
 Q-Q plot of independent variables against the test of normal distribution for males. The abscissa represents the observed value while the ordinate represents the expected normal value. (a) knee varus-valgus moment (BH.BW); (b) knee int.-ext. rotation moment (BH.BW); (c) COP to ankle distance (m); (d) tibial tilting angle (deg); (e) knee flexion angle (deg).

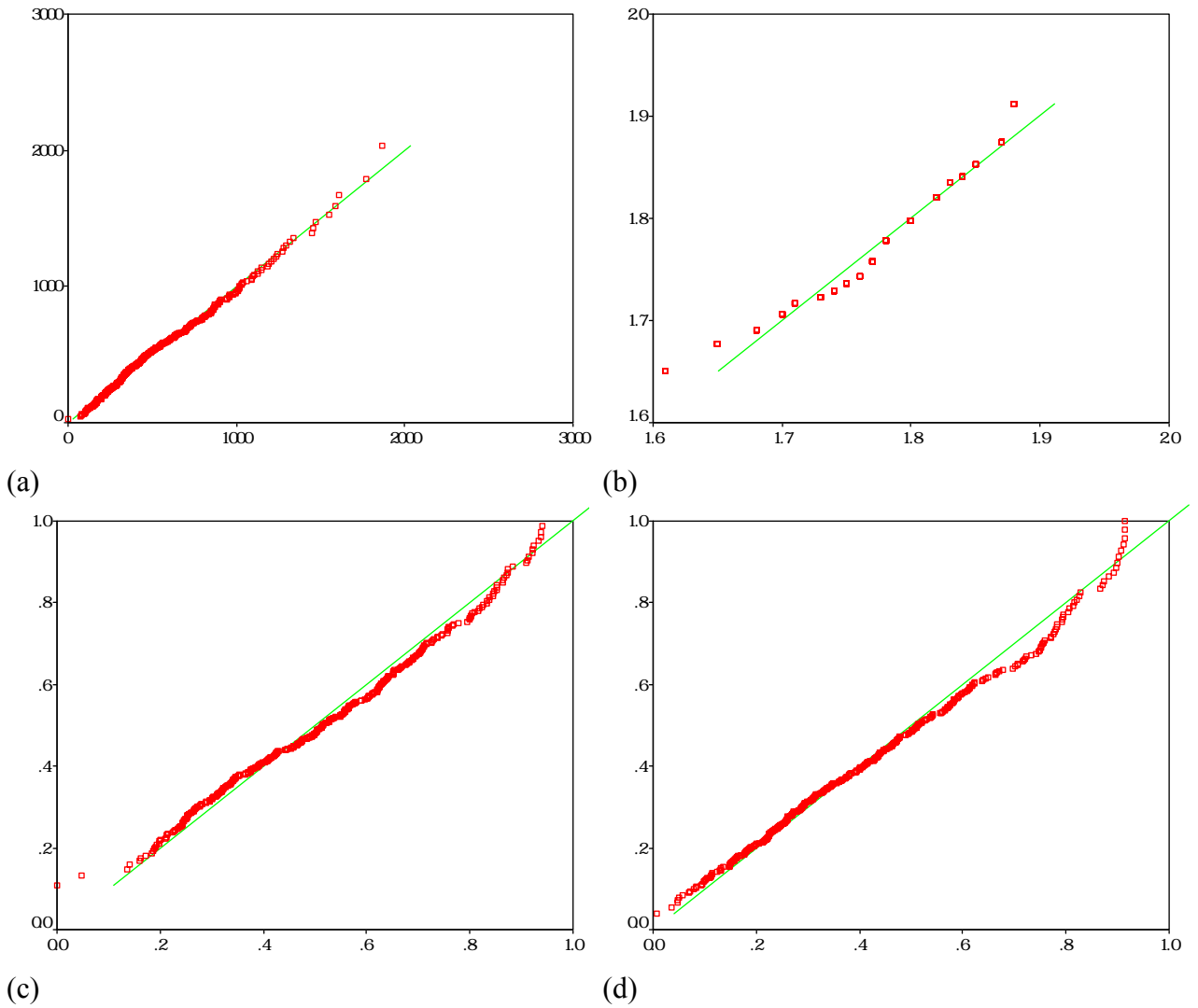


Figure 4.18. Q-Q plot of independent variables against the test of gamma distribution for males. The abscissa represents the observed value while the ordinate represents the expected gamma value. (a) posterior GRF (N); (b) standing height (m); (c) normalized linear envelope hamstring EMG ; (d) normalized linear envelope gastrocnemius EMG.

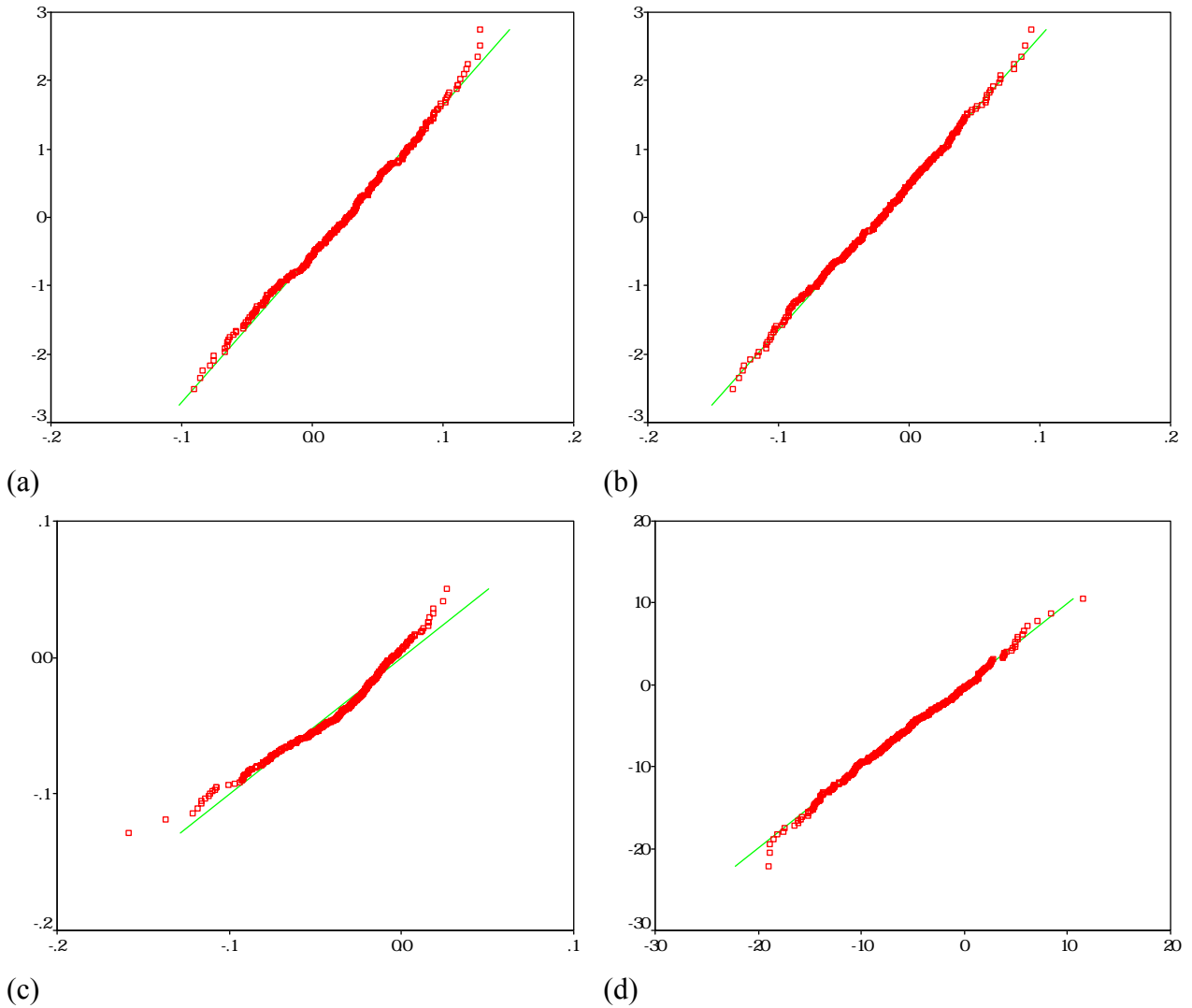


Figure 4.19. Q-Q plot of independent variables against the test of normal distribution for females. The abscissa represents the observed value while the ordinate represents the expected normal value. (a) knee varus-valgus moment (BH.BW); (b) knee int.-ext. rotation moment (BH.BW); (c) COP to ankle distance (m); (d) tibial tilting angle (deg).

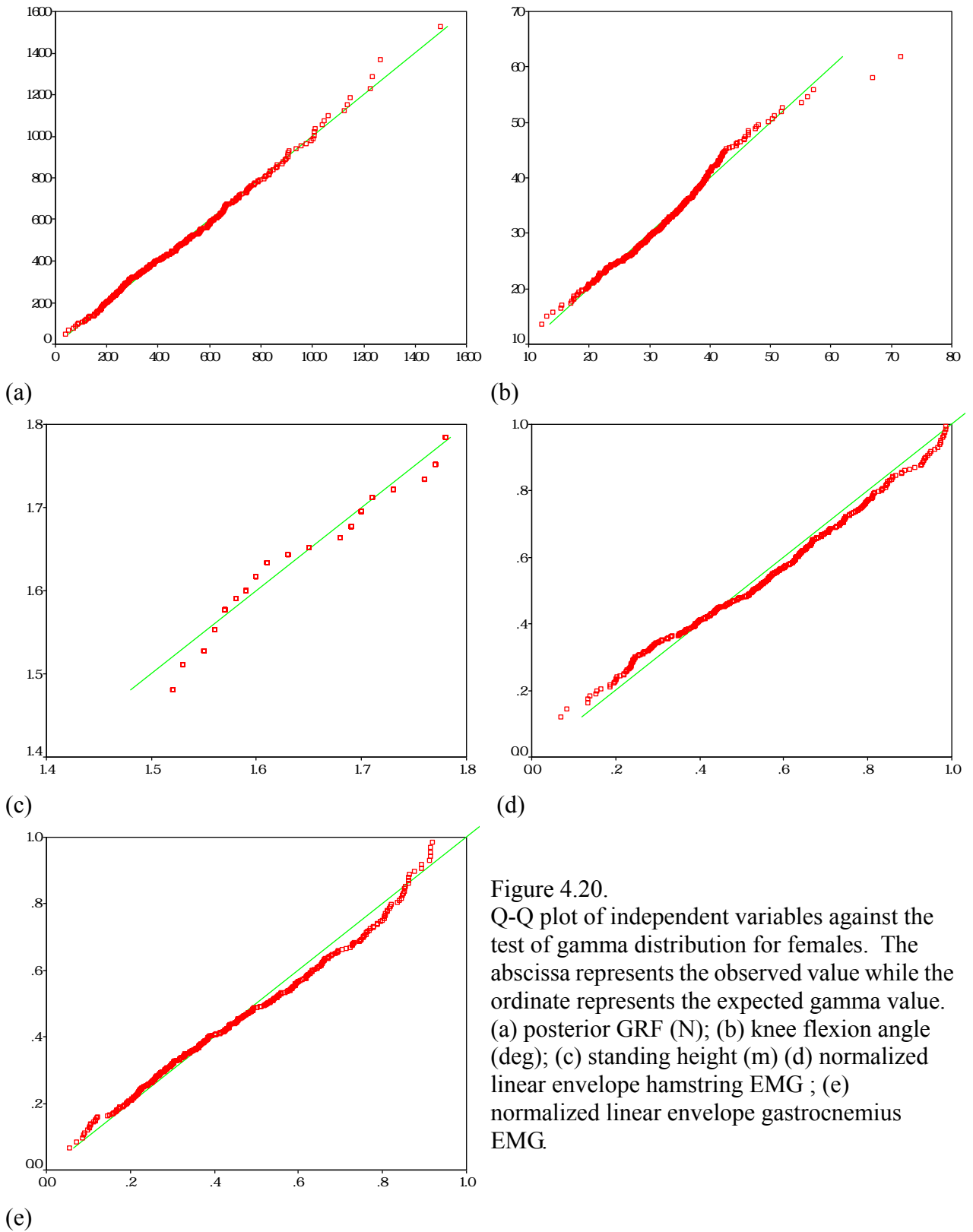


Figure 4.20. Q-Q plot of independent variables against the test of gamma distribution for females. The abscissa represents the observed value while the ordinate represents the expected gamma value. (a) posterior GRF (N); (b) knee flexion angle (deg); (c) standing height (m) (d) normalized linear envelope hamstring EMG ; (e) normalized linear envelope gastrocnemius EMG.

The mean and standard deviation of independent variables simulated as normal distribution and shape and scale parameters of those simulated as gamma distribution were calculated from empirical data of males and females (Tables 4.5 to 4.7). Mean and standard deviation of independent variables simulated as gamma distribution were provided also to aid in the understanding of the variation of the value of the independent variable.

Table 4.5 Mean and standard deviation (SD) of variables simulated as normal distribution in the stochastic biomechanical knee model.

	Male		Female	
	Mean	SD	Mean	SD
Knee Varus Moment (BH.BW)	0.01	0.05	0.02	0.05
Knee Ext. Rot. Moment (BH.BW)	0.01	0.04	0.02	0.05
COP to Ankle Distance (m)	-0.03	0.03	-0.04	0.03
Tibial Tilting Angle (deg)	-5.10	6.45	-5.85	5.62
Residual of GRF (BW)	0	0.75	0	0.71
Knee Flexion Angle (Deg)	36.70	9.66		

Table 4.6. Shape and scale parameters and mean and standard deviation (SD) of independent variables with gamma distribution for males.

	Male			
	Shape	Scale	Mean	SD
Posterior GRF (BW)	2.66	0.26	0.68	0.42
Standing Height (m)	910.81	0.002	1.78	0.06
Normalized Hamstring EMG			0.52	0.21
Hamstring Force (N)	6.01	83.13	500	203.87
Normalized Gastrocnemius EMG			0.42	0.23
Gastrocnemius Force (N)	3.35	59.69	200	109.24

Table 4.7. Shape and scale parameters and mean and standard deviation (SD) of independent variables as gamma distribution for females.

	Female			
	Shape	Scale	Mean	SD
Knee Flexion Angle (deg)	15.47	2.10	32.51	8.25
Posterior GRF (BW)	3.91	0.21	0.81	0.41
Standing Height (m)	576.08	0.003	1.63	0.07
Normalized Hamstring EMG			0.57	0.23
Hamstring Force (N)	6.09	82.05	500	202.51
Normalized Gastrocnemius EMG			0.47	0.23
Gastrocnemius Force (N)	4.31	46.41	200	96.33

4.2.2. Sensitivity Analysis of ACL Ultimate Load during the Stop-jump Task

The pair of ACL ultimate load of 2250 N for males and 1800 N for females in the stochastic biomechanical knee model resulted in a female to male non-contact ACL injury rate ratio of 4.96:1 that is essentially the same as the reported female to male ACL injury rate ratio of 5:1 (Arendt and Dick, 1995). In addition, the average of the pair of ACL ultimate load of 2250 N and 1800 N of ACL ultimate load was close to the averaged ACL ultimate load reported by Woo et al. (1991). Based on these results, the ACL ultimate load in Monte Carlo simulation of the probability of sustaining non-contact ACL injuries was set at 2250 N for males and 1800 N for females.

The ACL ultimate loads of 1800 N and 1250 N for males and females, respectively, and the ACL ultimate loads of 2550 N for males and 2025 N for females resulted in similar female to male ACL injury rate ratios that were greater than 5 (Table 4.8). The female to male ACL injury rate ratio with ACL ultimate loads set at 1800 N for males and 1250 N for females also close to 5, but the ACL injury rates were much greater than those simulated with higher ACL injury loadings.

The results also showed that the stochastic biomechanical model for the risk of sustaining non-contact ACL injuries could not appropriately predict the gender difference in the risk of sustaining non-contact if the gender difference in the strength of ACL was ignored. The female to male ACL injury rate ratio was 1.94 and 1.86 for ACL injury loading set as 2000 N and 2160 N, respectively. These two female to male ACL injury rate ratios were much lower than the ACL injury rate ratio reported in the literature.

Table 4.8. Average (SD) of number of simulated ACL injuries per 100,000 jumps and female to male non-contact ACL injury rate ratio with different ACL injury loadings.

	Source	ACL Ultimate Load (N)	Number of Injuries per 100,000 jumps	Female to Male Injury Rate Ratio
Male	McLean et al. (2003, 2004)	2000	1636 (27)	1.94 (0.05)
Female		2000	3168 (32)	
Male	Woo et al. (1991)& Mazzocca et al. (2003)	2160	1182 (24)	1.86 (0.10)
Female		2160	2202 (36)	
Male	Chandrashekar et al. (2006)	1800	2572 (25)	5.65 (0.13)
Female		1250	14540 (79)	
Male	Stapleton et al. (1998)	2250	972 (30)	<u>4.96 (0.22)</u>
Female		1800	4802 (51)	
Male	Stapleton et al. (1998)	2550	528 (10)	5.55 (0.26)
Female		2025	2930 (51)	

4.2.3. Probability and Characteristics of Simulated Injured and Uninjured Jumps

The probability of simulated non-contact ACL injuries during the stop-jump task was 0.0097 for males and 0.0480 for females in the stochastic biomechanical knee model with the ACL ultimate load as 2250 N for males and 1800 N for females. The simulated female non-contact injury rate was significantly greater than male's ($p = 0.000$).

The comparison of biomechanical characteristics between simulated injured and uninjured jumps showed that the injured jumps had smaller knee flexion angle ($p = 0.000$), posteriorly tilted tibial angle ($p = 0.000$), COP to ankle joint distance ($p = 0.000$), normalized hamstring force ($p = 0.000$), and normalized gastrocnemius force ($p = 0.028$ for males and $p = 0.000$ for females). The injured jumps also had greater normalized posterior and vertical ground reaction forces ($p = 0.000$ and $p = 0.000$), normalized knee extension moment ($p = 0.000$), normalized proximal tibial anterior shear force ($p = 0.000$), normalized patellar tendon force ($p = 0.000$), normalized quadriceps force ($p = 0.000$), normalized external valgus moment ($p = 0.000$), and normalized external internal rotation moment ($p = 0.000$) than uninjured jumps (Tables 4.9 and 4.10).

In simulated ACL injury jumps, male injured jumps had significantly smaller knee flexion angle ($p = 0.000$), posteriorly tilted tibial angle ($p = 0.000$), COP to ankle joint distance ($p = 0.000$), normalized posterior ground reaction force ($p = 0.022$), normalized external internal rotation moment ($p = 0.000$), normalized hamstring and gastrocnemius forces ($p = 0.000$, $p = 0.000$) than female injury jumps did (Table 4.11). Male injured jumps also had significantly greater normalized external valgus moment ($p = 0.000$), normalized knee extension moment ($p = 0.000$), normalized proximal tibial anterior shear force ($p = 0.000$), normalized patellar tendon force ($p = 0.000$), and normalized quadriceps

force ($p = 0.000$) when compared with female injury cases (Table 4.11).

In simulated uninjured jumps, male uninjured jumps had significantly greater knee flexion angle ($p = 0.000$) than female uninjured jumps (Table 4.12). Male simulated uninjured jumps also had significantly smaller posteriorly-tilted tibial tilting angle ($p = 0.000$), COP to ankle joint distance ($p = 0.000$), normalized posterior ground reaction force ($p = 0.000$), normalized vertical ground reaction force ($p = 0.000$), normalized external valgus moment ($p = 0.000$), normalized external internal rotation moment ($p = 0.000$), normalized hamstring and gastrocnemius force ($p = 0.000$ and $p = 0.000$), normalized patellar tendon force ($p = 0.000$), normalized quadriceps force ($p = 0.000$), normalized knee extension moment ($p = 0.000$), and normalized proximal tibial anterior shear force ($p = 0.000$) when compared with female uninjured jumps (Table 4.12).

Sagittal plane lower extremity biomechanics had significantly greater contribution to total ACL injury loading than non-sagittal plane biomechanics did in simulated injured jumps for both genders ($p = 0.000$, $p = 0.000$). The contribution of sagittal plane lower extremity biomechanics to the total ACL injury loading was 1839.86 (894.81) N for males and 1773.27 N (603.83) for females, while the contribution of non-sagittal plane biomechanics to the total ACL loading was 926.83 (666.45) N for males and 501.20 (388.81) N for females.

Replacement of density distribution of females' varus-valgus moment with that from Hewett et al. (2005) significantly decreased the contribution from non-sagittal loadings to total ACL loading from 501.20 (388.81) N to 183.69 (168.02) N ($p = 0.000$) (Table 4.13).

Table 4.9. Mean (SD) of biomechanical characteristics of simulated injured and uninjured jumps with 2250 N as ACL ultimate load for males.

	Injured	Uninjured	P-Value
Knee Flexion Angle (Deg)	21.95 (8.03)	36.83 (9.56)	0.000
Tibial Tilting Angle (Deg)	-1.98 (6.19)	-5.13 (6.45)	0.000
COP to Ankle Distance (m)	0.02 (0.03)	0.04 (0.03)	0.000
Posterior GRF (BW)	1.44 (0.57)	0.67 (0.41)	0.000
Vertical GRF (BW)	2.69 (1.09)	1.72 (0.90)	0.000
Knee Ext. Valgus Moment (BH.BW)	0.07 (0.07)	0.01 (0.05)	0.000
Knee Ext. Int. Rot. Moment (BH.BW)	0.02 (0.04)	0.01 (0.04)	0.000
Hamstrings Force (BW)	0.62 (0.26)	0.67 (0.28)	0.000
Gastrocnemius Force (BW)	0.26 (0.14)	0.27 (0.15)	0.028
Patellar Tendon Force (BW)	13.06 (5.27)	4.86 (3.84)	0.000
Quadriceps Force (BW)	11.42 (4.59)	4.25 (3.37)	0.000
Knee Extension Moment (BH.BW)	0.38 (0.16)	0.13 (0.12)	0.000
Proximal Tibial Ant Shear Force (BW)	1.33 (0.59)	0.51 (0.42)	0.000
Sagittal Contribution (N)	1839.86 (894.81)	60.61 (408.68)	0.000
Non-Sagittal Contribution (N)	926.83 (666.45)	187.30 (427.75)	0.000

BH.BW: moment normalized to body height (m) and body weight (kgw).

Table 4.10. Mean (SD) of biomechanical characteristics of simulated injured and uninjured jumps with 1800 N as ACL ultimate load for females.

	Injured	Uninjured	P-Value
Knee Flexion Angle (Deg)	24.87 (5.61)	32.88 (8.20)	0.000
Tibial Tilting Angle (Deg)	-3.36 (5.38)	-5.97 (5.60)	0.000
COP to Ankle Distance (m)	0.02 (0.03)	0.04 (0.03)	0.000
Posterior GRF (BW)	1.45 (0.47)	0.78 (0.38)	0.000
Vertical GRF (BW)	2.56 (0.97)	1.76 (0.85)	0.000
Knee Ext. Valgus Moment (BH.BW)	0.06 (0.05)	0.02 (0.05)	0.000
Knee Ext. Int. Rot. Moment (BH.BW)	0.03 (0.04)	0.02 (0.05)	0.000
Hamstrings Force (BW)	0.78 (0.33)	0.86 (0.36)	0.000
Gastrocnemius Force (BW)	0.33 (0.16)	0.34 (0.17)	0.000
Patellar Tendon Force (BW)	12.91 (4.15)	5.64 (3.50)	0.000
Quadriceps Force (BW)	11.27 (3.62)	4.93 (3.06)	0.000
Knee Extension Moment (BH.BW)	0.37 (0.13)	0.15 (0.11)	0.000
Proximal Tibial Ant Shear Force (BW)	1.30 (0.47)	0.59 (0.38)	0.000
Sagittal Contribution (N)	1773.27 (603.83)	346.71 (444.85)	0.000
Non-sagittal Contribution (N)	501.20 (388.81)	165.96 (297.93)	0.000

BH.BW: moment normalized to body height (m) and body weight (kgw).

Table 4.11. Mean (SD) of injured biomechanical characteristics of simulated jumps with 2250 N for males and 1800 N for females as ACL ultimate load.

	Male	Female	P-Value
Knee Flexion Angle (Deg)	21.95 (8.03)	24.87 (5.61)	0.000
Tibial Tilting Angle (Deg)	-1.98 (6.19)	-3.36 (5.38)	0.000
COP to Ankle Distance (m)	0.015 (0.03)	0.019 (0.03)	0.000
Posterior GRF (BW)	1.44 (0.57)	1.45 (0.47)	0.022
Vertical GRF (BW)	2.69 (1.09)	2.56 (0.97)	0.000
Knee Ext. Valgus Moment (BH.BW)	0.07 (0.07)	0.06 (0.05)	0.000
Knee Ext. Int. Rot. Moment (BH.BW)	0.02 (0.04)	0.03 (0.04)	0.000
Hamstrings Force (BW)	0.62 (0.26)	0.78 (0.33)	0.000
Gastrocnemius Force (BW)	0.26 (0.14)	0.33 (0.16)	0.000
Patellar Tendon Force (BW)	13.06 (5.27)	12.91 (4.15)	0.013
Quadriceps Force (BW)	11.42 (4.59)	11.27 (3.62)	0.010
Knee Extension Moment (BH.BW)	0.38 (0.16)	0.37 (0.13)	0.000
Proximal Tibial Ant Shear Force (BW)	1.33 (0.59)	1.30 (0.47)	0.000
Sagittal Contribution (N)	1839.86 (894.81)	1773.27 (603.83)	0.001
Non-Sagittal Contribution (N)	926.83 (666.45)	501.20 (388.81)	0.000

BH.BW: moment normalized to body height (m) and body weight (kgw).

Table 4.12. Mean (SD) of uninjured biomechanical characteristics of simulated jumps with 2250 N for males and 1800 N for females as ACL ultimate load.

	Male	Female	P-Value
Knee Flexion Angle (Deg)	36.83 (9.56)	32.88 (8.20)	0.000
Tibial Tilting Angle (Deg)	-5.13 (6.45)	-5.97 (5.60)	0.000
COP to Ankle Distance (m)	0.035 (0.032)	0.04 (0.03)	0.000
Posterior GRF (BW)	0.67 (0.41)	0.78 (0.38)	0.000
Vertical GRF (BW)	1.72 (0.90)	1.76 (0.85)	0.000
Knee Ext. Valgus Moment (BH.BW)	0.01 (0.05)	0.02 (0.05)	0.000
Knee Ext. Int. Rot. Moment (BH.BW)	0.01 (0.04)	0.02 (0.05)	0.000
Hamstrings Force (BW)	0.67 (0.28)	0.86 (0.36)	0.000
Gastrocnemius Force (BW)	0.27 (0.15)	0.34 (0.17)	0.000
Patellar Tendon Force (BW)	4.86 (3.84)	5.64 (3.50)	0.000
Quadriceps Force (BW)	4.25 (3.37)	4.93 (3.06)	0.000
Knee Extension Moment (BH.BW)	0.13 (0.12)	0.15 (0.11)	0.000
Proximal Tibial Ant Shear Force (BW)	0.51 (0.42)	0.59 (0.38)	0.000
Sagittal Contribution (N)	60.61 (408.68)	346.71 (444.85)	0.000
Non-sagittal Contribution (N)	187.30 (427.75)	165.96 (297.93)	0.000

BH.BW: moment normalized to body height (m) and body weight (kgw).

Table 4.13. Mean of contribution from non-sagittal loadings to total ACL loading in injured jumps subjected to the change of varus-valgus moment from literature in female stochastic biomechanical model and 1800 N as ACL injury criterion.

Independent Variable	Non-Sagittal Contribution (SD)	Difference in Non-Sagittal Contribution (p-value)
Original Non-Sagittal Contribution	501.20 (388.81)	
Hewett et al. (2005)	183.69 (168.02)	-351 (0.000)*

*: Significance at Type I error rate = 0.05.

4.3. Risk Factors of Simulated Non-contact ACL Injuries

The numbers of non-contact ACL injuries in females were significantly reduced when their density distributions of independent variables were replaced with males' density distributions of independent variables (Table 4.14). The simulated female to male non-contact ACL injury rate ratios with males' density distributions of knee flexion angle at the peak posterior ground reaction force and peak posterior ground reaction force decreased by 1.52 ($p = 0.000$) and 1.49 ($p = 0.000$), respectively. Although replacing female subjects' density distributions of knee valgus-varus moment, internal-external rotation moment, and hamstring muscle force with those of male subjects' also resulted in decreases in simulated female-to-male injury rate ratios, the decreases were generally less than 0.22. The numbers of non-contact ACL injuries in females and female-to-male injury rate ratio were significantly increased when female subjects' density distributions of tibial tilting angle and COP to ankle joint distance were replaced with those of male subjects' ($p = 0.000$ and $p = 0.000$). The numbers of non-contact ACL injuries in females and

female-to-male injury rate ratio were not significantly decreased when female subjects' density distributions of gastrocnemius force was replaced with that of male subjects' ($p = 0.481$ and $p = 0.563$)

The numbers of non-contact ACL injuries in females were significantly reduced compared with the original numbers of non-contact ACL injury resulted from females' motion patterns and females' ACL injury loading (Table 4.14). The female to male non-contact ACL injury rate ratio with all males' lower extremity motion patterns but females' ACL injury loading was 2.79 (Table 4.14). The female to male non-contact ACL injury rate ratio with males' lower extremity motion patterns that would reduce females' ACL loading was 2.36 (Table 4.14).

Table 4.14. Mean of numbers of non-contact ACL injury per 100,000 jumps and female to male non-contact ACL injury rate ratio subjected to the change of each independent variable in female Monte Carlo simulations and 1800 N as ACL injury criterion.

Independent Variable	Number of Injuries (SD)	Difference in Number of Injuries (p-value)*	Injury Rate Ratio (SD)	Difference in Injury Rate Ratio (p-value)*
Female Motion Patterns	4802 (51)		4.96 (0.22)	
Males' Knee Flexion Angle	3328 (42)	-1474 (0.000)	3.44 (0.25)	-1.52 (0.000)
Males' Posterior GRF	1683 (43)	-1436 (0.000)	3.47 (0.20)	-1.49 (0.000)
Males' Var-Val Moment	3366 (52)	-212 (0.000)	4.74 (0.22)	-0.22 (0.000)
Males' Int.-Ext. Rot. Moment	4678 (45)	-124 (0.034)	4.83 (0.31)	-0.13 (0.040)
Males' Tibial Tilting Angle	5106 (24)	304 (0.000)	5.27 (0.32)	0.31 (0.000)
Males' COP to Ankle Distance	5288 (29)	486 (0.000)	5.46 (0.32)	0.50 (0.000)
Males' Hamstring Force	4690 (41)	-112 (0.045)	4.85 (0.31)	-0.11 (0.046)
Males' Gastrocnemius Force	4766 (42)	-36 (0.481)	4.92 (0.33)	-0.04 (0.563)
Positive Male Motion Patterns [†]	2282 (44)	-2520 (0.000)	2.36 (0.18)	-2.60 (0.000)
All Male Motion Patterns ^{††}	2702 (55)	-2100 (0.000)	2.79 (0.19)	-2.18 (0.000)

*: Significance at Type I error rate = 0.05.

†: Positive male motion patters included knee flexion angle, posterior GRF, varus-valgus moment, internal-external rotation moment, hamstring force and gastrocnemius force.

††: All male motion patters were knee flexion angle, posterior GRF, COP to ankle joint distance, tibial tilting angle, varus-valgus moment, internal-external rotation moment, hamstring and gastrocnemius force.

CHAPTER V

DISCUSSION

The assumptions of the sagittal plane biomechanical model of the knee and the stochastic biomechanical model of the risk of sustaining non-contact ACL injuries are discussed in this chapter. Also, the results of computer simulations of ACL loading using the sagittal plane inverse dynamic model of the knee are interpreted in this Chapter. Further, the results of Monte Carlo simulations of the probability of sustaining non-contact ACL injuries in the stop-jump task using the stochastic biomechanical model of the ACL loading are discussed. Furthermore, the limitations of this study and future studies that are needed are discussed.

5.1. Effects of Assumptions on the Validity of the Sagittal Plane Inverse Dynamic Model of the Knee

A sagittal plane inverse dynamic knee model was developed in this study to determine the effects of sagittal plane lower extremity biomechanics on the ACL loading. This sagittal plane inverse dynamic knee model then served as a major component of the stochastic biomechanical model of non-contact ACL injuries. The sagittal plane inverse dynamic knee model of the ACL loading developed in this study has the following assumptions:

1. the masses and moments of inertia of the foot and lower leg segments were small and negligible;
2. the tibial plateau was perpendicular to the longitudinal axis of the tibia; and

3. the tibiofemoral joint compressive loading had not effect on ACL loading.

These assumptions should not affect the validity of the sagittal plane inverse dynamic knee model of the ACL loading.

Omitting the masses and moments of inertia of the foot and lower leg segments should not affect the validity of the inverse dynamic knee model for ACL loading. The total mass of the foot and lower leg segments was less than 6% of total body mass (Hinrichs, 1990) while the moments of inertia of the foot and lower leg segments relative to their own centers of mass are 0.0038 kg.m² and 0.0505 kg.m² (Hinrichs, 1990). The errors in the calculated joint resultant forces and moments due to omitting these small inertia properties of the foot and lower leg segments were less than 3% of the calculated joint resultant forces and moments without omitting the inertia properties of the foot and lower leg. The error in the estimated ACL loading due to these errors in the calculated joint resultant forces and moments were less than 2%, which should not significantly affect results of this study.

Ignoring the tibial plateau posterior slope should not affect the validity of the inverse dynamic knee model of the ACL loading. Giffin et al. (2004) tested 10 cadaver knees using robotic manipulator under three loading conditions: 200 N axial compression, 134 N anterior-posterior tibial load, and combined 200 N axial compression and 134 N anterior-posterior loads at different knee flexion angles and different slopes of tibial plateau. The slope of tibial plateau was $8.8 \pm 1.8^\circ$ in intact knees and $13.2 \pm 2.1^\circ$ after osteotomy. They found that an increase of the tibial posterior slope at conditions of anterior-posterior load and combined loads did not significantly increase the *in situ* force of the ACL and anterior tibial translation at all knee flexion angles tested in their cadaver knee model. For a 1000 N proximal tibial anterior shear force perpendicular to the longitudinal axis of the tibia, the projection of

this force parallel to the tibial plateau with tibial plateau posterior tilt angle of 8° is about 990 N. This means that the error in estimated ACL anterior shear force bearing is about 1%, and that the error in estimated ACL loading is about 2%.

The omission of the tibiofemoral joint compressive loading in the inverse dynamic knee model of ACL loading should not affect the validity of the computer simulation results of ACL loading at the peak posterior ground reaction force during the landing of the stop-jump task. Torzilli et al. (1994) investigated the effect of the joint compressive force and quadriceps force on the tibial translation of nine intact cadaver knees at different knee flexion angles. The results of their study demonstrated that combined quadriceps load and joint compressive load resulted in a small increase of anterior tibial translation ($<2\text{mm}$). The addition of 100 N anterior shear force to the combined joint compressive load and quadriceps force also resulted in a small increase in forced anterior tibial translation (1 to 3 mm). This result indicated the ACL strain was likely to be increased when the compressive joint load was applied, but the effect should be minimal. Pandy and Shelburne (1997) used a sagittal plane knee model to predict the relationships between the forces developed by muscles, external loads applied to the leg, and forces induced in the cruciate ligaments during isometric exercises. Their results indicated that the tibiofemoral joint compressive force did not significantly affect the ACL force. Fleming et al. (2003) measured the ACL strain when the knee was doing flexion and extension exercises against the external torque with and without the compressive load applied. Their results showed that the applied external load to produce the tibiofemoral compressive load did not significantly change the ACL strain. Based on these results, the omission of the tibiofemoral joint load should not significantly affect our interpretation of simulated ACL loading.

The sagittal plane inverse dynamic knee model of ACL loading is a useful tool to understand the major determinant of peak ACL loading in studies on non-contact ACL injuries. Literature repeatedly demonstrated that sagittal plane biomechanics are the major determinant of ACL loading. Markolf et al. (1995) presented that the combined valgus and external rotation loading resulted in smaller ACL loading than that due to either knee valgus or external rotation moment loading alone. The non-sagittal plane biomechanics is not necessary to increase the ACL loading but the sagittal plane biomechanics does. It would depend on how the individual lands and what the lower extremity motion patterns are. Berns et al. (1992) and Fleming et al. (2001) also demonstrated that sagittal plane biomechanics are the major determinant of ACL loading, and that non-sagittal plane biomechanics has limited effects on the ACL loading. The literatures support the importance of the sagittal plane inverse dynamic knee model of ACL loading developed in this study and the application of this model in studies on non-contact ACL injuries. This model is a useful tool to provide the important knowledge and understandings of non-contact ACL injuries.

The sagittal plane inverse dynamic model of ACL loading developed in this study, however, has limited ability to study how the lower extremity motor control affect ACL loading. The sagittal plane inverse dynamic model of ACL loading developed in this study can only be used to estimate ACL loading at a given lower extremity configuration with a given external loading condition. This model can not provide information regarding the development of ACL loading as a function of continuous lower extremity motion as the forward dynamic model of ACL loading developed by McLean et al. (2003a) does.

5.2. Effects of Assumptions on the Validity of the Stochastic Biomechanical Model of the Probability of Sustaining Non-contact ACL injuries

The stochastic biomechanical model of non-contact ACL injuries developed in this study has the following additional assumptions:

1. the muscle force has linear relationship with normalized EMG;
2. the sagittal plane knee loading, valgus-varus knee loading, and internal-external rotation loading are independent to each other.

These assumptions should not affect the validity of the stochastic biomechanical model developed in this study.

The assumption of linear relationship between normalized EMG and muscle force is well supported by the literature (Hatze, 1981; Kaufman et al., 1991). Hatze (1981) and Kaufman et al. (1991) demonstrated that muscle activation level measured by normalized EMG was the major determinant of the muscle force even in dynamic condition. Using the standard deviation of the normalized hamstring and gastrocnemius EMG to predict the standard deviation of the muscle forces for the stochastic biomechanical knee model, therefore, should be adequate.

The effects of non-sagittal plane biomechanics on peak ACL loading in the stochastic biomechanical model of non-contact ACL injuries are likely to be overestimated. The effects of knee valgus-varus moment and knee internal-external rotation moment on ACL loading were assumed to be independent to each other. Markolf et al. (1995), however, has demonstrated the *in vitro* ACL force resulted from the combined loading of anterior tibial shear force and either valgus-varus or internal-external rotation moment did not increase in proportion to that from single loading in either plane. The combined loading of valgus

moment with either internal or external torque applied did not always increase the ACL loading and the force was not the simple summation of two forces applied. The contribution of non-sagittal plane biomechanics on non-contact ACL injuries calculated in this study, therefore, was likely to be overestimated. As a result of overestimate of the contribution of non-sagittal plane biomechanics to the non-contact ACL injuries, the non-contact ACL injury rate for each gender may also be over estimated. This overestimate of the non-contact ACL injury rate, however, should not significantly affect the female to male non-contact ACL injury rate ratio because (1) the results of this study demonstrated that non-sagittal plane biomechanics were not major contributors to peak ACL loading even when their effects were over estimated, and (2) most of the over estimated non-contact ACL injury rates in two genders were canceled out each other when calculating the female to male non-contact ACL injury rate ratios.

5.3. Effects of Sagittal Plane Biomechanics on the ACL loading

5.3.1. Effect of the Knee Flexion Angle on the ACL Loading

The knee flexion angle affects the ACL loading. Decreasing knee flexion angle results in an increase in ACL loading while the other lower extremity kinematic and kinetic conditions are the same. The increased ACL loading caused by the decrease in the knee flexion angle is attributed to the increases in the patellar tendon-tibial shaft angle and ACL elevation angle (Figure 5.1). Nunley et al. (2003) demonstrated that the patellar tendon-tibial shaft angle increases as the knee flexion angle decreases. An increase in patellar tendon-tibial shaft angle tends to increase the anterior shear component of the patellar tendon force that increases proximal tibial anterior shear force and the ACL loading, especially at a small knee flexion

angle. Li et al. (2005) demonstrated the *in vivo* ACL elevation angle was correlated to the knee flexion angle while weight bearing. The ACL elevation angle was expressed as an exponential function of the knee flexion angle in this study based on the relationship reported by Li et al. (2005). The relationship between the ACL elevation angle and the knee flexion angle shows that the ACL elevation angle increases as the knee flexion angle decreases. An increase in the ACL elevation angle tends to increase the ACL loading, especially when the knee flexion angle is small.

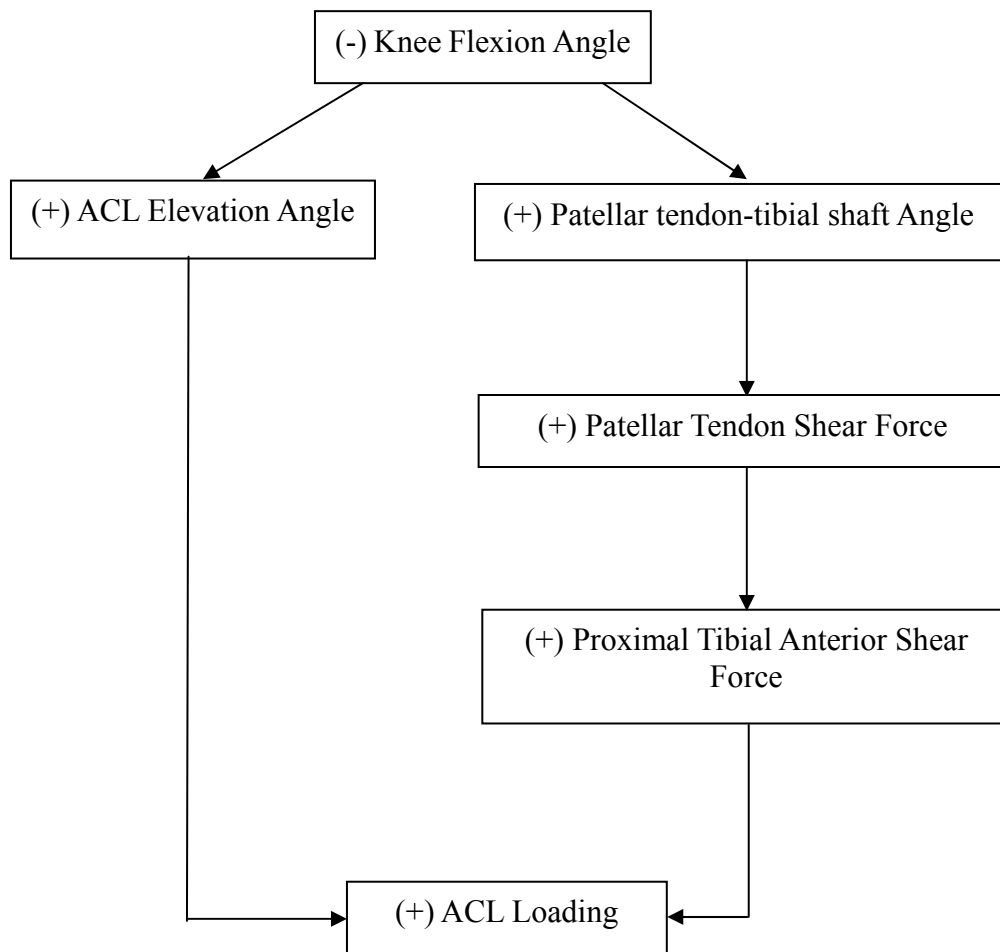


Figure 5.1 A flow chart of how the knee flexion angle affects the ACL Loading. (+): indicates increase; (-): indicates decrease.

The relationship between simulated ACL loading and the knee flexion angle is consistent with the result of *in vitro* and *in vivo* studies (Markolf et al., 1990, 1995; Fleming et al., 1999; Li et al., 1999) and computer simulation (Pandy and Shelburne, 1997) in the literature. Markolf et al. (1990, 1995) measured the ACL force with various resultants at different knee flexion angle. They showed that the *in situ* ACL force decreases with increase of knee flexion angles. Li et al. (1999) investigated the effect of muscle forces on the *in situ* ACL force at knee flexion angles of 15°, 30°, 60°, 90°, and 120°. They found that the *in situ* ACL force peaked at 15° and decreased as the knee flexion angle increased to 90°. Pandey and Shelburne (1997) used a sagittal plane knee model to predict the relationship between the muscle forces, external load, and cruciate ligament force at various knee flexion angles. Their results demonstrated that the ACL force decreased as the knee flexion angle increased during isometric quadriceps contraction. Fleming et al. (1999) studied the *in vivo* ACL strain during stair climbing activity. They reported the ACL strain increased as the knee flexion angle decreased where the ACL is more susceptible to injury. These studies investigating the relationship between the ACL loading or ACL strain and the knee flexion angles support our simulated results of that the ACL loading increases as the knee flexion angle decreases.

The difference in the ACL loading at large knee flexion angle between present study and Markolf et al. (1995) should be noticed. The ACL is unloaded when the knee flexion angle is greater than 55 degrees for males and 65 degrees for females in our model, while the ACL was loaded even when the knee flexion angle was greater than 65 degrees in the study by Markolf et al. (1995). This difference can be explained by the different ways to load the ACL in the two studies. The ACL was loaded by a constant external shear force on the proximal end of the tibia in the study by Markolf et al. (1995) while the ACL was loaded by the patellar

tendon force in the present study. The ACL loading will be a function of ACL elevation angle affected by the knee flexion angle when a constant external shear force is applied at the proximal end of the tibia to load the ACL. The ACL loading will be a function of patellar tendon-tibial shaft angle and ACL elevation angle if the ACL is loaded by the patellar tendon force. Literature has demonstrated that the patellar tendon-tibial shaft angle becomes negative at large knee flexion angle (Smidt, 1973; Nisell, 1985; Nunley et al., 2003). The patellar tendon force, therefore, will not be able to load the ACL at large knee flexion angle.

The ACL is more likely at risk when landing at a small knee flexion angle accompanied by a large posterior ground reaction force. The rate of increase (slope) of the ACL loading increases as the peak posterior ground reaction force increases indicates the small amount of decrease of knee flexion angle can dramatically increase the ACL loading if lands with large peak posterior ground reaction force than that lands with small peak posterior ground reaction force (Figure 4.1 and 4.2). This simulation result also indicates that the knee flexion angle and peak posterior ground reaction force has an interaction effect on the ACL loading.

Sagittal plane biomechanics alone may not be able to injure the ACL when the knee flexion angle is greater than 25 degrees for males and 35 degrees for females. The results of this study demonstrated that the ACL loading due to sagittal plane biomechanics was not greater than 2000 N when the knee flexion angle is greater than 25 degrees for males and 35 degrees for females within the range of the observed magnitudes of peak posterior ground reaction force during landing of the stop-jump task (Figures 4.3 and 4.4). Considering that the sagittal plane biomechanics is the major loading mechanism of the ACL, these knee flexion angles, therefore, can be considered as ACL Safe Knee Flexion Angles, which may be used as

specific training objectives of lower extremity configuration in future training programs for the prevention of non-contact ACL injuries.

The ACL Safe Knee Flexion Angle for female athletes is greater than that for male athletes. This gender difference can be explained by the gender difference in the patellar tendon-tibial shaft angle and the gender differences in the moment arms of the patellar tendon, hamstrings and gastrocnemius muscles. Nunley et al. (2003) showed that females have larger patellar tendon-tibial shaft angle than males do at the same knee flexion angle. With the other conditions the same, female athletes need to have greater knee flexion angle than male athletes do to keep ACL loading below 2000 N because of the gender difference in the relationship between knee flexion angle and patellar tendon-tibial shaft angle. Also, female athletes have smaller moment arm of the patellar tendon, hamstring and gastrocnemius muscles than male athletes do. Because of this gender difference in the patellar tendon-tibial shaft angle and the knee flexion and extension muscles, the ACL loading is greater for females than for males with the same knee flexion angle and posterior ground reaction force. Females need to have larger knee flexion angle than males do to ensure the ACL loading is below the injury loading. These results indicate that the targeted lower extremity configurations in future training programs for the prevention of non-contact ACL injuries should be different for different genders.

5.3.2. Effect of the Posterior Ground Reaction Force on the ACL Loading

Posterior ground reaction force affects ACL loading. Increase of the posterior ground reaction force during landing increases the ACL loading by increasing the quadriceps force. Increasing posterior ground reaction force applied on the foot during landing results in an increase in external knee flexion moment. The increase in the external knee flexion moment

demands an increase in internal knee extension moment, which will result in an increase in quadriceps muscle forces because the quadriceps muscles are the major generator of this internal knee extension moment. Increased quadriceps force results in an increase in patellar tendon force and, therefore, an increase in anterior shear force at the proximal end of the tibia, especially at small knee flexion angles. The increased proximal tibial anterior shear force tends to increase the ACL loading (Figure 5.2). The ground reaction forces are also affected by the lower extremity motions which include the hip and knee angular velocities. The lower extremity configuration, knee flexion angle, does not directly affect the ground reaction forces, but instead, affects the patellar tendon force distribution to the ACL.

Sagittal plane biomechanics may not be able to injure the ACL when the posterior ground reaction force is below 670 N for males and 545 N for females. The results of this study demonstrated that ACL loading due to sagittal plane biomechanics was not greater than 2000 N when the posterior ground reaction force is less than 670 N for males and 545 N for females even if the knee is at the full extension position during landing of the stop-jump task (Figures 4.1 and 4.2). These magnitudes of posterior ground reaction force, therefore, can be considered as the ACL Safe Posterior Ground Reaction Force, which can also be used as specific training objectives for soft landing in future training programs for the prevention of non-contact ACL injuries.

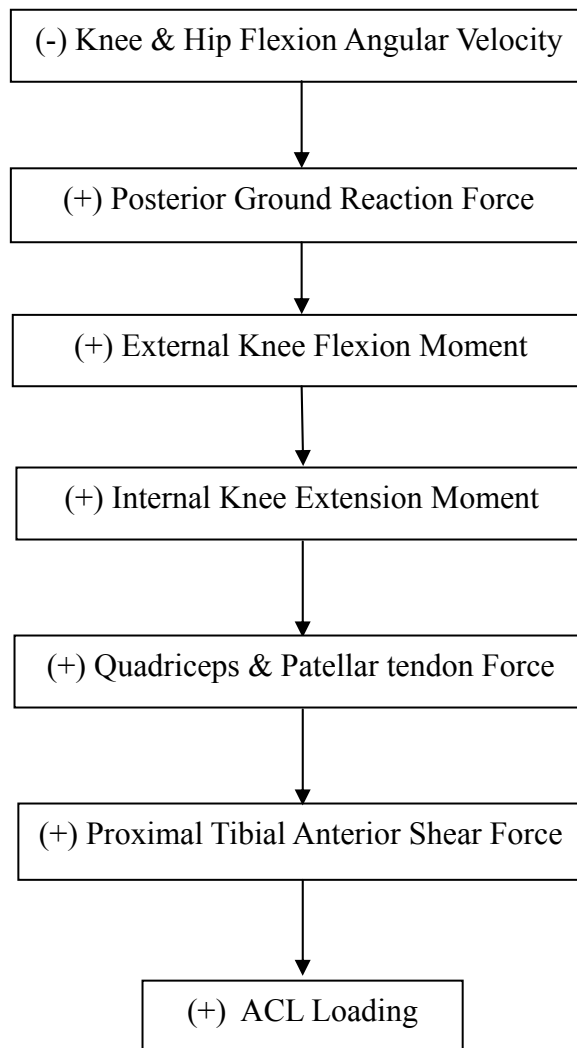


Figure 5.2 A flow chart of how the posterior ground reaction force affects the ACL Loading. (+): indicates increase; (-): indicates decrease.

The ACL Safe Posterior Ground Reaction Force for males is greater than that for females. This can also be explained by the greater patellar tendon-tibial shaft angle the females have than males do at the same knee flexion angle and the gender differences in the moment arm of the knee flexion and extension muscles. With a greater patellar tendon-tibial shaft angle female athletes have than male athletes do, female athletes have to have a lower posterior ground reaction force than male athletes do to keep the anterior shear force applied at the proximal end of the tibia by the patellar tendon below such a magnitude that the ACL loading is below 2000 N. These results indicate that females may need to be trained to land even softer than males do to prevent ACL injury in future training programs for the prevention of non-contact ACL injuries.

Literature has shown that posterior ground reaction force is an important factor to ACL loading. McNair and Marshall (1994) found a significant positive correlation between vertical ground reaction force and the tibial anterior acceleration during a hop-landing task and concluded that the ground reaction forces may be important parameters affecting the tibial anterior shear force. Simonsen et al. (2000) demonstrated the first peak knee extension moment after initial foot contact was in conjunction with the onset of peak posterior ground reaction force during a side-cutting activity. Yu et al. (2006b) found both peak posterior ground reaction force and peak vertical ground reaction force had significantly positive correlation with peak proximal tibial anterior shear force and peak knee extension moment during a stop-jump task. As discussed earlier, knee extension moment, quadriceps force, patellar tendon force, and proximal tibial anterior shear force are contributors to the ACL loading and are affected by posterior ground reaction force. These results, therefore, support the importance of posterior ground reaction force to ACL loading.

The effect of peak posterior ground reaction force on the ACL loading depends on the knee flexion angle. The rate of increase of ACL loading as the peak posterior ground reaction force increases. This rate of increase of the ACL loading increases as the knee flexion angle decreases (Figure 4.3 and 4.4). The smaller the knee flexion angle is, the greater the effect of the peak posterior ground reaction force on ACL loading is. A small increase in the peak posterior ground reaction force can cause a large increase in the ACL loading at a small knee flexion angle. These results further demonstrate the importance of knee flexion angle to the ACL loading.

5.3.3. Effect of Landing Styles on the ACL Loading

Landing styles affects the ACL loading. The landing style was represented by the horizontal location of the center of pressure of the ground reaction force relative to the ankle joint center at the time of peak posterior ground reaction force occurs. A short horizontal distance between the center of pressure of the ground reaction force indicates a landing on the heel while a large magnitude of this horizontal distance indicates a landing on the toe. Landing on the heels exaggerates the external knee flexion moment for a specific tibial tilting angle. Landing on the heels with the knee joint center anterior to the center of pressure enables both the vertical and posterior ground reaction forces to produce external knee flexion moments. This requires large quadriceps muscle force to balance this exaggerated external knee flexion moment. Also, landing on the heels places the center of mass behind the knee joint center which provokes large quadriceps contractions to bring the center of mass forward. The increased quadriceps force threatens the ACL if an individual lands on the heel at a small knee flexion angle (Figure 5.3). Literature has shown that the more anteriorly placed center of

pressure predicted a greater plantar flexion moment and a less knee extension moment (Shimokochi et al., 2006). A decreased knee extension moment requires less contribution of the quadriceps force and can prevent excessive loadings on the ACL. Landing on the toes, compared with landing on the heels, may be a protective landing style for the non-contact ACL injuries.

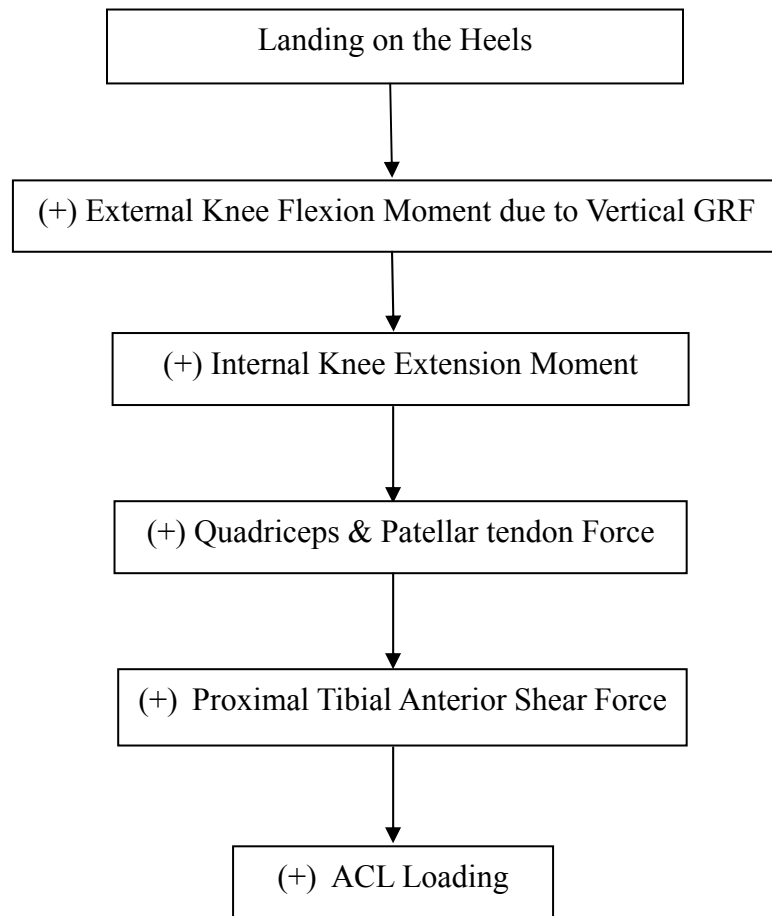


Figure 5.3 A flow chart of how the landing style affects the ACL Loading. (+): indicates increase; (-): indicates decrease.

The simulated peak ACL loading decreased with the increase of the posterior-tilted tibial angle because of the protection of the vertical ground reaction force. The vertical ground reaction force produces an external knee flexion moment if an individual lands with the tibia tilted forward in such a way that the knee joint center is anterior to the center of pressure. The external knee flexion moment produced by the vertical ground reaction force increases the demand for internal knee extension moment and quadriceps muscle force (Figure 5.4). In contrast, the vertical ground reaction force produces an external knee extension moment if the tibia is tilted backward in such a way that the knee joint center is posterior to the center of pressure. The external knee extension moment produced by the vertical ground reaction force reduces the demand for internal knee extension moment and quadriceps muscle force. These results combined indicate that a large vertical ground reaction force is not necessarily a risk factor for the non-contact ACL injuries because the landing styles and tibial tilting angle affects the role of the vertical ground reaction forces on the ACL loading. In contrast, a large posterior ground reaction force is a risk factor of non-contact ACL injuries regardless of the landing style and tibial tilting angle.

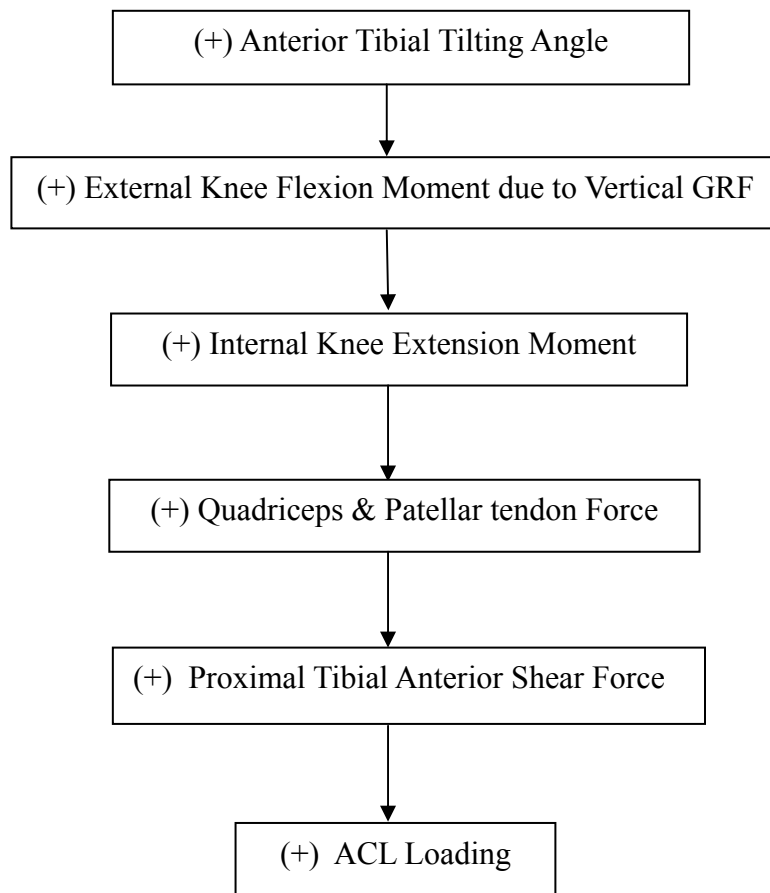


Figure 5.4 A flow chart of how the tibial tilting angle affects the ACL Loading. (+): indicates increase.

5.3.4. Effect of the Hamstrings Force on the ACL Loading

The effect of the hamstring force on the ACL loading depends on the knee flexion angle. The contraction of hamstrings muscle generates a posterior shear force on the tibia, which is considered as a protection mechanism for ACL (Renstrom et al., 1986; Yasuda and Sasaki, 1987a; MacWilliams et al., 1999). The computer simulation results in this study, however, demonstrate that the hamstring muscle co-contraction did not protect the ACL when the knee flexion angle is small. The hamstrings muscle contraction is ineffective to resist anterior shear force at proximal end of the tibia at small knee flexion angles because of (1) small posterior shear force generated by the hamstrings due to small knee flexion angles, (2) increased anterior shear force at the proximal end of the tibia due to increased quadriceps force, and (3) increased patellar tendon shear force due to the increased patellar tendon-tibial shaft angle. The hamstrings muscle force application line is essentially parallel to the femur. The smaller the knee flexion angle is, the smaller the projection of the hamstring muscle force in the posterior direction. On the other hand, the hamstring co-contraction generates a knee flexion moment, and thus increases the demand for quadriceps muscle force to generate knee extension moment to equalize a given external knee flexion moment due to the ground reaction forces and the knee flexion moment due to hamstring co-contraction (Figure 5.5). As previously discussed, the anterior shear force applied at the proximal end of the tibia by the quadriceps muscle through the patellar tendon increases as the knee flexion angle decreases. The protection of the hamstring muscle force to the ACL, therefore, diminishes as the anterior shear force applied at the proximal end of the tibia by the quadriceps muscles through the patellar tendon increases and the posterior shear force applied at proximal end of the tibia by the hamstring muscles decreases when the knee flexion angle decreases.

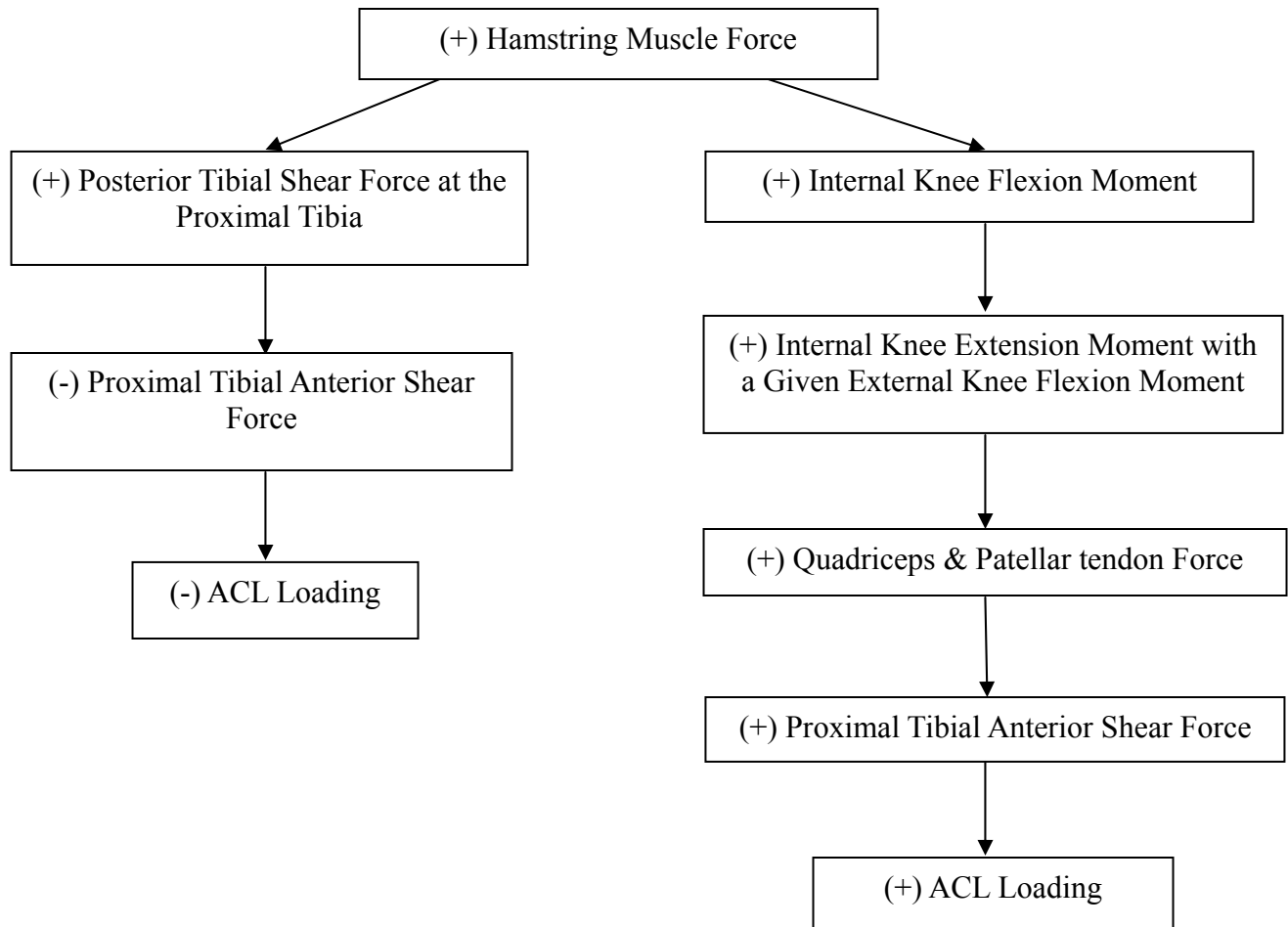


Figure 5.5 A flow chart of how the hamstring force affects the ACL Loading. (+): indicates increase; (-): indicates decrease.

Literature also demonstrates that the hamstring muscle force cannot protect the ACL at small knee flexion angles (More et al., 1993; O'Connor, 1993; Pandy and Shelburne, 1997; Li et al., 1999). Pandy and Shelburne (1997) reported that the knee flexion angle had to be greater than 10 degrees for the hamstring to generate significant posterior shear force to reduce ACL loading. More et al. (1993) and Li et al (1999) showed the hamstrings muscle force could significantly decrease the ACL graft tension until the knee flexion angle was greater than 15 degrees. O'Connor (1993) showed that hamstring force could not produce an effective posterior shear force until the knee flexion angle was greater than 22 degrees. Restrom et al. (1986) reported that the hamstring force can not overcome the force generated by the quadriceps muscle unless the knee flexion angle was greater than 30 degrees. The results of present study demonstrated that knee flexion angle greater than 13 degrees for males and 16 degrees for females can generate sufficient posterior draw force at proximal tibia to reduce the load on the ACL. Although inconsistent in the exact knee flexion angle at which the hamstring muscle force can generate meaningful posterior shear force to reduce ACL loading, the results of all these studies consistently demonstrate that hamstring muscle co-contraction can not protect ACL when knee flexion angle is small. These results indicate that knee flexion angle is even more important than just affecting anterior shear force applied at the proximal end of the tibia by the quadriceps muscles through the patellar tendon.

The gender difference in the knee flexion angle at which the hamstring muscles can generate meaningful posterior shear force to protect the ACL found in this study is mainly due to the gender difference in the patellar tendon-tibial shaft angle. Using the results by Nunley et al. (2003), the female subjects have larger patellar tendon-tibial shaft angle than male subjects do at the same knee flexion angle in the sagittal plane knee model for the computer simulation

in this study. The hamstring tendon-tibial shaft angle, on the other hand, is the same for male and female subjects in the sagittal plane knee model in this study. Female subjects, therefore, need a larger knee flexion angle than male subjects do. In such a case, the posterior shear force at the proximal end of the tibia generated by the hamstring muscles can actually reduce the anterior shear force applied at the proximal tibia by the quadriceps muscles through patellar tendon that is increased because of the hamstring co-contraction.

5.3.5. Effect of the Gastrocnemius Force on the ACL Loading

The ACL loading increases as the gastrocnemius muscle force increases. The gastrocnemius muscle force generates an internal knee flexion moment. An increase in gastrocnemius muscle force results in an increase in the internal knee flexion moment that increases the internal knee extension moment for a given external knee flexion moment (Figure 5.6). The results of computer simulation, however, demonstrate that the effect of the gastrocnemius force on the ACL loading is limited. O'Connor (1993) and Fleming et al. (2001) both showed that the co-contraction of gastrocnemius and quadriceps muscles resulted in a larger ACL loading or ACL strain than that of quadriceps contraction alone. Pflum et al. (2004) used a 3-D model of body to simulate the drop-landing task. They reported that the gastrocnemius muscle applied an anteriorly directed force on the tibia, but that may have limited effects on the ACL loading because the gastrocnemius muscle applied a relatively small anterior shear force to the lower leg.

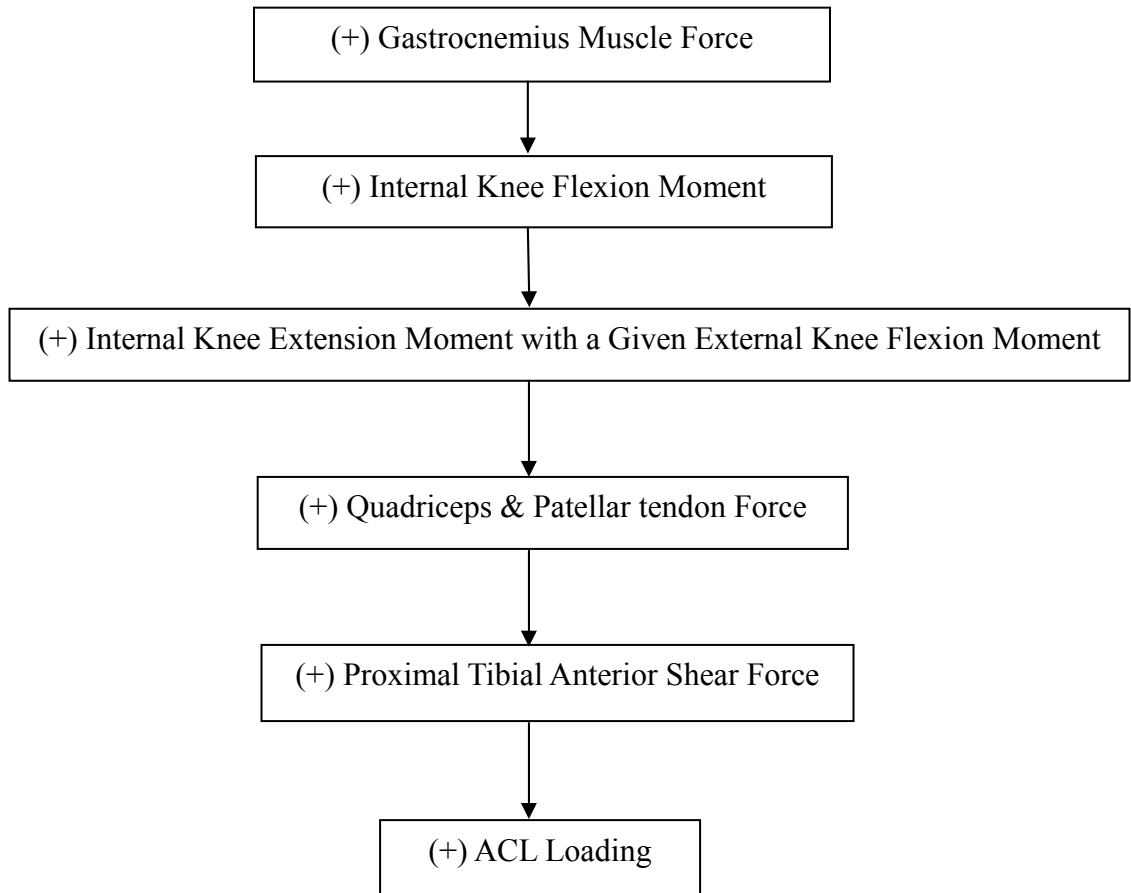


Figure 5.6 A flow chart of how the gastrocnemius force affects the ACL Loading. (+): indicates increase.

5.4. Monte Carlo Simulation of the Probability of Sustaining Non-contact ACL Injuries during the Stop-jump Task

5.4.1. Sensitivity of Simulated Relative Risk of Non-contact ACL injury

Although the probability of sustaining non-contact ACL injuries significantly increased as the ACL ultimate load used in the Monte Carlo simulation decreased, the female-to-male non-contact ACL injury rate ratio essentially remained constant as long as the gender difference in the ACL ultimate load is considered (Table 4.8). These results suggest that the simulated relative risk of sustaining non-contact ACL injuries is not sensitive to the ACL ultimate strength as long as the gender difference in ACL ultimate load is considered. Using 2250 N as the ACL ultimate load for males and 1800 N for females in the Monte Carlo simulation in this study resulted in a female-to-male non-contact ACL injury rate ratio as 5:1, which is essentially the same as the reported female-to-male non-contact ACL injury rate ratio for basketball players in the literature (Arendt and Dick, 1995; Agel et al., 2005). The athletic task used in the stochastic biomechanical model in this study was the stop-jump task which is frequently performed in basketball practice and games. Many non-contact ACL injuries occur in athletic tasks similar to the stop-jump task with a fast whole body horizontal movement before the landing and a quick deceleration and sudden change in movement direction during the landing. The similarity of the estimated female-to-male non-contact ACL injury rate ratio in this study to that reported in literature; therefore, support the validity of the stochastic biomechanical model of the relative risk for non-contact ACL injuries and the selection of non-contact ACL ultimate load in this study.

The use of 2250 N as the ACL ultimate load for males and 1800 N for females (Stapleton et al., 1998) in the stochastic biomechanical model of the probability of non-contact

ACL injuries is supported by literature. The age range of 80 subjects in this study was between 19 to 30 years old and falls in the younger group (22 to 35 years) defined in Woo et al. (1991). Woo et al. (1991) determined the *in vitro* ultimate tensile strength of the ACL in the younger group was 2160 N on average. In addition, Mazzocca et al. (2003) reported as well that the ACL strength of the uninjured knees was 2110 N on average. Both studies included male and female cadaver knees and reported the averaged ACL strength without separating genders. The averaged ACL strength of 2250 N for males and 1800 N for females is 2025 N and is fairly close to the values reported in these two studies. This similarity in the averaged strength of the ACL, to a certain degree, also supports the validity of the selection of ACL ultimate load in this study.

Two other pairs of gender specific ACL ultimate loads (Stapleton et al., 1998; Chandrashekar et al., 2006) used in the sensitivity test also resulted in female-to-male non-contact ACL injury rate ratios similar to that reported in the literature (Arendt and Dick, 1995; Agel et al., 2005) (Table 4.8). The main reason to reject the use of 1800 N as the ACL ultimate load for males and 1250 N for females (Chandrashekar et al., 2006) in the stochastic biomechanical model in this study is that this pair of ACL ultimate loads is apparently underestimates of the strength of the ACL for the subjects in this study. Chandrashekar et al. (2006) investigated ACL strength at failure of 10 male and 10 female cadavers. The age of cadavers ranged from 26 to 50 years of age for males and from 17 to 50 years of age for females. Woo et al. (1991) demonstrated that the ACL ultimate strength decreases as the age increases. They investigated three groups including the younger group from 22 to 35 years of age, middle group from 40 to 50 years of age, and older group from 60 to 97 years of age. The corresponding averaged ultimate strength for each group was 2160 N, 1503 N, and 658 N. The

strengths of the ACL reported by Chandrashekar et al. (2006) fell into the strengths of the ACL between younger and middle groups based on the age classification by Woo et al. (1991). This means that the strengths of the ACL reported by Chandrashekar et al. (2006) are likely to be underestimates of the actual strengths of the ACL of the subjects in this study.

The main reason to reject the use of the pair of ACL ultimate loads reported by Stapleton et al. (1998) was that this pair of ACL ultimate loads may be overestimates of the actual strengths of the ACL of the subjects in this study. The size of the physique affected the ultimate strength of ACL (Stapleton et al., 1998). The pair of ultimate loads of 2550 N for males and 2025 N for females was obtained from the large size of cadavers (Stapleton et al., 1998). The investigators, however, did not report the criteria of how the size for each group was determined. The corresponding mean height and weight were 1.78 m and 78 kg for the 40 male subjects and 1.63 m and 60 kg for the 40 female subjects in this study, which should be considered as medium sizes. The pair of ACL ultimate loads reported by Stapleton et al. (1998), therefore, may be overestimates of the actual strength of ACL for the subjects in the present study.

The gender difference in the strength of the ACL significantly affects gender difference in the risk of sustaining non-contact ACL injuries. As previously discussed, the estimated female-to-male non-contact ACL injury rate ratios using the stochastic biomechanical modeling in this study were similar to those reported in literature as long as the gender difference in the strength of the ACL was considered. The estimated female-to-male non-contact ACL injury rate ratios, however, were 1.86 ± 0.10 and 1.94 ± 0.05 when the gender difference in the strength of the ACL was considered (Table 4.8). These estimated female-to-male non-contact ACL injury rate ratios were below the lower limit of the

confidence interval reported in the literature (Agel et al., 2005). These results indicate that gender difference in the strength of ACL may play a major role in the gender difference in the risk of sustaining non-contact ACL injuries, and should be considered in the stochastic biomechanical model in this study.

The gender difference in the ACL ultimate load may be explained by the gender differences in the structure and material properties in the ACL. Muneta et al. (1997) have shown the cross-sectional area in females is smaller than that in males. Chandrashekar et al. (2005) also found that females have significantly smaller midsubstance area and ACL volume than those of males. Chandrashekar et al. (2006) further showed the ACL in females have significantly lower stiffness and modulus of elasticity than males do. These results support the use of different ACL ultimate loads in corresponding male and female stochastic biomechanical knee model.

5.4.2. Biomechanical Characteristics of Simulated Non-contact ACL Injuries

Comparison of Injured and Uninjured Jumps

The lower extremity kinematics and kinetics differ significantly between injured and uninjured jumps. The injured jumps exhibited significantly small knee flexion angle, large peak posterior ground reaction force, quadriceps force, patellar tendon force, and proximal tibial anterior shear force, which has adverse effect to the ACL especially at a small knee flexion angle as mentioned in the sagittal plane inverse dynamic knee model. Small knee flexion angle accompanied by a large ground reaction force has been demonstrated to increase the loading on the ACL (Yu et al., 2006a). Fleming et al. (1993) found a significantly positive correlation between an externally applied anterior shear load at tibia and ACL strain at 30

degrees of knee flexion, but not at 90 degrees of knee flexion. Yu et al. (2006b) then demonstrated a significant positive correlation between the peak posterior ground reaction force and knee extension moment. The large knee extension moment is mainly attributed by large quadriceps force.

Literature has repeatedly demonstrated that large quadriceps force applied at the proximal end of the tibia through the patella and patellar tendon at small knee flexion angles can injure the ACL. Arms et al. (1984) have found that quadriceps force can significantly increase the *in vitro* ACL strain from 0 to 45 degrees of knee flexion. This result is consistent with the result of Drahanich and Vahey (1990) in that isometric quadriceps loads significantly increased the ACL strain at 0 to 40 degrees of knee flexion angle when compared with the reference strains. Dürselen et al. (1995) showed that the applied quadriceps force makes the ACL sustain a high level of strain from full extension to 30 degrees of knee flexion and then the ACL strain starts to decrease when knee flexion angle greater than 30 degrees. Beynnon et al. (1995) had similar results in that the *in vivo* isometric quadriceps force significantly strain the ACL at knee flexion of 15 and 30 degrees relative to the relaxed condition. Withrow et al. (2006) investigated the relationship between the ACL strain and the quadriceps force. They found that the change of the ACL strain had significant correlation with the quadriceps force during the simulated one-footed landing. The mean maximum quadriceps force applied in their study was 1238 N and that force was more close to real situation than previous studies investigating the relationship between quadriceps force and ACL strain/force. Shoemaker et al. (1993) showed that the quadriceps has significant effect on increasing the tibial anterior displacement and the ACL graft tension. The largest graft tension due to quadriceps occurred at 35 degrees of knee flexion. These results show that the quadriceps force is indeed

responsible to the increase of the ACL strain and anterior tibial displacement although most of the studies applied low amplitude of quadriceps force. DeMorate et al. (2004) further presented that a large quadriceps force of 4500 N at 20 degrees knee flexion angle injured the ACL. A large quadriceps force even produces larger patellar tendon force when the knee flexion angle is smaller than 30 degrees (Hurberti et al., 1984; Nisell and Ekholm, 1985; Buff et al., 1988). The small knee flexion angle results in a large patellar tendon-tibial shaft angle and incurs a larger patellar tendon shear force compared with the large knee flexion angle (Nunley et al., 2003). All these literature support our simulation results in terms of large quadriceps force with small knee flexion angle increases the ACL loading. The difference in the biomechanical characteristics between injured and uninjured jumps during landing indicates the injured jumps have altered motion patterns and those may be the reasons attribute to non-contact ACL injuries and should be avoided during activities.

Although the difference was small, the hamstring muscle force was significantly greater in the uninjured jumps than in the injured jumps. Studies showed that hamstring muscle can provide a posterior-directed drawer force to protect ACL except for the knee flexion angle near extension (O'Connor, 1993; Pandey and Shelburne, 1997; Imran and O'Connor, 1998). *In vitro* studies have demonstrated the hamstring force can significantly decrease the ACL graft tension (More et al., 1993) or ACL force (Li et al., 1999; Markolf et al., 2004) beyond certain knee flexion angles. The combination of greater knee flexion angle and greater hamstring co-contraction in the simulated uninjured jumps than in the simulated injured jumps, to a certain degree, indicate that the hamstring co-contraction might provide some protections to the ACL in the simulated uninjured jumps.

The gastrocnemius force is similar between injured and uninjured jumps. The effect of

the gastrocnemius on the ACL is inconsistent in the literature. Dürselen et al. (1995) showed that the contraction of gastrocnemius force cannot significantly increase the ACL strain. Computer simulation studies have anterior-directed forces generated by gastrocnemius force, but the effect of the force on the ACL is relatively small and negligible (Pflum et al., 2004; Pandy and Shelburne, 1997). The differences of the gastrocnemius force between injured and uninjured cannot directly be compared with the literature because none of them recorded the gastrocnemius force to the status that the ACL is ruptured during *in vitro* or simulation studies. The present simulation results along with the literature, however, give the message of that the gastrocnemius force may not play important role in the risk of non-contact ACL injuries.

External valgus moment and internal rotation moment are significantly larger in the injured jumps than those in uninjured jumps, which are supported by the literature. Hewett et al. (2005) has reported that the injured subjects had significantly larger external knee valgus moment when compared with uninjured subjects during a drop-jump task in a prospective study. Kanamori et al. (2002) showed the applied external internal torque resulted in larger *in situ* force in the ACL than that from external torque. The ACL *in situ* force increases as the external internal torque increases. Markolf et al. (1995) also concluded that the internal tibial torque is a relatively important mechanism to generate loading on the ACL while the external tibial torque alone or with varus or valgus moment did not significantly increase forces on the ACL. These literatures support the simulated results and express the association between the injured jumps and external valgus and internal rotation moment.

Stochastic biomechanical models demonstrate the consistent results with the results from sagittal plane inverse dynamic knee model in which less posterior-tilted tibial angle and a landing close to the ankle joint instead of toes increase the ACL loading. As mentioned

previously, the vertical ground reaction force can have a protective effect on the ACL by generating an external knee extension moment if an individual lands with a more posterior-tilted tibial angle and lands closer to the toes. The injured jumps, however, have smaller posterior-tilted tibial angle and less COP to ankle joint distance but large posterior and vertical ground reaction forces. These features combined may explain why the ACL loading is increased during an awkward landing style and why the injured jumps sustain higher ACL loading than uninjured.

Sagittal plane biomechanics alone can injure the ACL while the non-sagittal plane biomechanics alone may not be able to injure the ACL. The ACL loading due to sagittal plane biomechanics in simulated injured jumps were 1840 ± 895 N for males and 1773 ± 603 N for females, that were $82 \pm 40\%$ and $99 \pm 34\%$ of the ACL ultimate load for the corresponding genders (Table 4.11). These results suggest that the ACL loading due to sagittal plane biomechanics alone can be greater than the ACL ultimate load in the simulated injured jumps for each gender. The ACL loading due to non-sagittal plane biomechanics in simulated injured jumps were 927 ± 666 N for males and 501 ± 389 N for females, that were $41 \pm 30\%$ and $28 \pm 22\%$ of ACL ultimate load for the corresponding genders (Table 4.11). These results suggest that ACL loading due to non-sagittal plane biomechanics alone was not greater than the ACL ultimate load for each gender. The ACL loading due to non-sagittal plane biomechanics in injured jumps was even lower when the knee valgus moment data reported by Hewett et al. (2005) were used in the Monte Carlo simulation. These results indicate that sagittal plane biomechanics is the major ACL loading mechanism and is the major risk factor of sustaining non-contact ACL injuries of the stop-jump task. Berns et al. (1992) and Markolf et al. (1995)

both demonstrated that the major ACL loading mechanism is anterior shear force at the proximal tibia. They also showed that the varus or valgus torque had significant effect on the ACL loading only when the proximal tibial anterior shear force was applied. Fukuda et al. (2003) evaluated the effect of different magnitudes of valgus torque on the *in situ* force of ACL. They found that the lower valgus torque resulted in corresponding lower magnitude of ACL *in situ* force at all flexion angles tested. The *in situ* force was still below 50 N when a 10 Nm valgus torque was applied. These studies support our result in that the sagittal plane biomechanics alone can possibly injure the ACL in the stop-jump task, but the non-sagittal loading alone may not.

In addition, the contributions of the sagittal loading and non-sagittal loadings to the total ACL loading are not the isolated contribution from each plane but are affected by each other. The knee flexion and extension muscles have the potential to support the valgus and varus moments because these muscles have the valgus and varus moment arms (Lloyd and Buchanan, 2001; Schipplein and Andriacchi, 1991). Activation of the knee flexion and extension muscles, therefore, contributes to the valgus-varus moment as well. Literature demonstrates the activation of quadriceps and hamstring muscles contributed to not only the knee flexion and extension moment, but also the varus-valgus moment during running, cutting, or static isometric contraction (Lloyd and Buchanan, 2001; Lloyd et al., 2005). Also, the applied external valgus load increased the muscle activation of the medial muscles of the thigh while the applied external varus moment increased the activation of the lateral muscles of the thigh (Buchanan et al., 1996). These results indicate that the sagittal plane biomechanics and the non-sagittal plane loadings may have coupling effect on the ACL loading

Comparison of Injured Jumps between Genders

Female simulated injured jumps had significantly larger knee flexion angle than that of male injured jumps. This result indicates that females may get injured even though the knee flexion angle at peak posterior ground reaction force is significantly greater than males. This can be explained by the larger patellar tendon-tibial shaft angle in females than that in males at the same knee flexion angle. Also, the stiff and hard landing of females may also contribute to the non-contact ACL injuries even though the knee flexion angle at peak posterior ground reaction force is larger than males.

Hamstring force may not be an important factor affecting the non-contact ACL injuries for females. The female simulated injured jumps have significant larger hamstring force than males do. This result indicates that hamstring force may not be the main factor affecting the gender differences in the non-contact ACL injuries. Female simulated injured jumps also exhibited significantly larger external internal rotation moment but smaller valgus moment than that of male simulated injured jumps. These results demonstrate that the gender differences in the non-contact ACL injuries may be more sensitive to internal rotation moment than valgus moment.

The simulated injured jumps for both genders have large knee extension moment, patellar tendon force, quadriceps force, and proximal tibial anterior shear force. These results demonstrate that the large magnitude of these kinetic variables contribute to non-contact ACL injuries regardless of the genders.

Comparison of Uninjured Jumps between Genders

The gender differences in the lower extremity motion patterns in the simulated

uninjured jumps are consistent with literature. Literature has repeatedly shown that females have smaller knee flexion angle (Malinzak et al., 2001; Chappell et al., 2002; Decker et al., 2003; Salci et al., 2004), large vertical and posterior ground reaction forces (James et al., 2004; Salci et al., 2004; Kernozek et al., 2005), large proximal tibial anterior shear force and knee extension moment (Chappell et al., 2002) when compared with their male counterparts during variety of sporting activities. The gender differences in the lower extremity motion patterns in the uninjured jumps imply that females are more susceptible to non-contact ACL injuries.

Much higher muscle activation in quadriceps than hamstrings has been observed in several EMG studies (Malinzak et al., 2001; Zeller et al., 2003, Urabe et al., 2005). Malinzak et al. (2001) and Zeller et al. (2003) both showed that female athletes have significantly higher activation in quadriceps than hamstring during variety of sporting activities including running, cutting, and squatting. Urabe et al (2005) found hamstring activation was significantly lower at 15, 20, and 25 degrees of knee flexion angle. These studies indicated that females rely more on the quadriceps and less on the hamstrings muscle. Our results also showed that much higher quadriceps force and lower hamstring force in both genders, however, females in the simulated uninjured jumps did not displayed smaller H/Q (hamstring-to-quadriceps) ratio. The little difference in muscle forces in simulated uninjured jumps between genders indicates the force ratio may not be an appropriate assessment factor to the risk of the non-contact ACL injuries for the uninjured jumps.

Males' landing patterns do not always protect the ACL. Males land with smaller posterior tibial tilting angle and with COP closer to the ankle joint when compared with females in the simulated stop-jumps. These landing styles place males in a riskier posture and increase the risk of the non-contact ACL injuries.

5.4.3. Risk Factors of Simulated Non-contact ACL Injuries

Knee flexion angle and peak posterior ground reaction force are two important risk factors of non-contact ACL injuries, and two main motor control related explanations of the gender difference in non-contact ACL injury rate. The probability of non-contact ACL injuries was significantly decreased when females' knee flexion angle and peak posterior ground reaction force were replaced with males' in the Monte Carlo simulation (Table 4.14). These results indicate that modification of females' knee flexion angle and posterior ground reaction force should effectively reduce the gender difference in the risk of non-contact ACL injuries.

Literature have repeatedly suggested the importance of knee flexion angle to the ACL loading for the prevention of non-contact ACL injuries (Boden et al., 2000; Colby et al., 2000; Malinzak et al., 2000; Salci et al., 2004; Yu et al., 2004), or for rehabilitation after ACL reconstruction surgery (Yasuda and Sasaki, 1987a,b; More et al., 1993; Beynnon et al., 1995, Li et al., 1999; Markolf et al., 2004). The *in vivo* studies showed that the females have smaller knee flexion angles than their male counterparts during cutting (Malinzak et al., 2000), jump-landing (Salci et al., 2004), and stop-jump (Yu et al., 2004). Boden et al. (2000) analyzed the videotapes taken during games. They found that the knee flexion angle was near full extension when the injury occurred. The *in vitro* studies showed that a large knee flexion angle is required to prevent excessive strain or stress on the ACL (Yasuda and Sasaki, 1987a, b; Li et al., 1999; Markolf et al., 2004) or to enhance the hamstring functions (More et al., 1993; Li et al., 1999). An *in vitro* study of Markolf et al. (1995) demonstrated that the ACL loading increased as knee flexion angle decreased. Also, Beynnon et al. (1995) found that *in vivo* ACL

strain increased as knee flexion angle decreased during active knee flexion-extension exercise with and without external load applied. As previously discussed, the effect of knee flexion angle on ACL loading is mainly due to the effects of knee flexion angle on the patellar tendon-tibial shaft angle (Nunley et al., 2003) and the ACL elevation angle (Li et al., 2005). The results of current study provide convincing evidence that supports the observations and indications regarding the effect of knee flexion angle on the risk of sustaining non-contact ACL injuries in the literature.

Increasing posterior ground reaction forces may increase the non-contact ACL injury rate. As previously discussed, the increase of posterior ground reaction force increases the ACL loading by increasing the external knee flexion moment that needs to be balanced by increasing internal knee extension moment. Females land with significantly larger peak posterior ground reaction force and that result in larger knee extension moment (Yu et al., 2006a). Increasing internal knee extension moment means increasing quadriceps muscle force. Literature, however, have not provided direct evidence to link the increased posterior ground reaction force with the risk of sustaining non-contact ACL injuries. The results of current study provide convincing evidence that fill this gap in the literature.

The simulation result of the stochastic biomechanical model is consistent with the result of the sagittal plane inverse dynamic knee model where the importance of knee flexion angle and peak posterior ground reaction force has been demonstrated. The results of both models show that the knee flexion angle and the peak posterior ground reaction force have interaction effect on the ACL loading. This can be seen in that the sum of the decreased non-contact injury rate ratio resulted from the corresponding factor of knee flexion angle and posterior ground reaction force is greater than the non-contact ACL injury rate ratio resulted

from that with part of males' motion patterns.

Cowling et al. (2003) investigated the effect of verbal instruction on the kinematics, EMG, and ground reaction forces during an abrupt single-limb jump. They found the knee flexion angle at initial foot contact and at peak ground reaction force was significantly increased while the peak ground reaction force was significantly reduced in the “knee angle instruction” condition. The instruction of knee angle condition “This time when you run to land I want you to land with your knee bending” is given to subject before the task. This result supports our simulations about the inherent interaction between knee flexion angle and posterior ground reaction force. This result also demonstrates the simple modification of knee flexion angle during landing makes landing softer with large knee flexion angle. This modification should be used for future training program in an effective way such as training with a constraint knee brace.

The gender differences in other lower extremity motion pattern measures, including the knee valgus-varus moment, knee internal-external rotation moment, and hamstrings and gastrocnemius co-contractions, do not appear to be the main cause of the gender difference in the non-contact ACL injury rate in the stop-jump task. Although replacing each of these female lower extremity motion pattern measures with males' more or less results in a change in the simulated probability of non-contact ACL injuries, the largest reduction in the female-to-male non-contact ACL injury rate ratio due to the change in any of these measures was less than 0.22 (Table 4.14). These results indicate that these lower extremity motion pattern measures may be risk factors for non-contact ACL injuries but could not explain the large gender difference in non-contact ACL injuries in the stop-jump task.

Although the results of the stochastic biomechanical modeling demonstrate that the

knee flexion angle and peak posterior ground reaction force are two important contributors to the risk of the non-contact ACL injuries, the interpretation of these two variables as risk factors of non-contact ACL injuries are limited to the stop-jump task only or to those landing tasks similar to the stop-jump. Lower extremity motion patterns may have different contributions to the risk of the non-contact ACL injuries in different athletic tasks because of the different demands of the tasks. McLean et al. (2004) demonstrated that the non-sagittal loadings, mainly the external valgus loading, are the dominant factors to the risk of the non-contact ACL injuries during sidestep cutting task. Their result and conclusion revealed that the sagittal plane biomechanics can not injure the ACL based on their forward dynamic model. The inconsistent risk factors of the non-contact ACL injuries determined in current project and McLean et al. (2004) may result from the different tasks performed for these two studies. The motion of the stop-jump task, horizontal approach run followed by the vertical take off, mainly occurs in the sagittal plane. Our results support well that the contributions of two sagittal plane biomechanical factors which are knee flexion angle and posterior ground reaction force explain most of the loading contributions to the ACL loading. The sidestep cutting task consists of the horizontal approach run followed by a direction change of 35° to 55° away from the original approaching direction. This direction change requires demand from the coronal and transverse planes and may explain why the non-sagittal loadings are important during sidestep cutting task.

Gender difference in the lower extremity motor control is a major cause of gender difference in the risk of non-contact ACL injuries, but not the only cause. Replacing female lower extremity motion pattern measures with those male lower extremity motion patterns that can reduce female's non-contact ACL injury rate decreased the female-to-male non-contact

ACL injury rate ratio to about 2.4:1. These results combined with the results of sensitivity test suggest that gender differences in the strength of the ACL and knee anatomy also significantly contribute to the gender difference in the risk of non-contact ACL injuries. These results indicate that training may reduce, but can not completely eliminate, the gender difference in the risk of non-contact ACL injuries.

5.4.4. Limitations of the Stochastic Biomechanical Model

Although the stochastic biomechanical model of the probability of sustaining non-contact ACL injuries developed in this study accurately estimated the female-to-male non-contact ACL injury rate ratio, it has four limitations

1. The estimated injury rates for basketball players in male and female stochastic biomechanical models were based on the stop-jump task only. The non-contact ACL injuries the basketball players sustained during the game, however, can occur in different tasks such as cutting or one-footed landing. The risk of sustaining non-contact ACL injuries may be different in different athletic tasks. The estimated non-contact ACL injury rate in this study may not be an accurate estimate of the overall non-contact ACL injury rate in basketball.
2. The combination of knee valgus-varus moment with knee internal-external rotation moment in the stochastic biomechanics model was completely random without constraints to represent the realistic combination of these two variables. In the reality, the valgus moment always accompanies with external rotation

moment while the varus moment occurs concurrently with internal rotation moment during landing tasks. The lack of constraint for realistic combination of knee valgus-varus moment may have result in overestimate of non-contact ACL injury rate.

3. The unit of the non-contact ACL injury rate estimated in the present stochastic biomechanical model was in injuries per 100,000 jumps, which was inconsistent with the unit of the non-contact injury rate reported in epidemiology studies.
4. The sagittal and non-sagittal loading contributions have coupling effect on the ACL loading and the isolated contribution to the ACL loading can not be determined. Activation of quadriceps and hamstring muscles contributed to not only the knee flexion and extension moment, but also the valgus-varus moment. The applied external valgus-varus moment affects the activation of the quadriceps and hamstring muscles. The isolated sagittal or non-sagittal loadings to the ACL loadings may not be able to be obtained because of the human anatomy and physiology.

5.5. Significance and Recommended Future Studies

A sagittal plane biomechanical model of the knee and a stochastic biomechanical model for the probability of non-contact ACL injuries were developed in this study. The applications of these two models in the current study provided significant new information for understanding the relationships between lower extremity motion patterns and ACL loading,

and between lower extremity motion patterns and the risk of non-contact ACL injuries. The results of this study advanced the literature on the prevention of non-contact ACL injuries and set the basis for future clinical applications of the models developed in this study and further research on the prevention of non-contact ACL injuries. The stochastic biomechanical model developed in this study can be directly applied to other athletic tasks in other studies on non-contact ACL injury prevention to evaluate the risk of sustaining non-contact ACL injuries in different tasks, different sports, and different populations. The models can also be applied to evaluate the efficiency of ACL injury prevention programs.

The distribution of each primary independent variable is constructed based on the empirical experimental data of uninjured recreational athletes during the stop-jump task. The distribution of the primary independent variable of the uninjured data can still construct the population variability if the sample mean and standard deviation and the distribution type are known. In addition, the non-contact ACL injury is attributed by a combination of the extreme values of primary independent variables that are tails of the distributions. These advantages enable the model to predict the injury case without the real injury data.

The validity of the sagittal plane knee model was well established. The sagittal plane knee model was developed based on the inverse dynamics and this method has been widely applied in the biomechanical studies with the well established validity (Nisell, 1985; Zatsiorsky, 2002). In addition, the ACL loading determined from sagittal plane knee model has the same pattern as the ACL loading determined in the cadaveric knee model (Markolf et al., 1995). This result further supports the validity of the sagittal plane inverse dynamic knee model.

The ACL loading model consists of the sagittal plane knee model as well as the

valgus-varus loading and internal-external rotation loading. It is necessary to determine the contribution of the non-sagittal loading to the total ACL loading because the ACL loading is attributed by the loading from sagittal plane, coronal and transverse planes. The non-sagittal loading contribution as functions of knee flexion angle in the current ACL loading model were determined based on the ACL loading data subjected to the non-sagittal loadings applied on the proximal tibia at different knee flexion angles in the cadaveric knee model (Markolf et al., 1995). Determining the non-sagittal loading contribution to the total ACL loading based on these *in vitro* data should be appropriate. In the current literature, only one ACL loading equation was reported by McLean et al. (2003a). The investigators, however, did not clearly describe how the ACL loading equation was determined. The non-sagittal loadings expressed as functions of the knee flexion angle in current ACL loading model have an advantage over that determined by McLean et al. (2003a) because the effects of the non-sagittal loadings and the effects of the knee flexion angle on the ACL loading were both considered. This determination should increase the validity of the current ACL loading model. The main concern of the current loading model is that these loadings imposed on the ACL are assumed to be independent and additive to each other. This assumption may result in the overestimate of the predicted ACL loading in the stop-jump task, but the influence should be small and would not affect the interpretation of model outcomes. A true 3-D knee model along with the more realistic loading equations for the ACL loading model are needed to improve the validity of the current model in predicting the ACL loading and probability of non-contact ACL injuries and to further understand the risk of non-contact ACL injuries for future study. Future studies include but are not limited to

1. Modify the current sagittal plane biomechanical model of the knee to a true 3-D model of the knee and instrument the new 3-D model of the knee into the stochastic biomechanical model for the probability of sustaining non-contact ACL injuries. Although the current stochastic biomechanical model includes the non-sagittal plane biomechanics by adding the knee valgus-varus moment and internal-external rotation moment in the ACL loading model, no detailed kinematic variables are included in the model to describe the effects of lower extremity motion on the non-sagittal plane kinetics. Adding detailed kinematic variables to describe the non sagittal plane kinetics will enable us to further understand the effects of knee valgus-varus and internal-external rotation moments on the ACL loading and the risk of sustaining non-contact ACL injuries.
2. Determine the ACL ultimate load as a function of the body mass for the corresponding male and female stochastic biomechanical models. The literature has demonstrated that the body mass has significantly positive correlation with the ACL volume and that can affect the ACL ultimate load (Chandrashekar et al., 2006). Females have smaller ACL volume than males do. The use of ACL ultimate load as a function of the body mass for corresponding male and female models considers the variability of the ACL ultimate load in the model and can increase the validity of the stochastic biomechanical model.
3. Determine a unit conversion factor to convert the unit of estimated probability of sustaining non-contact ACL injuries from number of injuries per 100,000

repetition of a task to number of injuries per 1,000 hours of exposure time as used in traditional epidemiology studies. Video survey can be conducted to find on average how many times an athletes perform a given athletic task per 1,000 hours of exposure time. The times of performance of a given task per 1,000 hour of exposure time can then be used as the conversion factor to convert unit of the estimated probability of sustaining non-contact ACL injuries in a given task to number of injuries per 1,000 hours of exposure time. Using a uniform unit will minimize the confusion between different studies and be convenient to further validate the stochastic biomechanical model developed in this study.

4. Determine the probability of sustaining non-contact ACL injuries in other athletic tasks. Non-contact ACL injuries occur in a variety of athletic tasks. The current study only determined the probability of sustaining non-contact ACL injuries and female-to-male non-contact ACL injury rate ratio in the stop-jump task. The risk and the major risk factors of sustaining non-contact ACL injuries in different athletic tasks may be different. To fully understand the non-contact ACL injuries, understanding the non-contact ACL injuries in different athletic tasks and different sports is important.
5. Analyze the overall risk of sustaining non-contact ACL injuries in each sport in which non-contact ACL injuries frequently occur. With known probability of sustaining non-contact ACL injuries in each athletic task, which athletic tasks have major contributions to the overall risk of sustaining non-contact ACL

injuries in a given sport can be determined using the stochastic modeling approach by adding a proportional stratified random sample control mechanism in the Monte Carlo simulation. This stratified random sample control mechanism can control the number of each athletic task included in a Monte Carlo simulation for a given sport, so that the number of each athletic task included in the simulation will be proportional to that in real training and competitions of the sports. Understanding which tasks have major contributions to the overall risk of sustaining non-contact ACL injuries will provide significant information for development of prevention strategies.

6. Evaluate the effectiveness of a given non-contact ACL injury prevention programs. The female-to-male non-contact ACL injury rate ratio estimated using the stochastic biomechanical model has been validated. The stochastic biomechanical model developed in this study is valid at least in estimating the relative risk of sustaining non-contact ACL injuries. The stochastic biomechanical model developed in this study, therefore, can be applied to determine how a prevention program changes the risk of sustaining non-contact ACL injuries. An efficient scientific method to evaluate the effectiveness of non-contact ACL injury prevention programs is critical for future development of prevention programs.
7. Determine the female hormone effect on the risk of sustaining non-contact ACL injuries. Female hormones have been suggested as a risk factor for non-contact

ACL injuries. The stochastic biomechanical model developed in this study can be applied to determine if female hormones are indeed a risk factor for non-contact ACL injuries. Literature has demonstrated that female hormones may affect the mechanical property of the ACL. The relative risk of sustaining non-contact ACL injuries in females during a menstrual cycle can be determined using the stochastic modeling approach if the variation of the mechanical properties of the ACL during a menstrual cycle is known.

5.7. Conclusion

The results of this study warrant the following conclusions:

1. The sagittal plane biomechanical model of the knee and the stochastic biomechanical model for the probability of sustaining non-contact ACL injuries are valid at least in estimating relative risk of sustaining non-contact ACL injuries.
2. Knee flexion angle and posterior ground reaction force are two major factors that affect the ACL loading in sagittal plane during landing of the stop-jump task.
3. Landing on the heels increases ACL loading during landing of the stop-jump task.
4. Knee flexion angle and peak posterior ground reaction force are two major risk factors for non-contact ACL injuries during the landing of the stop-jump task.

5. Lower extremity sagittal plane biomechanics alone can injure the ACL while the non-sagittal plane biomechanics may not during landing of the stop-jump task.
6. Gender differences in the knee flexion angle and peak posterior ground reaction force are two major motor control related contributors to the gender differences in the risk of non-contact ACL injuries.
7. The gender difference in the strength of the ACL also has major contribution to the gender difference in the risk of non-contact ACL injuries. Training of lower extremity motion patterns may reduce the risk of non-contact ACL injuries in females, but can not completely eliminate the gender difference in the risk of sustaining non-contact ACL injuries.
8. The training programs for the modification of the lower extremity motion patterns to prevent the non-contact ACL injuries should be gender specific.

APPENDIX A

Effect of Sagittal Plane Biomechanics on the Peak ACL Loading

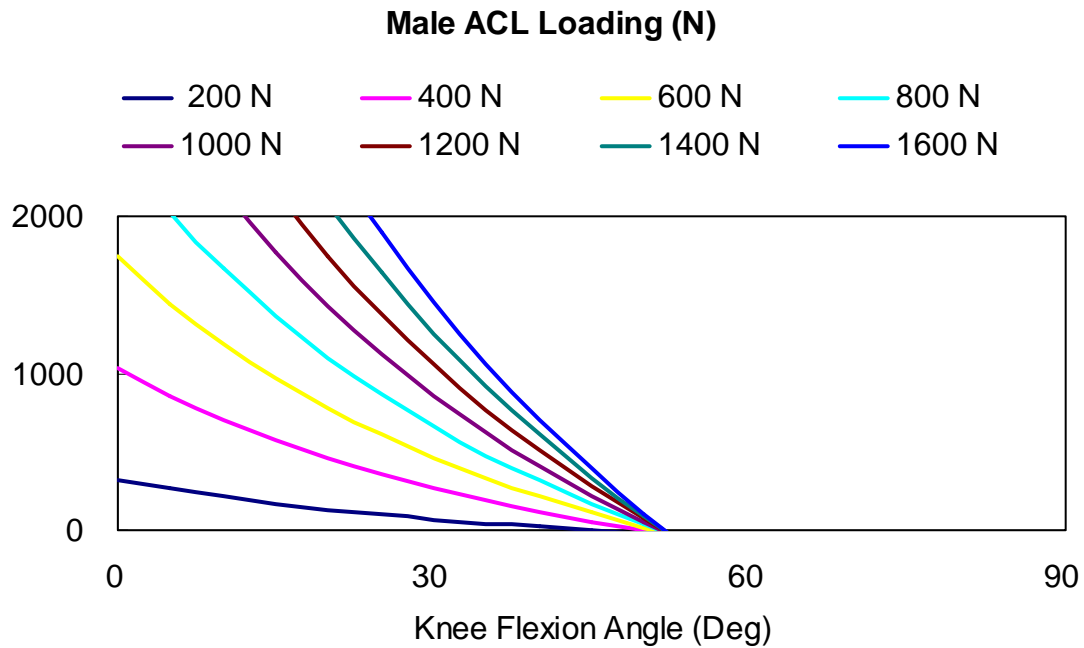


Figure A.1. Effect of the knee flexion angle at peak posterior ground reaction force on the simulated ACL loading for males at different posterior ground reaction forces during the landing of the stop-jump task.

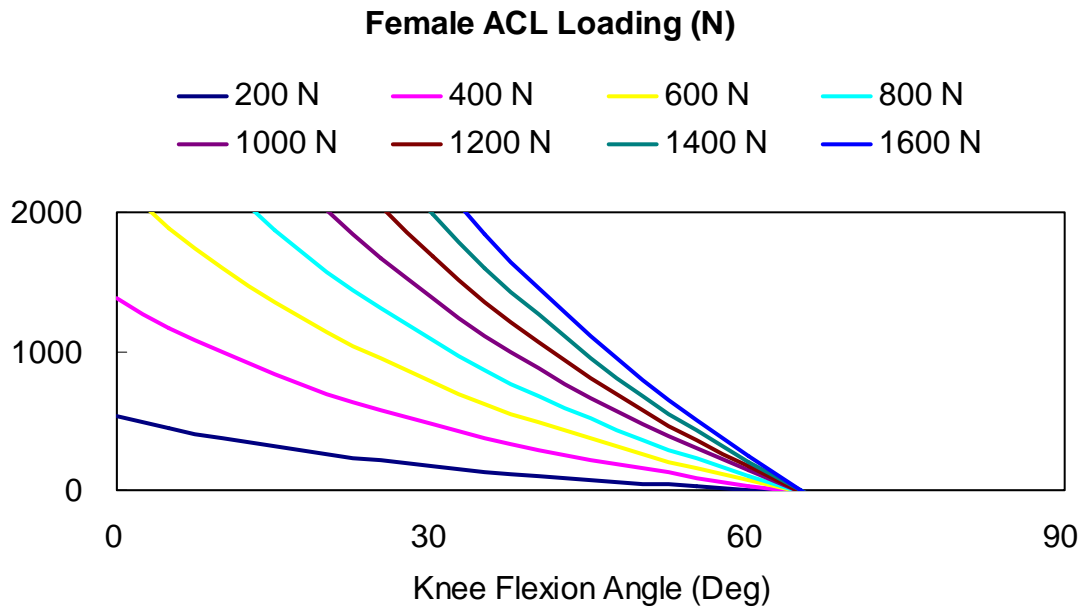


Figure A.2. Effect of the knee flexion angle at peak posterior ground reaction force on the simulated ACL loading for females at different posterior ground reaction forces during the landing of the stop-jump task.

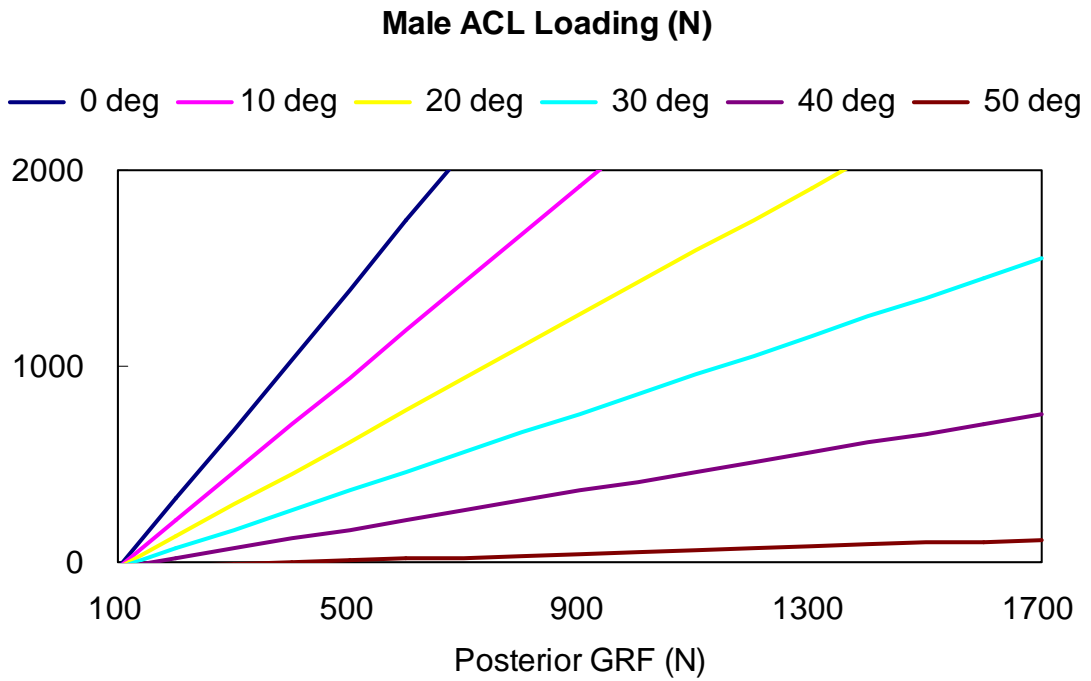


Figure A.3. Effect of the posterior ground reaction force on the simulated ACL loading for males at different knee flexion angles during the landing of the stop-jump task.

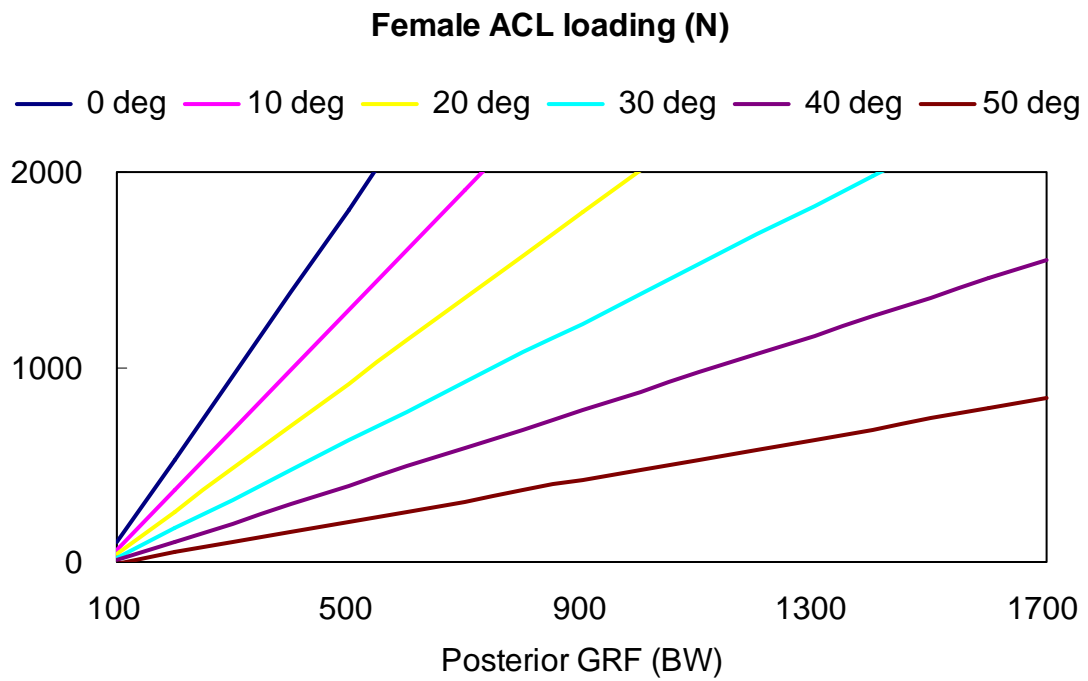


Figure A.4. Effect of the posterior ground reaction force on the simulated ACL loading for females at different knee flexion angles during the landing of the stop-jump task.

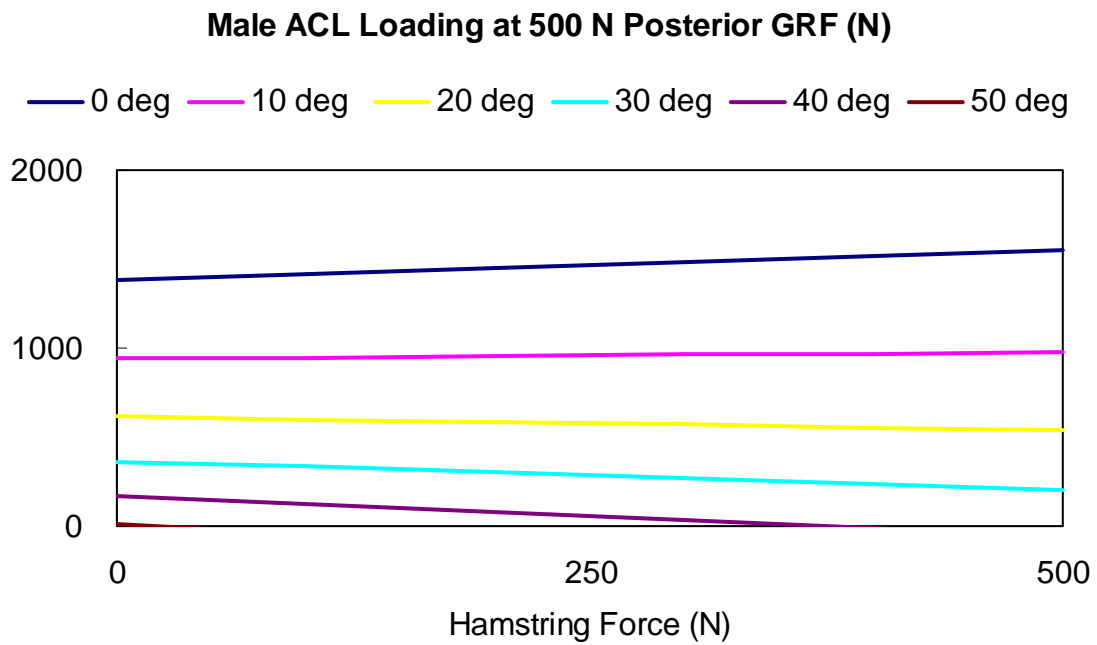


Figure A.5. Effect of the hamstring force on the simulated ACL loading for males at 500 N of posterior ground reaction force and at different knee flexion angles during the landing of the stop-jump task.

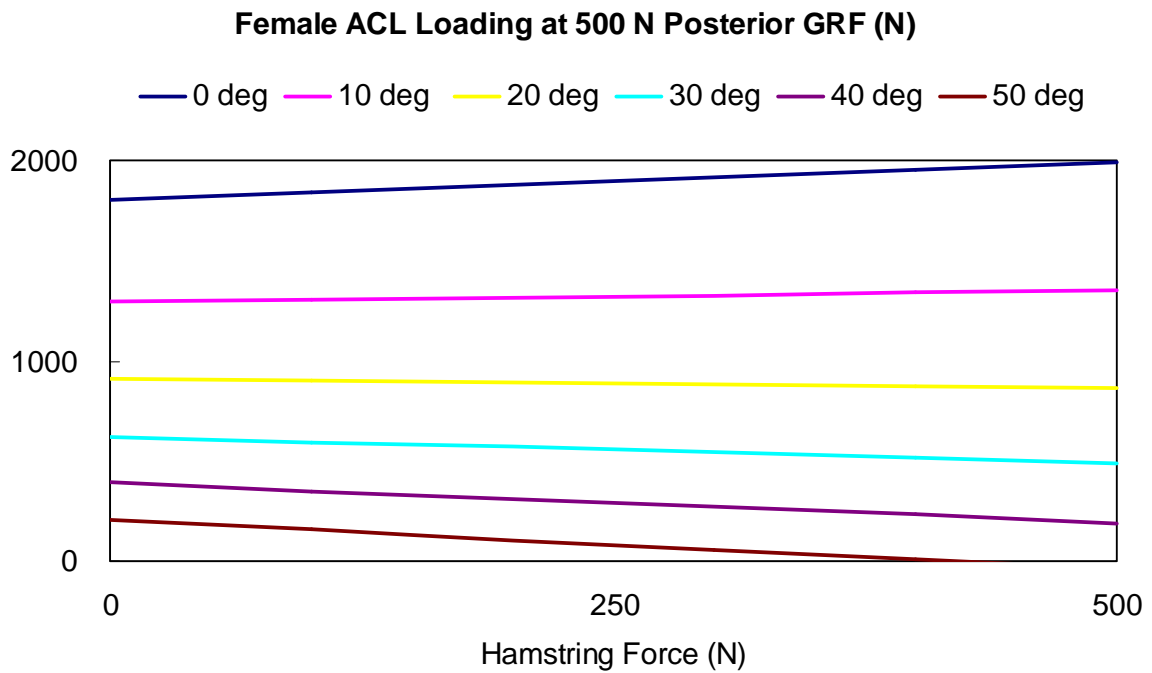


Figure A.6. Effect of the hamstring force on the simulated ACL loading for females at 500 N of posterior ground reaction force and at different knee flexion angles during the landing of the stop-jump task.

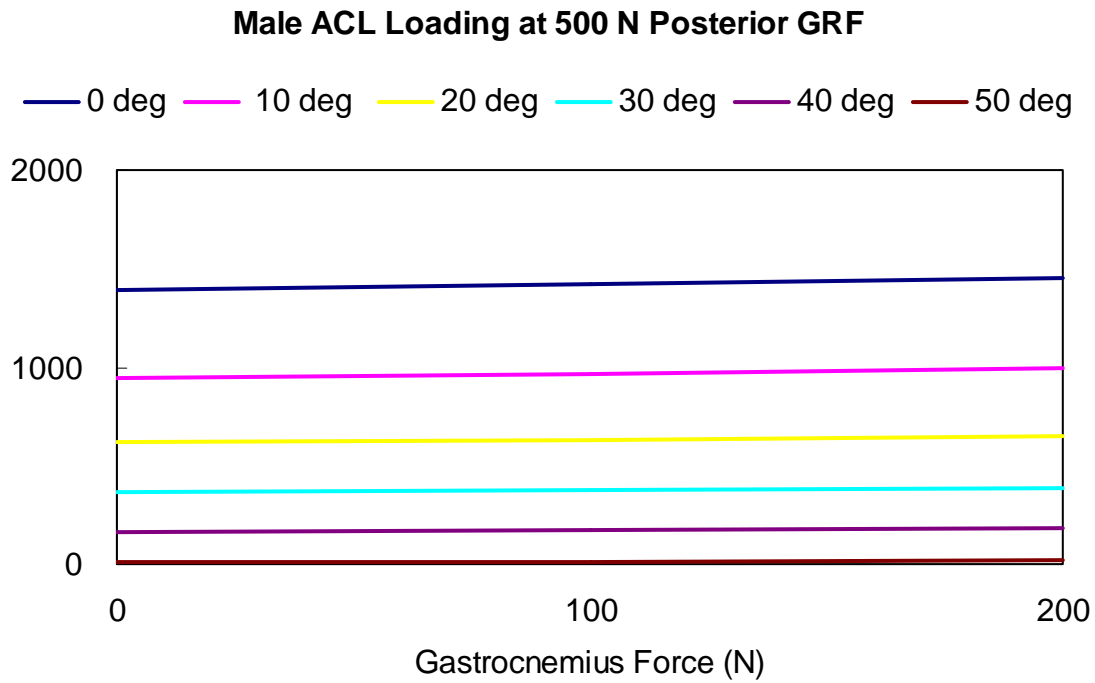


Figure A.7. Effect of the gastrocnemius force on the simulated ACL loading for males at 500 N of posterior ground reaction force and at different knee flexion angles during the landing of the stop-jump task.

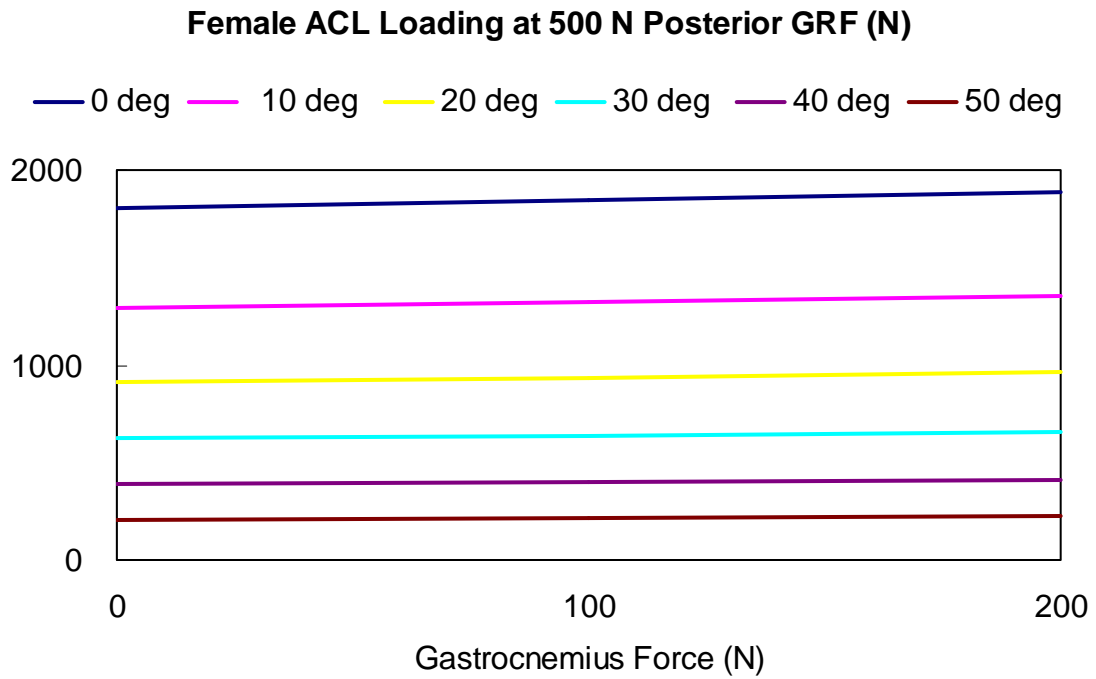
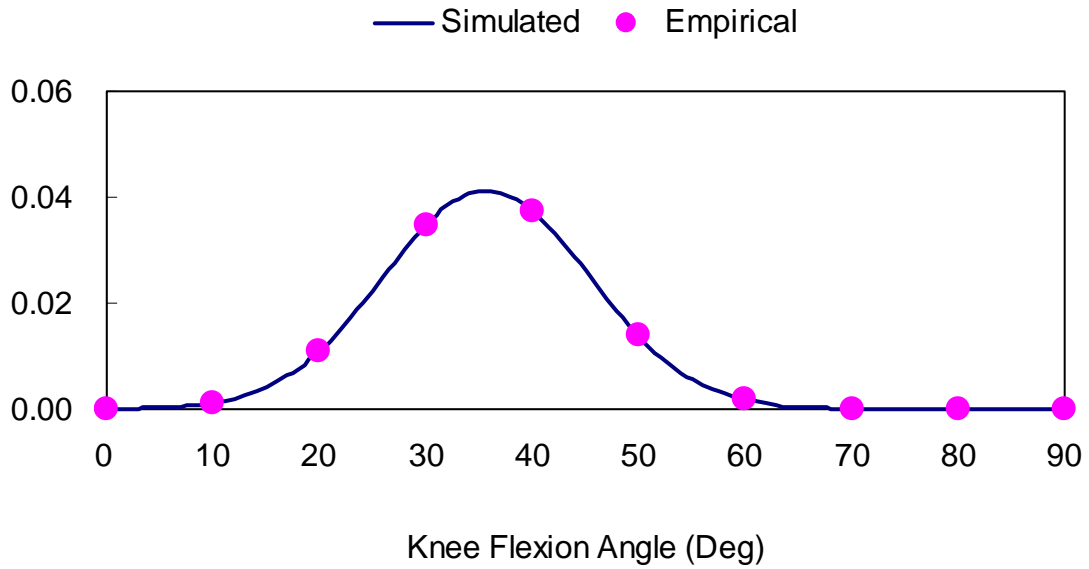


Figure A.8. Effect of the gastrocnemius force on the simulated ACL loading for females at 500 N of posterior ground reaction force and at different knee flexion angles during the landing of the stop-jump task.

APPENDIX B

Density Distribution of Independent Variables of Stochastic Biomechanical Models

Density Distribution of Male Knee Flexion Angle



Density Distribution of Female Knee Flexion Angle

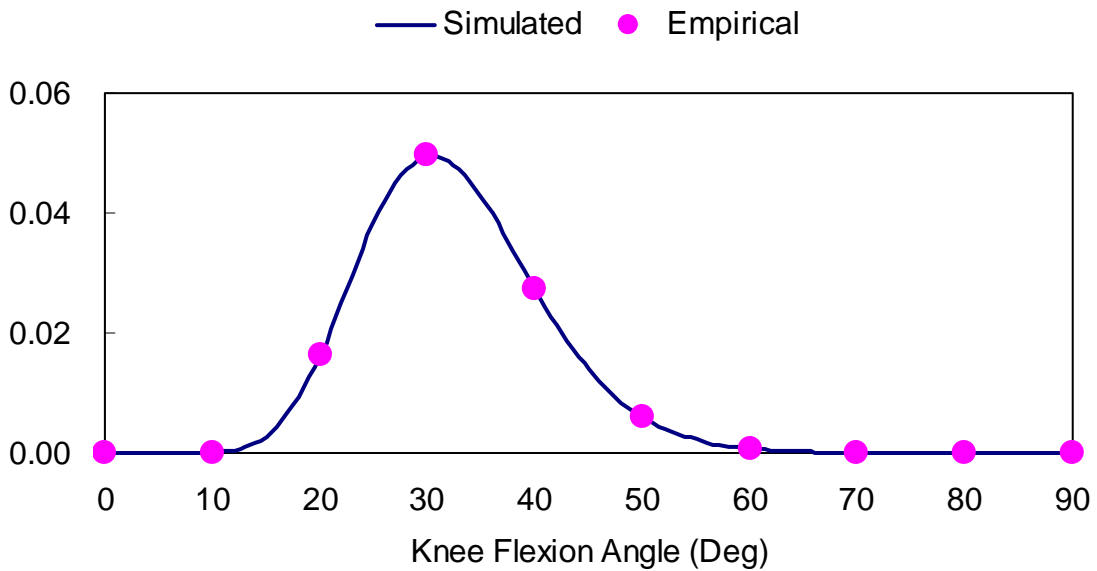


Figure B.1. Density distribution of knee flexion angle of males and females. Empirical indicates the distribution based on the experimental data.

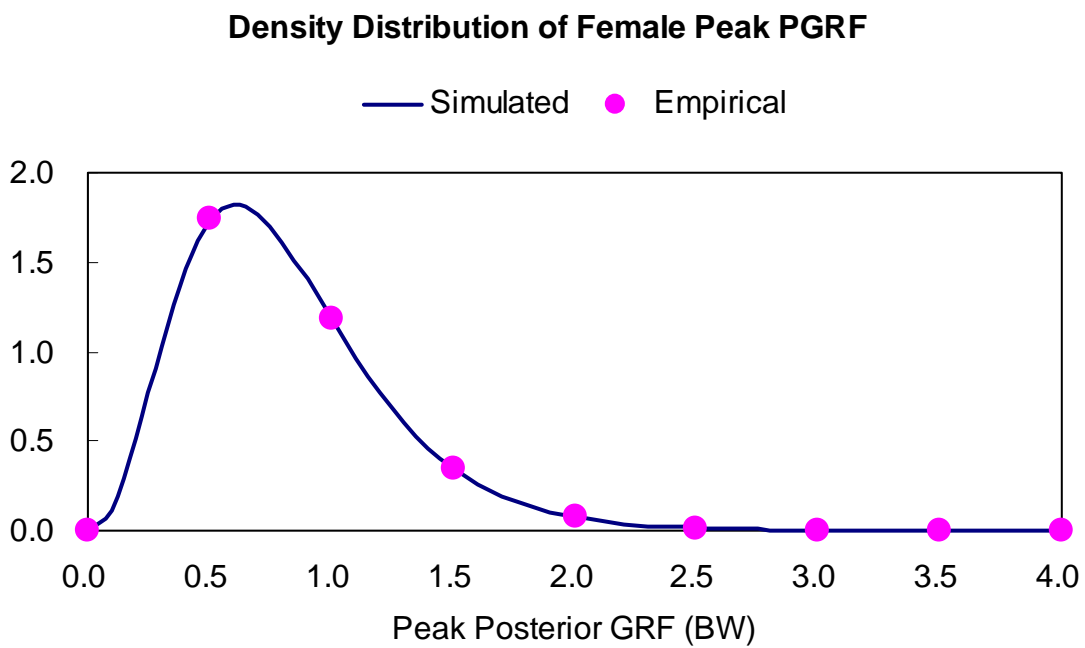
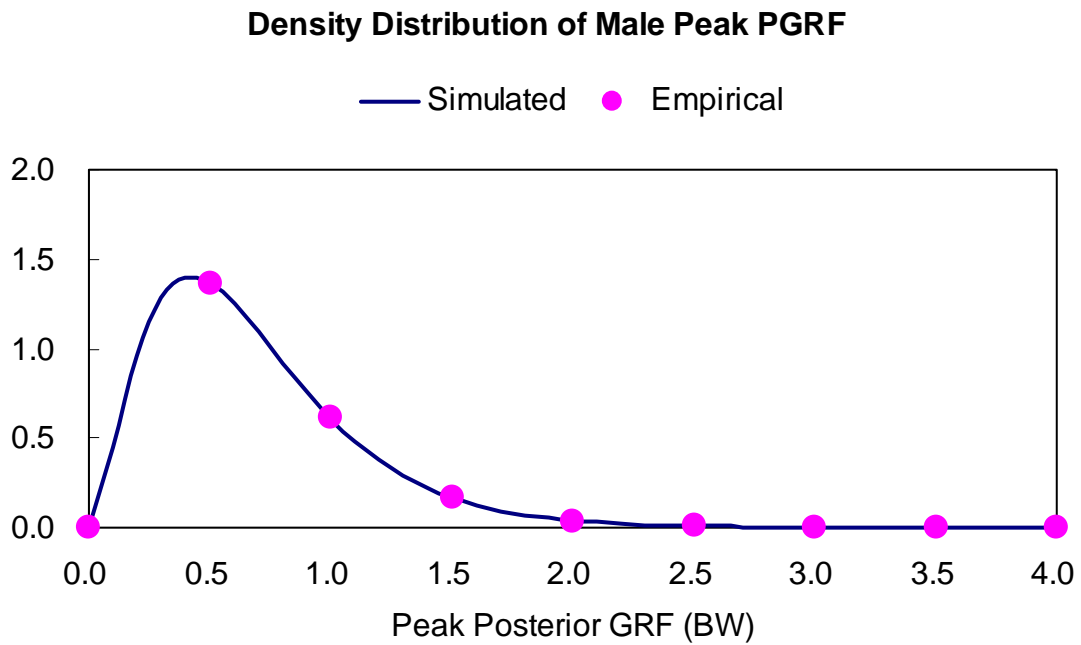
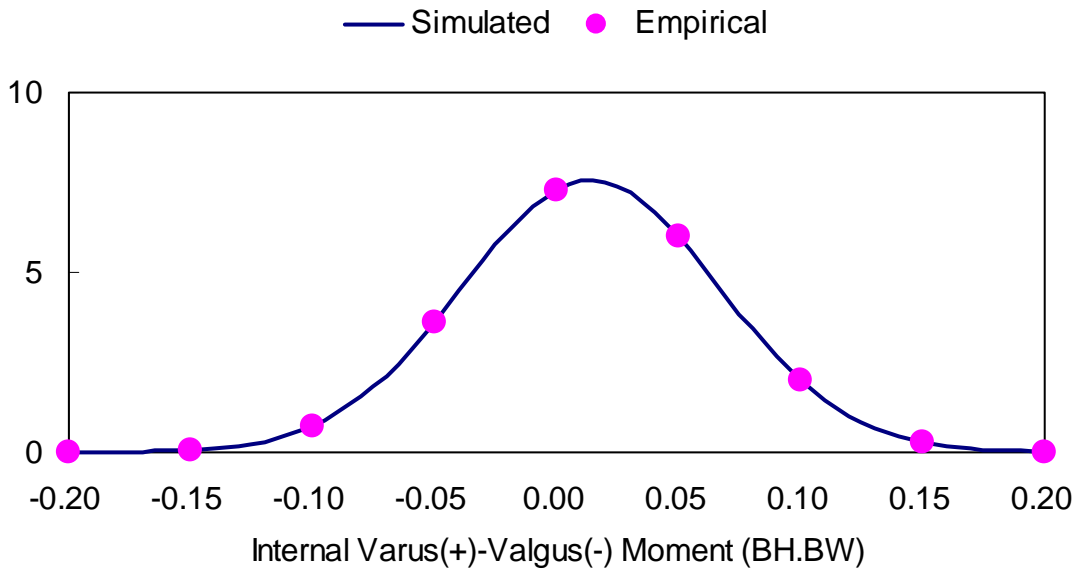


Figure B.2. Density distribution of normalized peak posterior ground reaction force of males and females. Empirical indicates the distribution based on the experimental data.

Density Distribution of Male Varus-Valgus Moment



Density Distribution of Female Varus-Valgus Moment

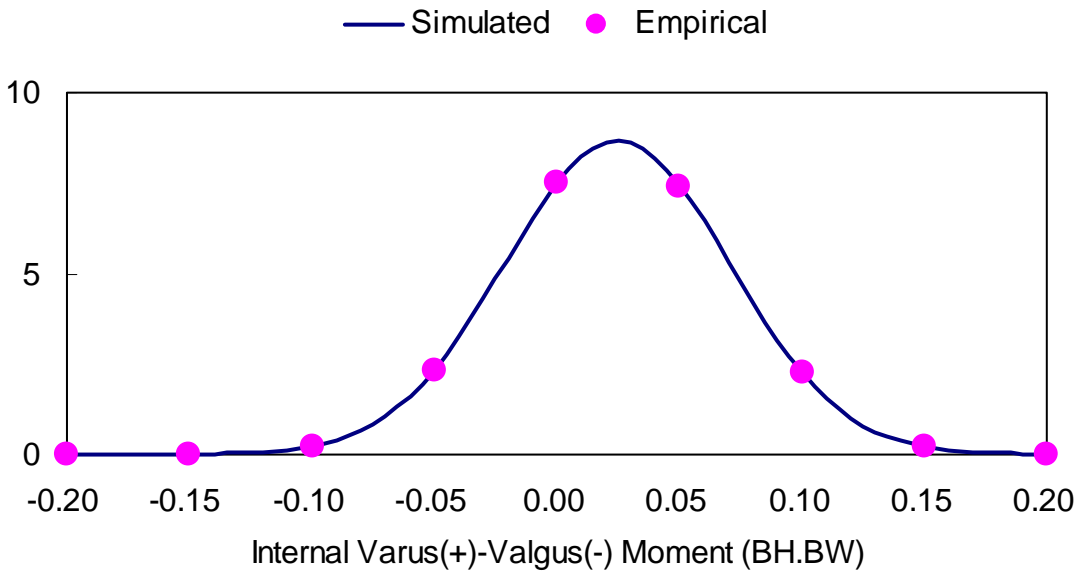


Figure B.3. Density distribution of normalized internal varus(+)-valgus(-) moment of males and females. Empirical indicates the distribution based on the experimental data.

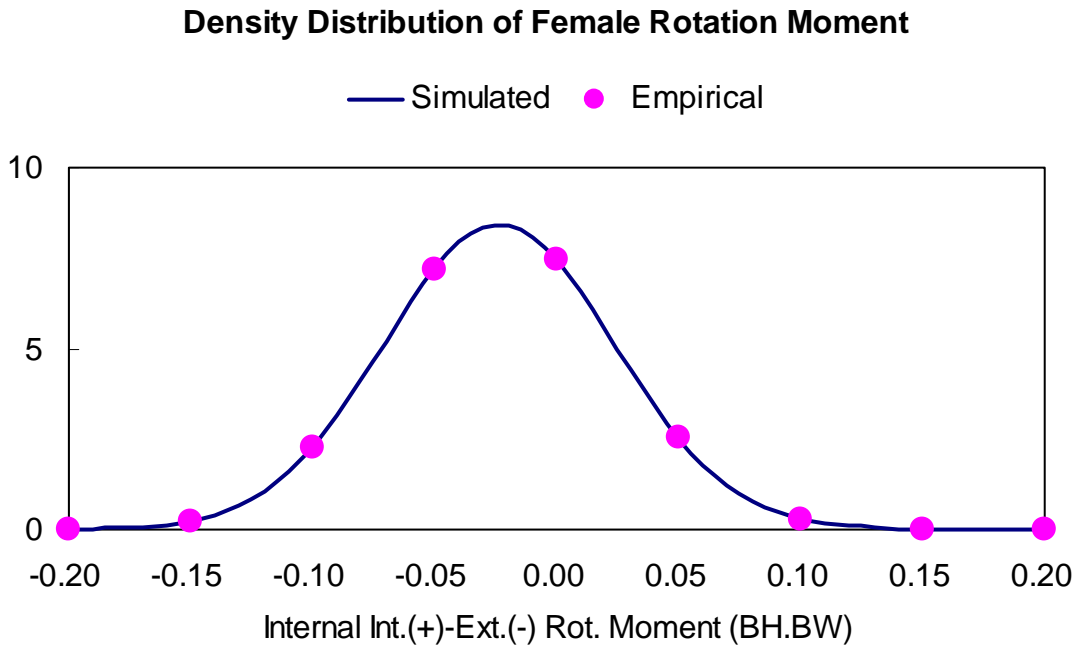
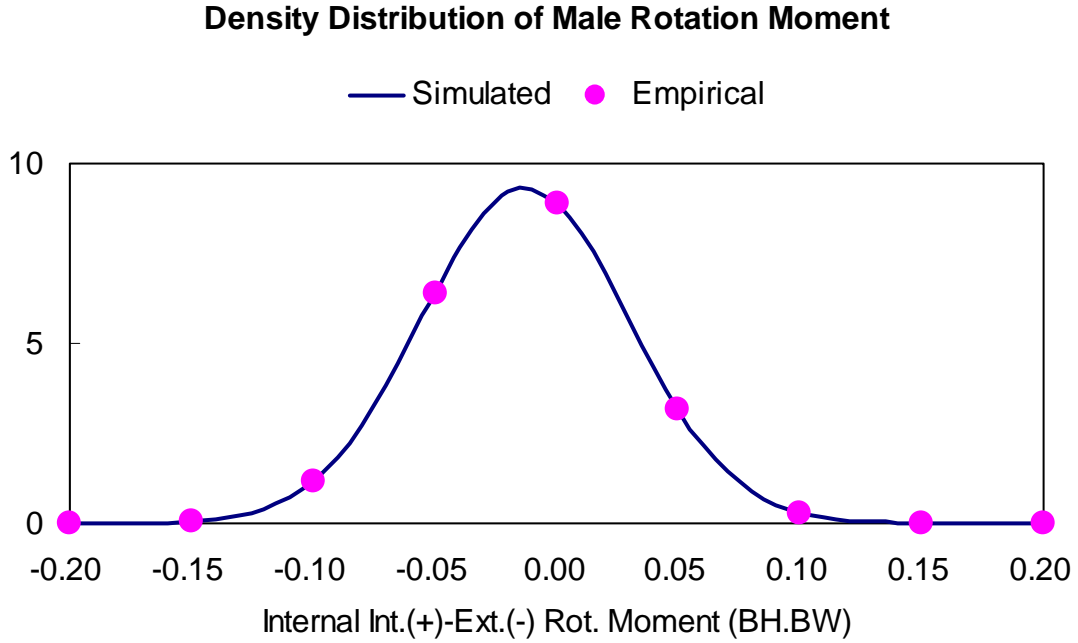
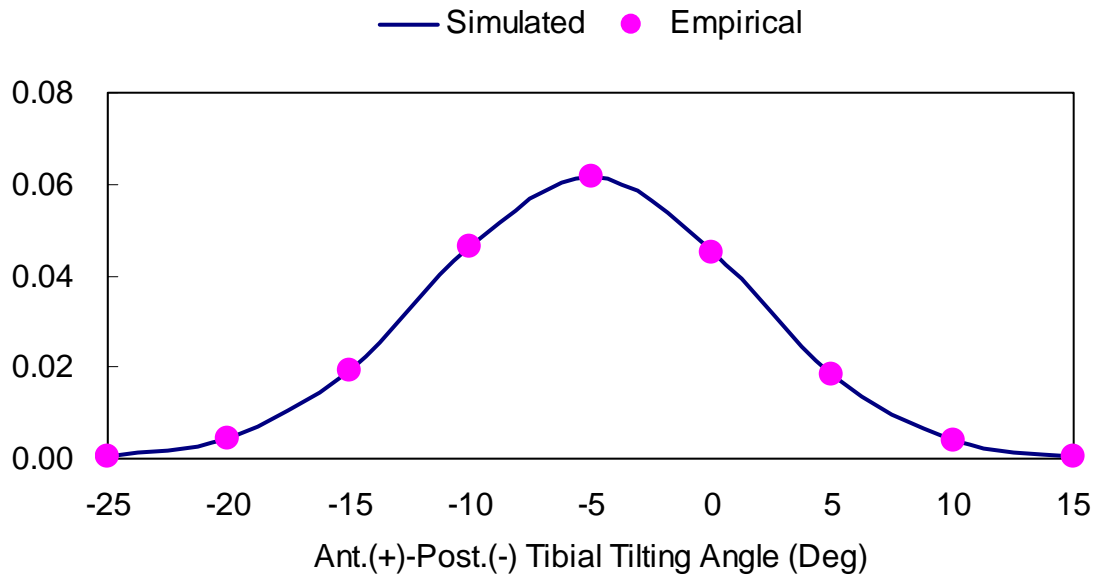


Figure B.4. Density distribution of normalized internal internal(+)-external(-) rotation moment of males and females. Empirical indicates the distribution based on the experimental data.

Density Distribution of Male Tibial Tilting Angle



Density Distribution of Female Tibial Tilting Angle

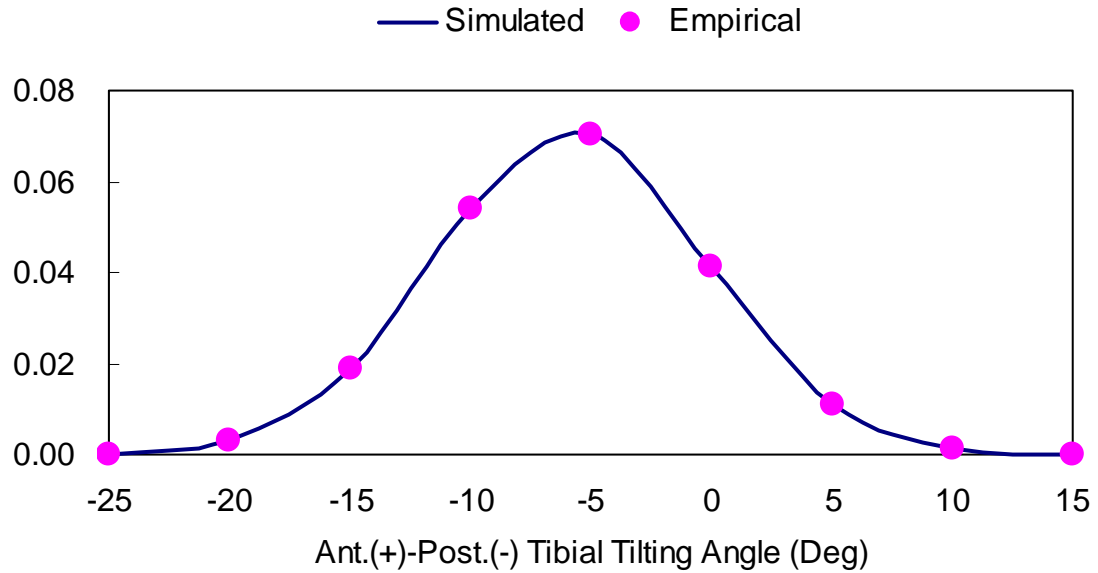
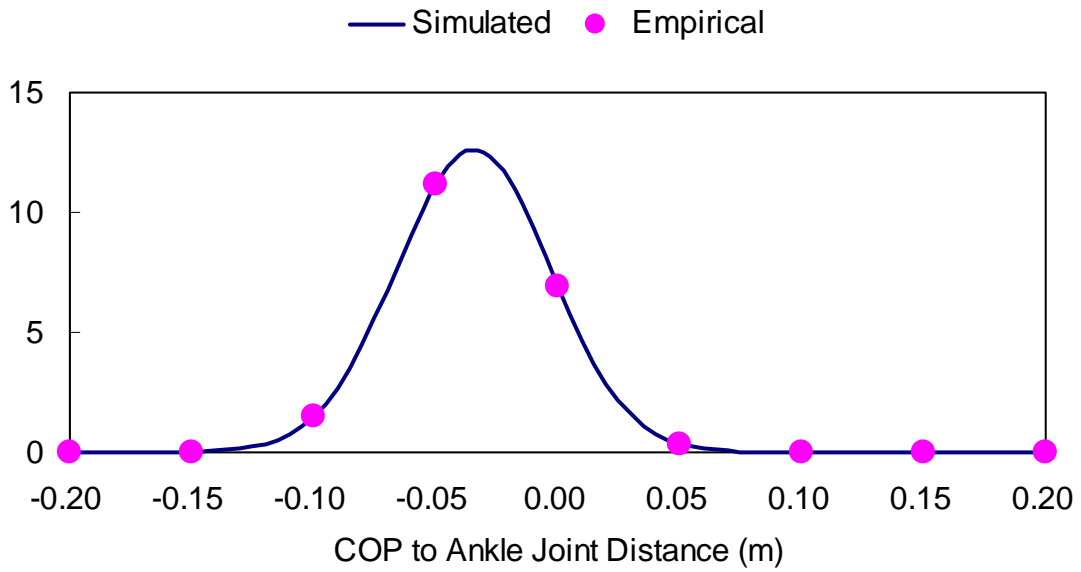


Figure B.5. Density distribution of anterior(+)-posterior(-) tibial tilting angle of males and females. Empirical indicates the distribution based on the experimental data.

Density Distribution of Male COP to Ankle Distance



Density Distribution of Female COP to Ankle Distance

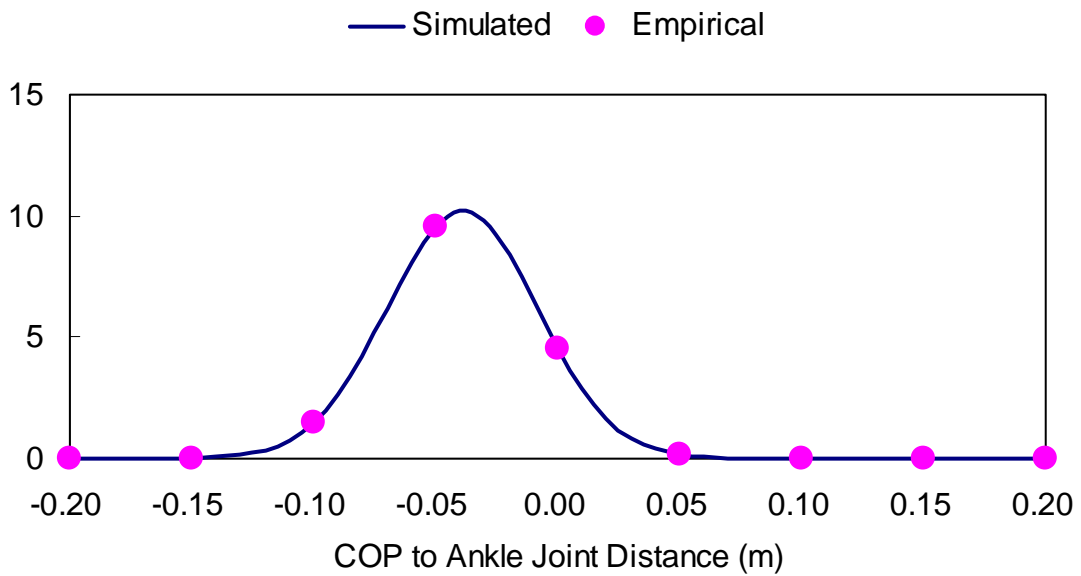
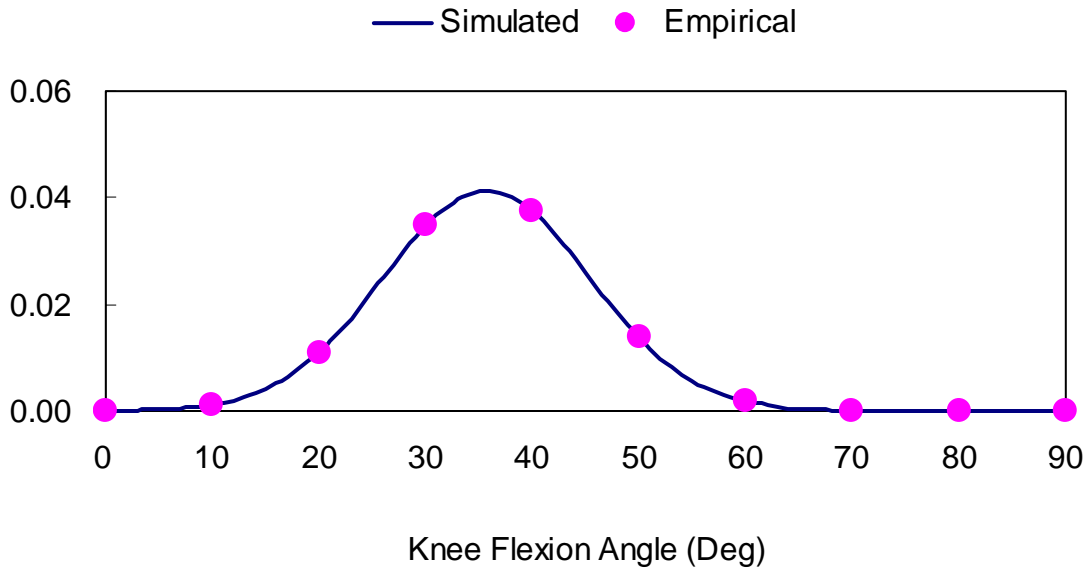


Figure B.6. Density distribution of COP to ankle joint distance of males and females. (+): prone to land on heel; (-): prone to land on toe. Empirical indicates the distribution based on the experimental data.

APPENDIX C

Probability Distribution of Independent Variables of Stochastic Biomechanical Models

Probability Distribution of Male Knee Flexion Angle



Probability Distribution of Female Knee Flexion Angle

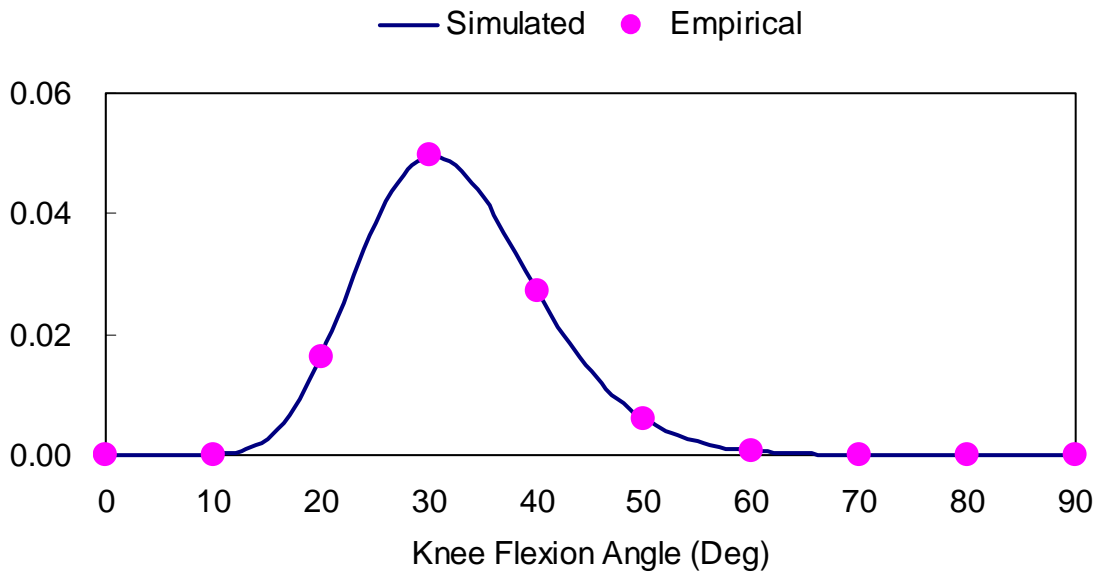


Figure C.1. Probability distribution of knee flexion angle of males and females. Empirical indicates the distribution based on the experimental data.

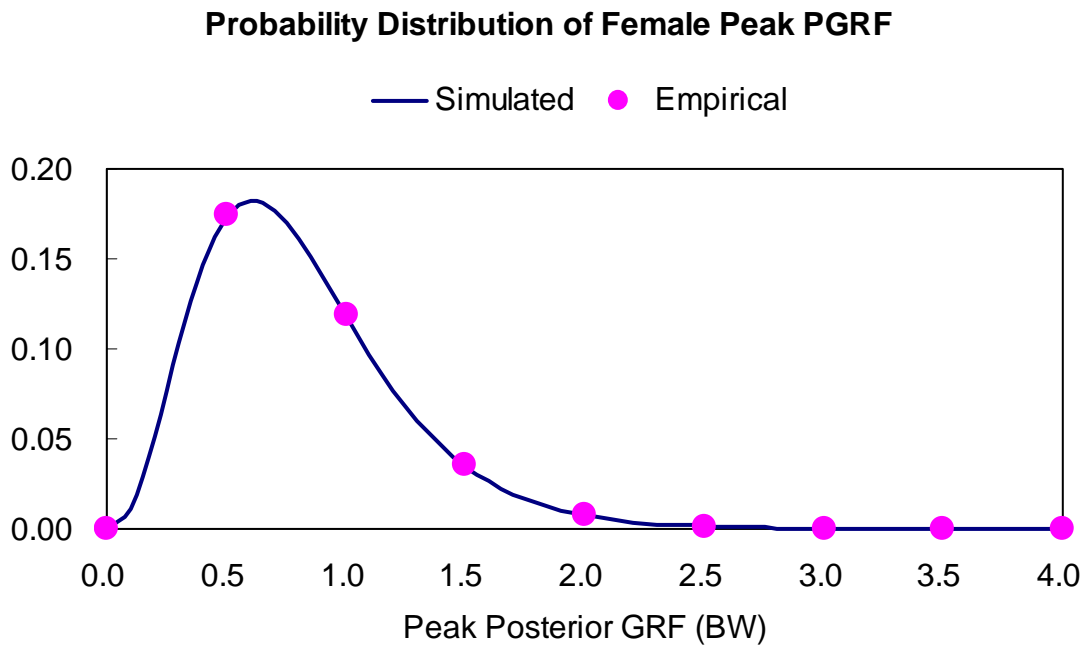
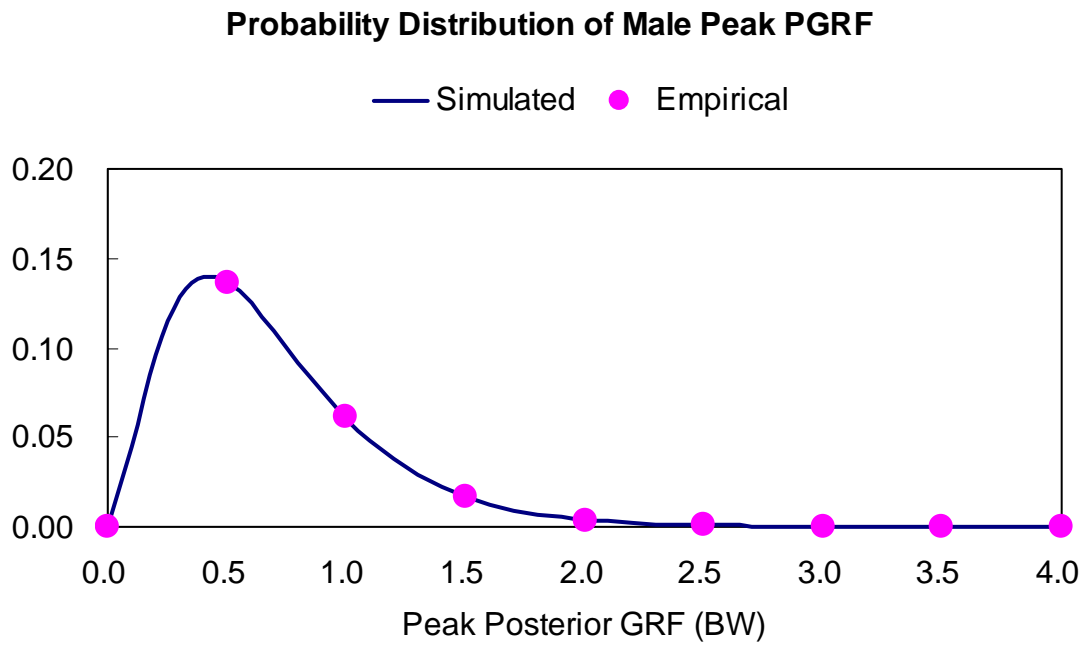
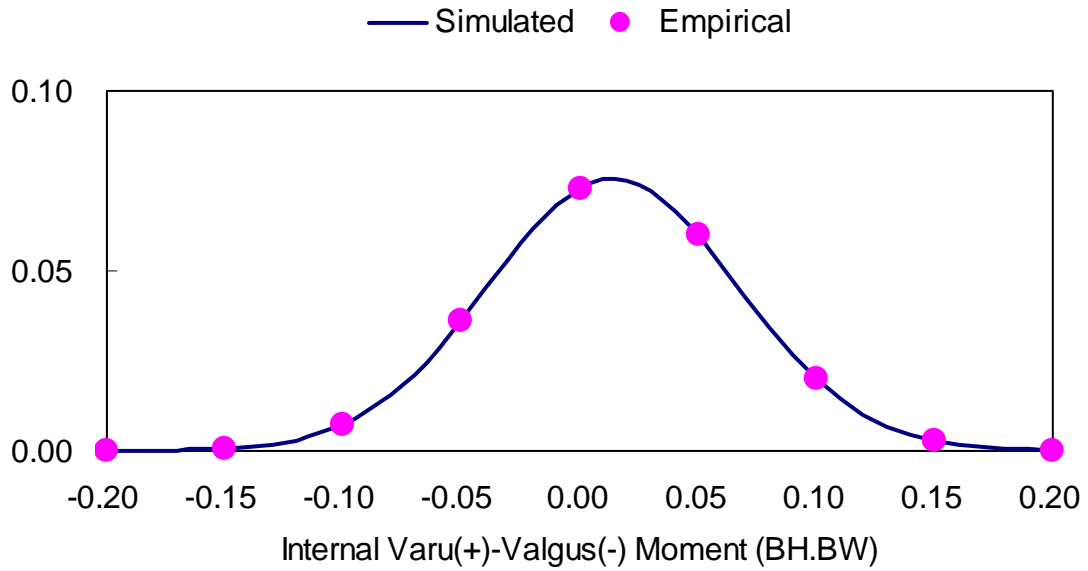


Figure C.2. Probability distribution of normalized posterior ground reaction force of males and females. Empirical indicates the distribution based on the experimental data.

Probability Distribution of Male Varus-Valgus Moment



Probability Distribution of Female Varus-Valgus Moment

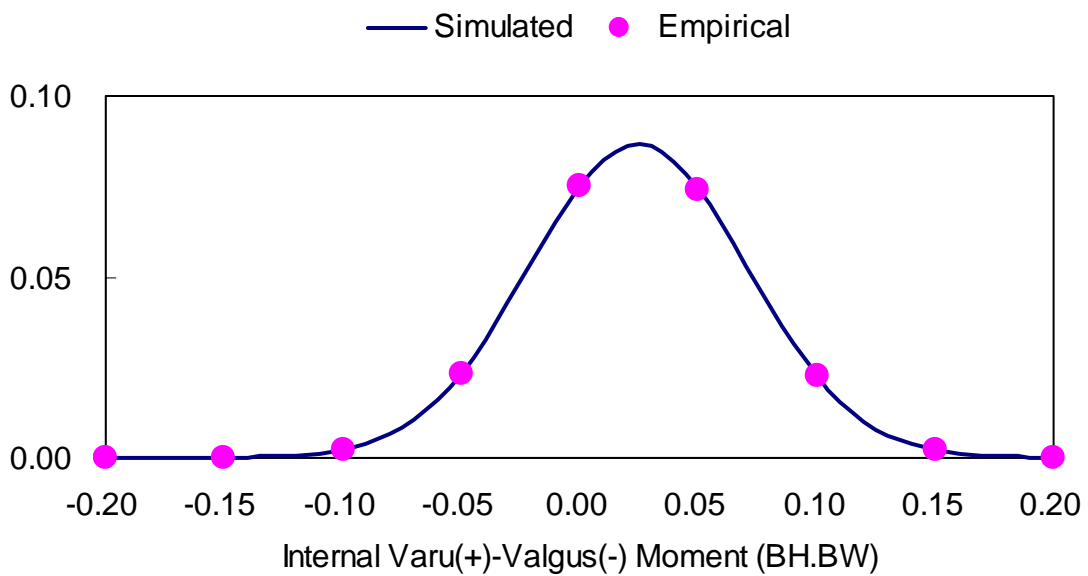
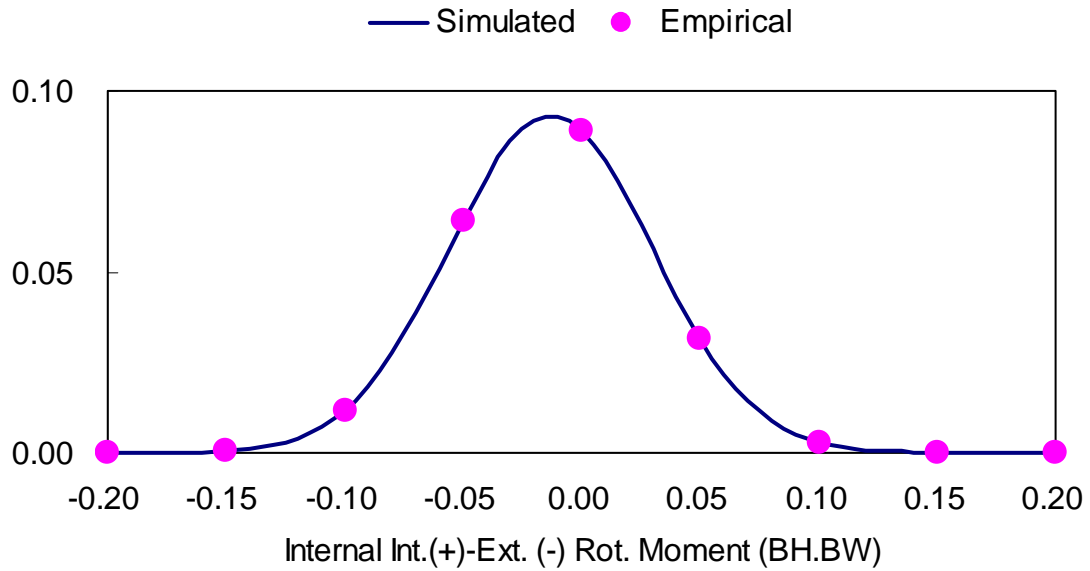


Figure C.3. Probability distribution of normalized internal varus(+)-valgus(-) moment of males and females. Empirical indicates the distribution based on the experimental data.

Probability Distribution of Male Rotation Moment



Probability Distribution of Female Rotation Moment

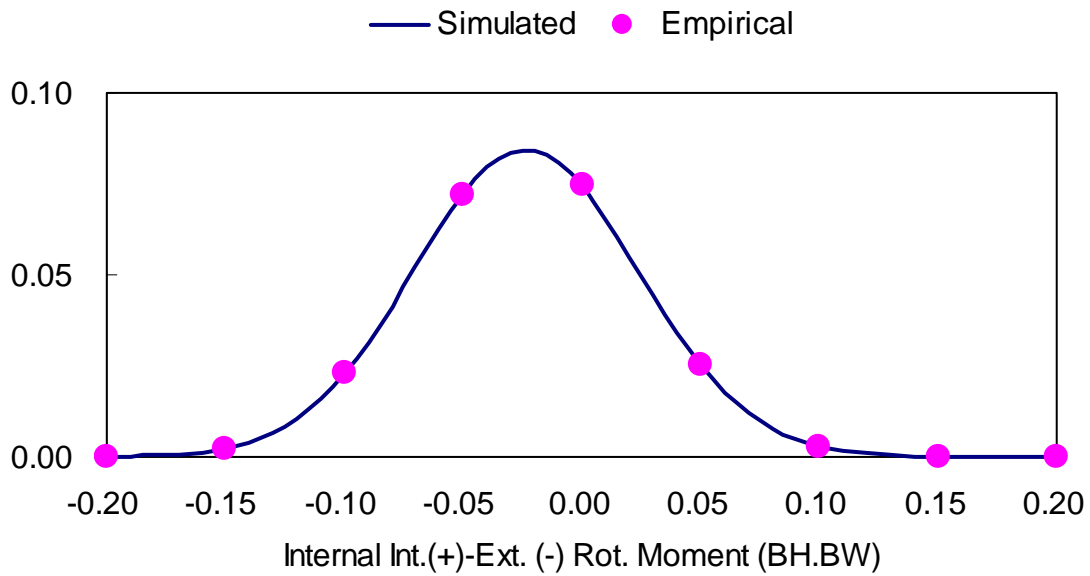
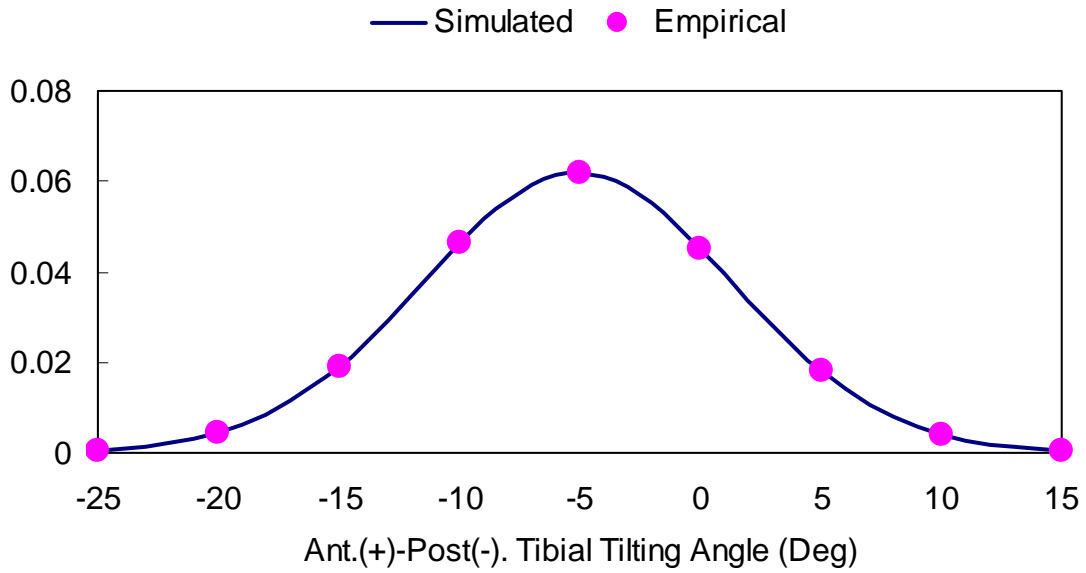


Figure C.4. Probability distribution of normalized internal internal(+)-external(-) rotation moment of males and females. Empirical indicates the distribution based on the experimental data.

Probability Distribution of Male Tibial Tilting Angle



Probability Distribution of Female Tibial Tilting Angle

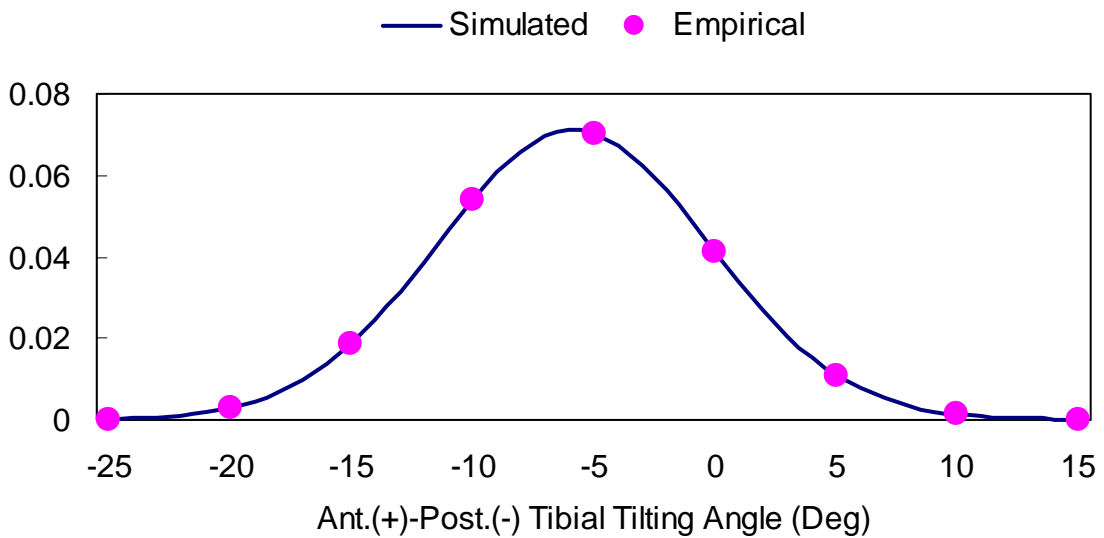
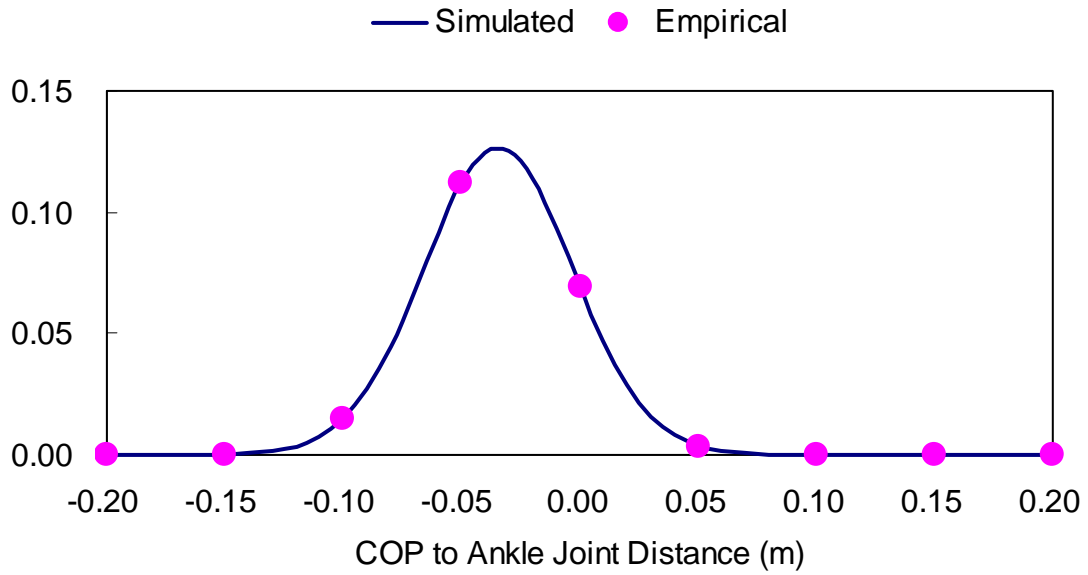


Figure C.5. Probability distribution of anterior(+)-posterior(-) tibial tilting angle of males and females. Empirical indicates the distribution based on the experimental data.

Probability Distribution of Male COP to Ankle Distance



Probability Distribution of Female COP to Ankle Distance

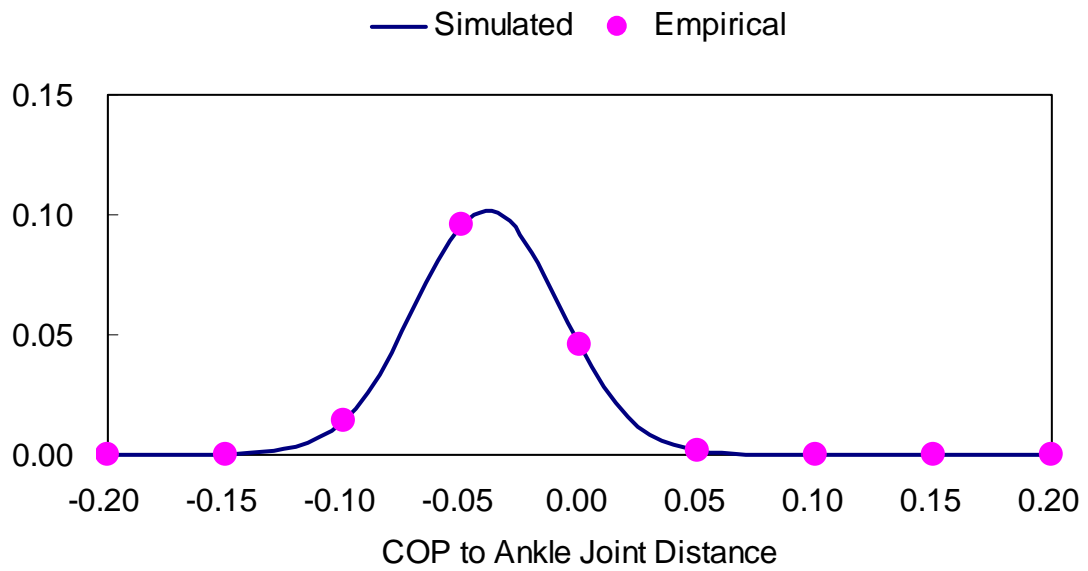


Figure C.6. Probability distribution of COP to ankle joint distance of males and females. (+):prone to land on heel; (-): prone to land on toe. Empirical indicates the distribution based on the experimental data.

REFERENCES

1. Agel, J., Arendt, E. A., and Bershadsky, B. (2005). Anterior cruciate ligament injury in national collegiate athletic association basketball and soccer: a 13-year review. Am J Sports Med, 33(4):524-30.
2. Anderson, A. F., Dome, D. C., Gautam, S., Awh, M. H., and Rennert, G. W. (2001). Correlation of anthropometric measurements, strength, anterior cruciate ligament size, and intercondylar notch characteristics to sex differences in anterior cruciate ligament tear rates. Am J Sports Med, 29(1):58-66.
3. Arendt, E., and Dick, R. (1995). Knee injury patterns among men and women in collegiate basketball and soccer. NCAA data and review of literature. Am J Sports Med, 23(6):694-701.
4. Arendt, E. A., Bershadsky, B., and Agel, J. (2002). Periodicity of noncontact anterior cruciate ligament injuries during the menstrual cycle. J Gend Specif Med, 5(2):19-26.
5. Arms, S. W., Pope, M. H., Johnson, R. J., Fischer, R. A., Arvidsson, I., and Eriksson, E. (1984). The biomechanics of anterior cruciate ligament rehabilitation and reconstruction. Am J Sports Med, 12(1):8-18.
6. Ball, K. A., Brooks-Hill, A. L., Richard, D., Marks, P., and Evans, R. J. (1999). Lack of hip flexion: A mechanism for ACL injury? Medicine & Science in Sports & Exercise, 31(5):S295.
7. Bell, A. L., Pedersen, D. R., and Brand, R. A. (1990). A comparison of the accuracy of several hip center location prediction methods. J Biomech, 23(6):617-21.
8. Bellchamber, T. L., and van den Bogert, A. J. (2000). Contributions of proximal and distal moments to axial tibial rotation during walking and running. J Biomech, 33(11):1397-403.
9. Bendjaballah, M. Z., Shirazi-Adl, A., and Zukor, D. J. (1997). Finite element analysis of human knee joint in varus-valgus. Clin Biomech, 12(3):139-148.
10. Berns, G. S., Hull, M. L., and Patterson, H. A. (1992). Strain in the anteromedial bundle of the anterior cruciate ligament under combination loading. J Orthop Res, 10(2):167-76.

11. Beynnon, B. D., Fleming, B. C., Johnson, R. J., Nichols, C. E., Renstrom, P. A., and Pope, M. H. (1995). Anterior cruciate ligament strain behavior during rehabilitation exercises in vivo. Am J Sports Med, 23(1):24-34.
12. Bjordal, J. M., Arnly, F., Hannestad, B., and Strand, T. (1997). Epidemiology of anterior cruciate ligament injuries in soccer. Am J Sports Med, 25(3):341-5.
13. Boden, B. P., Dean, G. S., Feagin, J. A., Jr., and Garrett, W. E., Jr. (2000). Mechanisms of anterior cruciate ligament injury. Orthopedics, 23(6):573-8.
14. Buchanan, T. S., Kim, A. W., and Lloyd, D. G. (1996). Selective muscle activation following rapid varus/valgus perturbations at the knee. Med Sci Sports Exerc, 28(7):870-6.
15. Buff, H. U., Jones, L. C., and Hungerford, D. S. (1988). Experimental determination of forces transmitted through the patello-femoral joint. J Biomech, 21(1):17-23.
16. Caraffa, A., Cerulli, G., Progetti, M., Aisa, G., and Rizzo, A. (1996). Prevention of anterior cruciate ligament injuries in soccer. A prospective controlled study of proprioceptive training. Knee Surg Sports Traumatol Arthrosc, 4(1):19-21.
17. Cerulli, G., Benoit, D. L., Lamontagne, M., Caraffa, A., and Liti, A. (2003). In vivo anterior cruciate ligament strain behaviour during a rapid deceleration movement: case report. Knee Surg Sports Traumatol Arthrosc, 11(5):307-11.
18. Chandrashekar, N., Mansouri, H., Slauterbeck, J., and Hashemi, J. (2006). Sex-based differences in the tensile properties of the human anterior cruciate ligament. J Biomech, 39(12):2307-12.
19. Chandrashekar, N., Slauterbeck, J., and Hashemi, J. (2005). Sex-based differences in the anthropometric characteristics of the anterior cruciate ligament and its relation to intercondylar notch geometry: a cadaveric study. Am J Sports Med, 33(10):1492-8.
20. Chang, Y. W., Hughes, R. E., Su, F. C., Itoi, E., and An, K. N. (2000). Prediction of muscle force involved in shoulder internal rotation. J Shoulder Elbow Surg, 9(3):188-95.
21. Chao, E. Y. (1980). Justification of triaxial goniometer for the measurement of joint rotation. J Biomech, 13(12):989-1006.

22. Chappell, J. D., Yu, B., Kirkendall, D. T., and Garrett, W. E. (2002). A comparison of knee kinetics between male and female recreational athletes in stop-jump tasks. *Am J Sports Med*, 30(2):261-7.
23. Chaudhari, A. M., and Andriacchi, T. P. (2006). The mechanical consequences of dynamic frontal plane limb alignment for non-contact ACL injury. *J Biomech*, 39(2):330-8.
24. Colby, S., Francisco, A., Yu, B., Kirkendall, D., Finch, M., and Garrett, W., Jr. (2000). Electromyographic and kinematic analysis of cutting maneuvers. Implications for anterior cruciate ligament injury. *Am J Sports Med*, 28(2):234-40.
25. Cowling, E. J., Steele, J. R., and McNair, P. J. (2003). Effect of verbal instructions on muscle activity and risk of injury to the anterior cruciate ligament during landing. *Br J Sports Med*, 37(2):126-30.
26. Decker, M. J., Torry, M. R., Wyland, D. J., Sterett, W. I., and Richard Steadman, J. (2003). Gender differences in lower extremity kinematics, kinetics and energy absorption during landing. *Clin Biomech*, 18(7):662-9.
27. Delagi, E. F., and Perotto, A. (1979). Anatomic guide for the electromyographer : the limbs. Springfield, Illinois: Charles C Thomas.
28. DeMorat, G., Weinhold, P., Blackburn, T., Chudik, S., and Garrett, W. (2004). Aggressive quadriceps loading can induce noncontact anterior cruciate ligament injury. *Am J Sports Med*, 32(2):477-83.
29. Devita, P., and Skelly, W. A. (1992). Effect of landing stiffness on joint kinetics and energetics in the lower extremity. *Med Sci Sports Exerc*, 24(1):108-15.
30. Draganich, L. F., and Vahey, J. W. (1990). An in vitro study of anterior cruciate ligament strain induced by quadriceps and hamstrings forces. *J Orthop Res*, 8(1):57-63.
31. Durselen, L., Claes, L., and Kiefer, H. (1995). The influence of muscle forces and external loads on cruciate ligament strain. *Am J Sports Med*, 23(1):129-36.
32. Feagin, J. A., Jr., and Lambert, K. L. (1985). Mechanism of injury and pathology of anterior cruciate ligament injuries. *Orthop Clin North Am*, 16(1):41-5.

33. Ferretti, A., Papandrea, P., Conteduca, F., and Mariani, P. P. (1992). Knee ligament injuries in volleyball players. Am J Sports Med, 20(2):203-7.
34. Finsterbush, A., Frankl, U., Matan, Y., and Mann, G. (1990). Secondary damage to the knee after isolated injury of the anterior cruciate ligament. Am J Sports Med, 18(5):475-9.
35. Fleming, B. C., Beynnon, B. D., Nichols, C. E., Johnson, R. J., and Pope, M. H. (1993). An in vivo comparison of anterior tibial translation and strain in the anteromedial band of the anterior cruciate ligament. J Biomech, 26(1):51-8.
36. Fleming, B. C., Beynnon, B. D., Renstrom, P. A., Johnson, R. J., Nichols, C. E., Peura, G. D., and Uh, B. S. (1999). The strain behavior of the anterior cruciate ligament during stair climbing: an in vivo study. Arthroscopy, 15(2):185-91.
37. Fleming, B. C., Ohlen, G., Renstrom, P. A., Peura, G. D., Beynnon, B. D., and Badger, G. J. (2003). The effects of compressive load and knee joint torque on peak anterior cruciate ligament strains. Am J Sports Med, 31(5):701-7.
38. Fleming, B. C., Renstrom, P. A., Beynnon, B. D., Engstrom, B., Peura, G. D., Badger, G. J., and Johnson, R. J. (2001). The effect of weightbearing and external loading on anterior cruciate ligament strain. J Biomech, 34(2):163-70.
39. Fleming, B. C., Renstrom, P. A., Ohlen, G., Johnson, R. J., Peura, G. D., Beynnon, B. D., and Badger, G. J. (2001). The gastrocnemius muscle is an antagonist of the anterior cruciate ligament. J Orthop Res, 19(6):1178-84.
40. Ford, K. R., Myer, G. D., and Hewett, T. E. (2003). Valgus knee motion during landing in high school female and male basketball players. Med Sci Sports Exerc, 35(10):1745-50.
41. Ford, K. R., Myer, G. D., Toms, H. E., and Hewett, T. E. (2005). Gender differences in the kinematics of unanticipated cutting in young athletes. Med Sci Sports Exerc, 37(1):124-9.
42. Fukuda, Y., Woo, S. L., Loh, J. C., Tsuda, E., Tang, P., McMahon, P. J., and Debski, R. E. (2003). A quantitative analysis of valgus torque on the ACL: a human cadaveric study. J Orthop Res, 21(6):1107-12.

43. Garrett, W. E., and Yu, B. (2004). Gender differences in lower extremity kinetics and probability for non-contact ACL injuries in a stop-jump task. Proceeding of 71st Annual Meeting of American Academy of Orthopaedic Surgery. San Francisco, CA. USA.
44. Garrick, J. G., and Requa, R. K. (1996). Football cleat design and its effect on anterior cruciate ligament injuries. Am J Sports Med, 24(5):705-6.
45. Giffin, J. R., Vogrin, T. M., Zantop, T., Woo, S. L., and Harner, C. D. (2004). Effects of increasing tibial slope on the biomechanics of the knee. Am J Sports Med, 32(2):376-82.
46. Gottlob, C. A., Baker, C. L., Jr., Pellissier, J. M., and Colvin, L. (1999). Cost effectiveness of anterior cruciate ligament reconstruction in young adults. Clin Orthop Relat Res, (367):272-82.
47. Greenwood, D. T. (1987). Principles of Dynamics. Englewood Cliffs, New Jersey: Prentice Hall.
48. Griffin, L. Y., Agel, J., Albohm, M. J., Arendt, E. A., Dick, R. W., et al. (2000). Noncontact anterior cruciate ligament injuries: risk factors and prevention strategies. J Am Acad Orthop Surg, 8(3):141-50.
49. Harmon, K. G., and Ireland, M. L. (2000). Gender differences in noncontact anterior cruciate ligament injuries. Clin Sports Med, 19(2):287-302.
50. Hatze, H. (1981). Estimation of myodynamic parameter values from observations on isometrically contracting muscle groups. Eur J Appl Physiol Occup Physiol, 46(4):325-38.
51. Henry, J. C., and Kaeding, C. (2001). Neuromuscular differences between male and female athletes. Curr Womens Health Rep, 1(3):241-4.
52. Herzog, W., and Read, L. J. (1993). Lines of action and moment arms of the major force-carrying structures crossing the human knee joint. J Anat, 182 (Pt 2):213-30.
53. Hewett, T. E. (2000). Neuromuscular and hormonal factors associated with knee injuries in female athletes. Strategies for intervention. Sports Med, 29(5):313-27.

54. Hewett, T. E., Myer, G. D., Ford, K. R., Heidt, R. S., Jr., Colosimo, A. J., McLean, S. G., van den Bogert, A. J., Paterno, M. V., and Succop, P. (2005). Biomechanical measures of neuromuscular control and valgus loading of the knee predict anterior cruciate ligament injury risk in female athletes: a prospective study. Am J Sports Med, 33(4):492-501.
55. Hewett, T. E., Stroupe, A. L., Nance, T. A., and Noyes, F. R. (1996). Plyometric training in female athletes. Decreased impact forces and increased hamstring torques. Am J Sports Med, 24(6):765-73.
56. Hinrichs, R. N. (1990). Adjustments to the segment center of mass proportions of Clauser et al. (1969). J Biomech, 23(9):949-51.
57. Huberti, H. H., Hayes, W. C., Stone, J. L., and Shybut, G. T. (1984). Force ratios in the quadriceps tendon and ligamentum patellae. J Orthop Res, 2(1):49-54.
58. Hughes, R. E., and An, K. N. (1997). Monte Carlo simulation of a planar shoulder model. Med Biol Eng Comput, 35(5):544-8.
59. Huston, L. J., Greenfield, M. L., and Wojtys, E. M. (2000). Anterior cruciate ligament injuries in the female athlete. Potential risk factors. Clin Orthop Relat Res, (372):50-63.
60. Huston, L. J., Vibert, B., Ashton-Miller, J. A., and Wojtys, E. M. (2001). Gender differences in knee angle when landing from a drop-jump. Am J Knee Surg, 14(4):215-9; discussion 219-20.
61. Imran, A., Huss, R. A., Holstein, H., and O'Connor, J. J. (2000). The variation in the orientations and moment arms of the knee extensor and flexor muscle tendons with increasing muscle force: a mathematical analysis. Proc Inst Mech Eng [H], 214(3):277-86.
62. Imran, A., and O'Connor, J. J. (1998). Control of knee stability after ACL injury or repair: interaction between hamstrings contraction and tibial translation. Clin Biomech (Bristol, Avon), 13(3):153-162.
63. Inman, V. T., Ralston, H. J., and Todd, F. (1981). Human Walking. Baltimore, MD, USA: Williams and Wilkins.

64. Inoue, M., McGurk-Burleson, E., Hollis, J. M., and Woo, S. L. (1987). Treatment of the medial collateral ligament injury. I: The importance of anterior cruciate ligament on the varus-valgus knee laxity. Am J Sports Med, 15(1):15-21.
65. Irmischer, B. S., Harris, C., Pfeiffer, R. P., DeBeliso, M. A., Adams, K. J., and Shea, K. G. (2004). Effects of a knee ligament injury prevention exercise program on impact forces in women. J Strength Cond Res, 18(4):703-7.
66. Irvine, G. B., and Glasgow, M. M. (1992). The natural history of the meniscus in anterior cruciate insufficiency. Arthroscopic analysis. J Bone Joint Surg Br, 74(3):403-5.
67. James, C. R., Sizer, P. S., Starch, D. W., Lockhart, T. E., and Slauterbeck, J. (2004). Gender differences among sagittal plane knee kinematic and ground reaction force characteristics during a rapid sprint and cut maneuver. Res Q Exerc Sport, 75(1):31-8.
68. Kanamori, A., Zeminski, J., Rudy, T. W., Li, G., Fu, F. H., and Woo, S. L. (2002). The effect of axial tibial torque on the function of the anterior cruciate ligament: a biomechanical study of a simulated pivot shift test. Arthroscopy, 18(4):394-8.
69. Kannus, P., and Jarvinen, M. (1990). Knee flexor/extensor strength ratio in follow-up of acute knee distortion injuries. Arch Phys Med Rehabil, 71(1):38-41.
70. Kaufman, K. R., An, K. N., Litchy, W. J., and Chao, E. Y. (1991). Physiological prediction of muscle forces--II. Application to isokinetic exercise. Neuroscience, 40(3):793-804.
71. Kernozek, T. W., Torry, M. R., H, V. A. N. H., Cowley, H., and Tanner, S. (2005). Gender differences in frontal and sagittal plane biomechanics during drop landings. Med Sci Sports Exerc, 37(6):1003-12; discussion 1013.
72. Kirkendall, D. T., and Garrett, W. E., Jr. (2000). The anterior cruciate ligament enigma. Injury mechanisms and prevention. Clin Orthop Relat Res, (372):64-8.
73. Lamontagne, M., Benoit, D. L., Ramsey, D. K., Caraffa, A., and Cerulli, G. (2005). What can we learn from in vivo biomechanical investigations of lower extremity? XXIII International Symposium of Biomechanics in Sports. Beijing, China.
74. Lephart, S. M., Abt, J. P., Ferris, C. M., Sell, T. C., Nagai, T., Myers, J. B., and Irrgang,

- J. J. (2005). Neuromuscular and biomechanical characteristic changes in high school athletes: a plyometric versus basic resistance program. Br J Sports Med, 39(12):932-8.
75. Lephart, S. M., Ferris, C. M., Riemann, B. L., Myers, J. B., and Fu, F. H. (2002). Gender differences in strength and lower extremity kinematics during landing. Clin Orthop Relat Res, (401):162-9.
76. Li, G., Defrate, L. E., Rubash, H. E., and Gill, T. J. (2005). In vivo kinematics of the ACL during weight-bearing knee flexion. J Orthop Res, 23(2):340-4.
77. Li, G., Rudy, T. W., Sakane, M., Kanamori, A., Ma, C. B., and Woo, S. L. (1999). The importance of quadriceps and hamstring muscle loading on knee kinematics and in-situ forces in the ACL. J Biomech, 32(4):395-400.
78. Lindenfeld, T. N., Schmitt, D. J., Hendy, M. P., Mangine, R. E., and Noyes, F. R. (1994). Incidence of injury in indoor soccer. Am J Sports Med, 22(3):364-71.
79. Lloyd, D. G., and Buchanan, T. S. (2001). Strategies of muscular support of varus and valgus isometric loads at the human knee. J Biomech, 34(10):1257-67.
80. Lloyd, D. G., Buchanan, T. S., and Besier, T. F. (2005). Neuromuscular biomechanical modeling to understand knee ligament loading. Med Sci Sports Exerc, 37(11):1939-47.
81. MacWilliams, B. A., Wilson, D. R., DesJardins, J. D., Romero, J., and Chao, E. Y. (1999). Hamstrings cocontraction reduces internal rotation, anterior translation, and anterior cruciate ligament load in weight-bearing flexion. J Orthop Res, 17(6):817-22.
82. Malinzak, R. A., Colby, S. M., Kirkendall, D. T., Yu, B., and Garrett, W. E. (2001). A comparison of knee joint motion patterns between men and women in selected athletic tasks. Clin Biomech, 16(5):438-45.
83. Mandelbaum, B. R., Silvers, H. J., Watanabe, D. S., Knarr, J. F., Thomas, S. D., Griffin, L. Y., Kirkendall, D. T., and Garrett, W., Jr. (2005). Effectiveness of a neuromuscular and proprioceptive training program in preventing anterior cruciate ligament injuries in female athletes: 2-year follow-up. Am J Sports Med, 33(7):1003-10.
84. Markolf, K. L., Burchfield, D. M., Shapiro, M. M., Shepard, M. F., Finerman, G. A., and Slauterbeck, J. L. (1995). Combined knee loading states that generate high anterior cruciate ligament forces. J Orthop Res, 13(6):930-5.

85. Markolf, K. L., Gorek, J. F., Kabo, J. M., and Shapiro, M. S. (1990). Direct measurement of resultant forces in the anterior cruciate ligament. An in vitro study performed with a new experimental technique. J Bone Joint Surg Am, 72(4):557-67.
86. Markolf, K. L., O'Neill, G., Jackson, S. R., and McAllister, D. R. (2004). Effects of applied quadriceps and hamstrings muscle loads on forces in the anterior and posterior cruciate ligaments. Am J Sports Med, 32(5):1144-9.
87. Matsumoto, H., Suda, Y., Otani, T., Niki, Y., Seedhom, B. B., and Fujikawa, K. (2001). Roles of the anterior cruciate ligament and the medial collateral ligament in preventing valgus instability. J Orthop Sci, 6(1):28-32.
88. Mazzocca, A. D., Nissen, C. W., Geary, M., and Adams, D. J. (2003). Valgus medial collateral ligament rupture causes concomitant loading and damage of the anterior cruciate ligament. J Knee Surg, 16(3):148-51.
89. McCarroll, J. R., Shelbourne, K. D., and Patel, D. V. (1995). Anterior cruciate ligament injuries in young athletes. Recommendations for treatment and rehabilitation. Sports Med, 20(2):117-27.
90. McConkey, J. P. (1986). Anterior cruciate ligament rupture in skiing. A new mechanism of injury. Am J Sports Med, 14(2):160-4.
91. McLean, S. G., Huang, X., Su, A., and Van Den Bogert, A. J. (2004). Sagittal plane biomechanics cannot injure the ACL during sidestep cutting. Clin Biomech, 19(8):828-38.
92. McLean, S. G., Su, A., and van den Bogert, A. J. (2003a). Determining neuromuscular contributions to ACL injury risk via computer simulation. Transactions of 49th Annual Meeting of the Orthopaedic Research Society. New Orleans, LA, USA.
93. McLean, S. G., Su, A., and van den Bogert, A. J. (2003b). Development and validation of a 3-D model to predict knee joint loading during dynamic movement. J Biomech Eng, 125(6):864-74.
94. McNair, P. J., and Marshall, R. N. (1994). Landing characteristics in subjects with normal and anterior cruciate ligament deficient knee joints. Arch Phys Med Rehabil, 75(5):584-9.

95. McNair, P. J., Marshall, R. N., and Matheson, J. A. (1990). Important features associated with acute anterior cruciate ligament injury. N Z Med J, 103(901):537-9.
96. McNair, P. J., Prapavessis, H., and Callender, K. (2000). Decreasing landing forces: effect of instruction. Br J Sports Med, 34(4):293-6.
97. Mirka, G. A., and Marras, W. S. (1993). A stochastic model of trunk muscle coactivation during trunk bending. Spine, 18(11):1396-409.
98. More, R. C., Karras, B. T., Neiman, R., Fritschy, D., Woo, S. L., and Daniel, D. M. (1993). Hamstrings--an anterior cruciate ligament protagonist. An in vitro study. Am J Sports Med, 21(2):231-7.
99. Muneta, T., Takakuda, K., and Yamamoto, H. (1997). Intercondylar notch width and its relation to the configuration and cross-sectional area of the anterior cruciate ligament. A cadaveric knee study. Am J Sports Med, 25(1):69-72.
100. Myer, G. D., Ford, K. R., Brent, J. L., and Hewett, T. E. (2006). The effects of plyometric vs. dynamic stabilization and balance training on power, balance, and landing force in female athletes. J Strength Cond Res, 20(2):345-53.
101. Myer, G. D., Ford, K. R., Palumbo, J. P., and Hewett, T. E. (2005). Neuromuscular training improves performance and lower-extremity biomechanics in female athletes. J Strength Cond Res, 19(1):51-60.
102. Myklebust, G., Engebretsen, L., Braekken, I. H., Skjølberg, A., Olsen, O. E., and Bahr, R. (2003). Prevention of anterior cruciate ligament injuries in female team handball players: a prospective intervention study over three seasons. Clin J Sport Med, 13(2):71-8.
103. Nisell, R. (1985). Mechanics of the knee. A study of joint and muscle load with clinical applications. Acta Orthop Scand Suppl, 216:1-42.
104. Nisell, R., and Ekholm, J. (1985). Patellar forces during knee extension. Scand J Rehabil Med, 17(2):63-74.
105. Nunley, R. M., Wright, D. W., Renner, J. B., Yu, B., and Garrett, W. E. (2003). Gender comparison of patella tendon-tibial shaft angle with weight-bearing. Res Sports Med, 11:173-185.

106. O'Connor, J. J. (1993). Can muscle co-contraction protect knee ligaments after injury or repair? J Bone Joint Surg Br, 75(1):41-8.
107. Ohkoshi, Y., Yasuda, K., Kaneda, K., Wada, T., and Yamanaka, M. (1991). Biomechanical analysis of rehabilitation in the standing position. Am J Sports Med, 19(6):605-11.
108. Onate, J. A., Guskiewicz, K. M., Marshall, S. W., Giuliani, C., Yu, B., and Garrett, W. E. (2005). Instruction of jump-landing technique using videotape feedback: altering lower extremity motion patterns. Am J Sports Med, 33(6):831-42.
109. Pandy, M. G., and Shelburne, K. B. (1997). Dependence of cruciate-ligament loading on muscle forces and external load. J Biomech, 30(10):1015-24.
110. Pflum, M. A., Shelburne, K. B., Torry, M. R., Decker, M. J., and Pandy, M. G. (2004). Model prediction of anterior cruciate ligament force during drop-landings. Med Sci Sports Exerc, 36(11):1949-58.
111. Pollard, C. D., Sigward, S. M., Ota, S., Langford, K., and Powers, C. M. (2006). The influence of in-season injury prevention training on lower-extremity kinematics during landing in female soccer players. Clin J Sport Med, 16(3):223-7.
112. Portney, L. G., and Watkins, M. P. (2000). Foundations of clinical research: applications to practice. Upper Saddle River, N.J.: Prentice Hall Health.
113. Powell, J. W., and Schootman, M. (1992). A multivariate risk analysis of selected playing surfaces in the National Football League: 1980 to 1989. An epidemiologic study of knee injuries. Am J Sports Med, 20(6):686-94.
114. Renstrom, P., Arms, S. W., Stanwyck, T. S., Johnson, R. J., and Pope, M. H. (1986). Strain within the anterior cruciate ligament during hamstring and quadriceps activity. Am J Sports Med, 14(1):83-7.
115. Salci, Y., Kentel, B. B., Heycan, C., Akin, S., and Korkusuz, F. (2004). Comparison of landing maneuvers between male and female college volleyball players. Clin Biomech, 19(6):622-8.
116. Schipplein, O. D., and Andriacchi, T. P. (1991). Interaction between active and passive knee stabilizers during level walking. J Orthop Res, 9(1):113-9.

117. Shea, K. G., Pfeiffer, R., Wang, J. H., Curtin, M., and Apel, P. J. (2004). Anterior cruciate ligament injury in pediatric and adolescent soccer players: an analysis of insurance data. J Pediatr Orthop, 24(6):623-8.
118. Shelburne, K. B., and Pandy, M. G. (1997). A musculoskeletal model of the knee for evaluating ligament forces during isometric contractions. J Biomech, 30(2):163-76.
119. Shelburne, K. B., Pandy, M. G., Anderson, F. C., and Torry, M. R. (2004a). Pattern of anterior cruciate ligament force in normal walking. J Biomech, 37(6):797-805.
120. Shelburne, K. B., Pandy, M. G., and Torry, M. R. (2004b). Comparison of shear forces and ligament loading in the healthy and ACL-deficient knee during gait. J Biomech, 37(3):313-9.
121. Shimokochi, Y., Schmitz, R. J., and Shultz, S. J. (2006). Knee extensor moment is related to plantar flexor moment and center of pressure in the anterior/posterior plane. 2006 Human Movement Science Research Symposium. Chapel Hill, NC.
122. Shoemaker, S. C., Adams, D., Daniel, D. M., and Woo, S. L. (1993). Quadriceps/anterior cruciate graft interaction. An in vitro study of joint kinematics and anterior cruciate ligament graft tension. Clin Orthop Relat Res, (294):379-90.
123. Simonsen, E. B., Magnusson, S. P., Bencke, J., Naesborg, H., Havkrog, M., Ebstrup, J. F., and Sorensen, H. (2000). Can the hamstring muscles protect the anterior cruciate ligament during a side-cutting maneuver? Scand J Med Sci Sports, 10(2):78-84.
124. Smidt, G. L. (1973). Biomechanical analysis of knee flexion and extension. J Biomech, 6(1):79-92.
125. Smith, B. A., Livesay, G. A., and Woo, S. L. (1993). Biology and biomechanics of the anterior cruciate ligament. Clin Sports Med, 12(4):637-70.
126. Stapleton, T. R., Waldrop, J. I., Ruder, C. R., Parrish, T. A., and Kuivila, T. E. (1998). Graft fixation strength with arthroscopic anterior cruciate ligament reconstruction. Two-incision rear entry technique compared with one-incision technique. Am J Sports Med, 26(3):442-5.
127. Urabe, Y., Kobayashi, R., Sumida, S., Tanaka, K., Yoshida, N., Nishiwaki, G. A., Tsutsumi, E., and Ochi, M. (2005). Electromyographic analysis of the knee during

- jump landing in male and female athletes. *Knee*, 12(2):129-34.
128. Withrow, T. J., Huston, L. J., Wojtys, E. M., and Ashton-Miller, J. A. (2006). The relationship between quadriceps muscle force, knee flexion, and anterior cruciate ligament strain in an in vitro simulated jump landing. *Am J Sports Med*, 34(2):269-74.
 129. Wojtys, E. M., Huston, L. J., Lindenfeld, T. N., Hewett, T. E., and Greenfield, M. L. (1998). Association between the menstrual cycle and anterior cruciate ligament injuries in female athletes. *Am J Sports Med*, 26(5):614-9.
 130. Wojtys, E. M., Huston, L. J., Schock, H. J., Boylan, J. P., and Ashton-Miller, J. A. (2003). Gender differences in muscular protection of the knee in torsion in size-matched athletes. *J Bone Joint Surg Am*, 85-A(5):782-9.
 131. Woo, S. L., Debski, R. E., Withrow, J. D., and Janaushek, M. A. (1999). Biomechanics of knee ligaments. *Am J Sports Med*, 27(4):533-43.
 132. Woo, S. L., Hollis, J. M., Adams, D. J., Lyon, R. M., and Takai, S. (1991). Tensile properties of the human femur-anterior cruciate ligament-tibia complex. The effects of specimen age and orientation. *Am J Sports Med*, 19(3):217-25.
 133. Yanagawa, T., Shelburne, K., Serpas, F., and Pandy, M. (2002). Effect of hamstrings muscle action on stability of the ACL-deficient knee in isokinetic extension exercise. *Clin Biomech*, 17(9-10):705-12.
 134. Yasuda, K., and Sasaki, T. (1987a). Exercise after anterior cruciate ligament reconstruction. The force exerted on the tibia by the separate isometric contractions of the quadriceps or the hamstrings. *Clin Orthop Relat Res*, (220):275-83.
 135. Yasuda, K., and Sasaki, T. (1987b). Muscle exercise after anterior cruciate ligament reconstruction. Biomechanics of the simultaneous isometric contraction method of the quadriceps and the hamstrings. *Clin Orthop Relat Res*, (220):266-74.
 136. Yu, B., Chappell, J. D., and Garrett, W. E. (2006a). Response to letter to the editor. *Am J Sports Med*, 34:312-315.
 137. Yu, B., Gabriel, D., Noble, L., and An, K. N. (1999). Estimate of optimum cutoff frequency for a low-pass digital filter. *Journal of Applied Biomechanics*, 15:318-329.

138. Yu, B., and Garrett, W. (2005). Hamstring co-contraction does not necessarily reduce ACL loading. XXth Meeting of the International Society of Biomechanics. Cleveland, OH, USA.
139. Yu, B., Herman, D., Preston, J., Lu, W., Kirkendall, D. T., and Garrett, W. E. (2004). Immediate effects of a knee brace with a constraint to knee extension on knee kinematics and ground reaction forces in a stop-jump task. Am J Sports Med, 32(5):1136-43.
140. Yu, B., Kirkendall, D. T., Taft, T. N., and Garrett, W. E., Jr. (2002). Lower extremity motor control-related and other risk factors for noncontact anterior cruciate ligament injuries. Instr Course Lect, 51:315-24.
141. Yu, B., Lin, C. F., and Garrett, W. E. (2006b). Lower extremity biomechanics during the landing of a stop-jump task. Clin Biomech, 21(3):297-305.
142. Zatsiorsky, V. M. (2002). Kinetics of Human Motion. Champaign, IL: Human Kinetics.
143. Zavatsky, A. B., and O'Connor, J. J. (1992a). A model of human knee ligaments in the sagittal plane. Part 2: Fibre recruitment under load. Proc Inst Mech Eng [H], 206(3):135-45.
144. Zavatsky, A. B., and O'Connor, J. J. (1992b). A model of human knee ligaments in the sagittal plane. Part 1: Response to passive flexion. Proc Inst Mech Eng [H], 206(3):125-34.
145. Zeller, B. L., McCrory, J. L., Kibler, W. B., and Uhl, T. L. (2003). Differences in kinematics and electromyographic activity between men and women during the single-legged squat. Am J Sports Med, 31(3):449-56.